The Impact of Sensory-guided Behavior on Neuronal Processing in the Mouse Barrel Cortex and a Novel Two-alternative Forced Choice Paradigm in Head-fixed Mice and Rats

Škreb, Vida

Abstract: Unspecified

The Impact of Sensory-guided Behavior on Neuronal Processing in the Mouse Barrel Cortex and a Novel Two-alternative Forced Choice Paradigm in Head-fixed Mice and Rats

---

Dissertation

zur

Erlangung der naturwissenschaftlichen Doktorwürde

(Dr. sc. nat.)

vorgelegt der

Mathematisch-naturwissenschaftlichen Fakultät

der

Universität Zürich

von

Vida Škreb

aus

Kroatien

Promotionskomitee

Prof. Dr. Bruno Weber (Vorsitz und Leitung der Dissertation)

Prof. Dr. Jean-Marc Fritschy

Prof. Dr. Fritjof Helmchen

Zürich, 2017

“Nothing has such power to broaden the mind
as the ability to investigate systematically and truly
all that comes under thy observation in life.”

Marcus Aurelius

Table of Contents

List of figures and tables

1. Summary

The reconfiguration of neuronal networks due to perceptual learning, and the impact of behavior in a task on online sensory processing are currently critical questions in neuroscience. In the work presented here, these topics were investigated in the barrel cortex of mice performing a sophisticated detection and discrimination task through the lens of two-photon calcium imaging. Layer 2/3 of the primary sensory cortex has been established as an essential locus of adult experience-dependent plasticity. Due to its unique topographical organization, the barrel cortex is an excellent area to investigate modulations of sensory processing in during whisker-dependent behavior. Before recording neuronal activity during learning of a sensory-guided task in project number two, we examined the ability of mice to perform a complex task successfully.

Thus, the primary goal of the first project was to establish if mice can learn complex behavior equally well as rats. In our two-alternative forced choice (2-AFC) paradigm, rodents learned to discriminate simultaneously applied single-whisker vibrotactile stimuli of different repetition rates. Both rats and mice could perform over 400 trials a day, with performance levels reaching over 90% of correct responses. The key finding of this project is that both species show comparable results regarding several behavioral readouts. Namely, their psychometric curves were similar with an average perceptual threshold of 53.0 Hz, and a 50.6- Hz frequency difference with corresponding Weber fractions of 0.58 and 0.56 respectively in rats and mice. Furthermore, their reaction times, the amount of omitted trials, rates of learning, and impulsivity were comparable among the two species. Additionally, we found that whisking before stimulus presentation impaired performance. A fundamental characteristic of our 2-AFC behavioral paradigm paired with whisker tracking is that it allows for a very precise control of the applied vibrotactile stimuli. Since the animal is head-fixed, additional recording and/or stimulating methods can be employed, such as electrophysiology or optogenetics. In the second project, its combination with long-term two-photon imaging will be presented. Furthermore, the task is very suitable for investigating interhemispheric interactions due to the possibility of bilateral stimulation. The main conclusion of the first project is that mice are equally adept as rats in learning complex behavior, such as the 2-AFC detection and discrimination tasks. This result opens up a

multitude of possible research avenues by virtue of fusing behavioral measurements with potent recording and/or stimulating methods and taking advantage of the rich array of transgenic lines created in mice.

In the second project, we investigated plasticity effects due to behavior in a sensory-guided task, along with the impact of attentional engagement on sensory processing in the barrel cortex. To achieve this goal, our 2-AFC task was combined with long-term two-photon calcium imaging in layer 2/3 in the somatosensory cortex. This layer is a major site of adult cortical plasticity. However, our understanding of it is limited, since most studies focused on the granular and infragranular layers. Our data revealed strong plasticity effects due to perceptual whisker-dependent learning. During the baseline recording sessions, mice were passively exposed to sensory stimuli. Once the animals engaged in the operant conditioning sensory-guided task, the stimuli gained behavioral relevance by becoming associated with a water reward. Hence, layer 2/3 neurons display flexible modulation depending on the behavioral context, showing a more complex role for the primary sensory cortex than solely a passive relay of sensory information. Plasticity effects were equally reflected in comparing anesthesia recordings from before and after learning. A robust trend in sensory representation is the increase of evoked calcium transients with increasing repetition rates of the vibrotactile stimulus, also shown in this thesis. However, this monotonic increment was disrupted after the learning took place, which exclusively involved the highest and lowest frequencies. The middle frequency, never applied during the task, received fewer calcium transients than the lowest frequency, thus eliminating the distinctive property of vibrotactile frequency representation. Furthermore, we report the excitatory effect on the cortical representation of somatosensory stimuli during active behavior in the task, as opposed to passive stimulus exposure during unattended trials. Our bilateral 2-AFC paradigm allowed for the comparison of contralateral and ipsilateral responses, which was previously unknown in layer 2/3. We report that contralateral calcium responses are substantially larger than ipsilateral ones, contrary to the infragranular layers, where they are similar in size. To summarize the second project, behavior in a sensory-guided paradigm shapes both online sensory processing and long-term plasticity effects in layer 2/3 of the barrel cortex.

2. Zusammenfassung

Die Neukonfiguration von neuronalen Netzwerken in Folge perzeptuellen Lernens sowie der Einfluss von Aufmerksamkeit auf die sensorische Verarbeitung sind zentrale neurowissenschaftliche Fragen. In der hier präsentierten Arbeit werden diese Themen mit Hilfe von zwei-Photonen Kalzium Bildgebung im Barrel Kortex von Mäusen untersucht, während diese eine komplexe Erkennungs-und Entscheidungsaufgabe ausführten. Die kortikale Schicht 2/3 des primären somatosensorischen Kortex wurde bereits früher als eines der zentralen Areale für erfahrungsabhängige Plastizität im erwachsenen Gehirn identifiziert. Aufgrund seiner charakteristischen topographischen Organisation ist der Barrel Kortex eine bestens geeignete Region um die Modulation der sensorischen Verarbeitung während der Ausführung komplexen Verhaltens zu untersuchen. In einem ersten Teil der Arbeit war das Ziel, eine komplexe Verhaltensaufgabe im Mausmodell zu etablieren. Die zentrale Frage dieses ersten Teils war, ob Mäuse komplexes Verhalten ähnlich gut wie Ratten erlernen können. In unserem two-alternative forced choice (2-AFC) Paradigma haben Nager gelernt, vibrotaktile Reize mit verschiedenen Wiederholungsraten zu unterscheiden, wobei diese Stimuli an einzelnen Schnurrhaaren, gleichzeitig auf beiden Seiten des Gesichts appliziert wurden. Sowohl Ratten als auch Mäuse konnten mehr als 400 Testläufe pro Tag durchführen, wobei das Leistungsniveau eine über 90% korrekte Antwortrate aufwies. Das Kernresultat dieses Projektes ist, dass beide Arten vergleichbare Ergebnisse im Hinblick auf mehrere Verhaltensparameter zeigen. Im Detail waren die psychometrischen Kurven von Ratten und Mäusen mit einer durchschnittlichen Wahrnehmungsschwelle von 53.0 Hz respektive 50.6 Hz und Weber-Fraktionen von 0.58 und 0.56 äusserst ähnlich. Zudem waren die Reaktionszeiten, die Menge an vermiedenen Testläufen und sowohl Lern-, als auch Impulsivitätsraten zwischen beiden Arten vergleichbar. Außerdem konnten wir zeigen, dass das aktive Bewegen der Schnurrhaare die Verhaltensleistung beeinträchtigt. Eine entscheidende Eigenschaft unseres Verhaltensparadigmas in Kombination mit der Bewegungsmessung von Schnurrhaaren ist die Tatsache, dass die verwendeten vibrotaktilen Stimuli präzise kontrolliert werden können. Da der Kopf des Tiers fixiert ist, können zusätzliche Technologien, wie zum Beispiel Elektrophysiologie oder Optogenetik, angewandt werden. Im zweiten Projekt wird eine Kombination mit chronischer zwei-Photonen Mikroskopie vorgestellt. Weiter ist der Test sehr gut geeignet, die Interaktion zwischen den

beiden Hirn-Hemisphären zu untersuchen, da bilateral stimuliert werden kann. Die wesentliche Schlussfolgerung des ersten Projekts ist also, dass es Mäusen in ähnlichem Ausmaß wie Ratten möglich ist, komplexes Verhalten, wie beispielsweise die 2-AFC Erkennungs- und Entscheidungsaufgabe, erfolgreich durchzuführen. Aufgrund der kombinierten Anwendung von Verhaltensmessungen und wirkungsvollen Aufnahme- und/oder Stimulationsmethoden, sowie die Möglichkeit eine grosse Bandbreite von genetisch modifizierten Mausstämmen zu untersuchen, öffnet dieses Ergebnis zahlreiche weitere Türen.

Im zweiten Projekt haben wir Plastizitätseffekte in einer sensorisch geführten Aufgabe zusammen mit dem Einfluss von Aufmerksamkeit auf die sensorische Verarbeitung im Barrel Kortex untersucht. Um dieses Ziel zu erreichen, wurde unser 2-AFC Paradigma mit Langzeit zwei-Photonen Kalzium Imaging in Schicht 2/3 im somatosensorischen Kortex kombiniert. Obwohl dieser Teil des Kortex für kortikale Plastizität im erwachsenen Gehirn zentral scheint, besteht nur ein sehr lückenhaftes Verständnis, da sich die meisten Studien bislang auf die granulären und infragranulären Schichten beschränkt haben. Unsere Daten weisen auf starke Plastizitätseffekte während Lernprozessen hin.

Während der Baseline-Aufnahmen wurden Mäuse passiv sensorischen Stimuli ausgesetzt, die zu einer progressiven Reduzierung von Reiz-induzierten Kalzium-Transienten geführt haben. Dieser Effekt änderte sich in eine Akzentuierung der Transienten, sobald das Tier einer operanten, sensorisch geführten Konditionierungsaufgabe ausgesetzt wurde, in die Relevanz des Reizes hoch ist, da er mit Belohnung in Form von Wasser assoziiert wurde. Die Neuronen in Schicht 2/3 weisen also eine kontextabhängige bidirektionale Modulation auf, wobei im primären somatosensorischen Kortex eine komplexere Rolle gefunden wurde als eine einfache passive Umschaltung sensorischer Informationen. Plastizitätseffekte spiegeln sich gleichermaßen wider, wenn Aufnahmen von anästhesierten Tieren vor und nach Lernen verglichen wurden. Ein robuster Trend in der sensorischen Repräsentation ist der Anstieg von Kalzium-Transienten in Abhängigkeit von zunehmenden Wiederholungsraten von vibrotaktilen Stimuli, was auch in der vorliegenden Arbeit gezeigt werden konnte. Allerdings wurde diese gleichbleibende Erhöhung nach dem Lernen unterbrochen, wobei hier nur die höchste und die niedrigste Frequenz eingeschlossen wurde. Die mittleren Frequenzen, die in dieser Aufgabe nie präsentiert wurden, haben, verglichen mit den anderen Frequenzen, die geringsten Kalzium-Transienten erzeugt. Wir konnten zudem exzitatorische Effekte auf die

kortikale Repräsentation von somatosensorischen Stimuli nachweisen, wenn die Tiere aktiv in die Verhaltensaufgabe involviert waren. Eine passieve Reizverarbeitung führte im Gegensatz dazu zu deutlich Abschwächung der kortikalen Repräsentation. Unser bilaterales 2-AFC Paradigma ermöglichte den Vergleich von kontra- und ipsilaterale Antworten, was vorher für Schicht 2/3 nicht hinlänglich untersucht wurde. Kontralaterale Kalzium-Anworten waren - im Gegensatz zu infragranularen Schichten -wesentlich höher als ipsilaterale. Zusammenfassend konnte im zweiten Teil der Dissertation gezeigt werden, es im Kontex von Lernvorgängen im somatosensorischen Kortex sowohl zu akuten Modulationen, als auch zu Langzeiteffekten in Schicht 2/3 des Barrel Kortex, kommt.

3. General Introduction

3.1. The cerebral cortex

The neocortex

The cerebral cortex is characterized by deep and intricate complexities of structure and function. This outer sheet of densely packed neuronal cells is highly convoluted to ensure the placement of its large surface within the confines of the skull. The wiring is thus economized since the cell bodies are close enough to facilitate an adequate speed of communication while the outgoing axons are joined together to form myelinated white matter. To ensure efficiency, it is regionally specialized according to different functions, such as sensory perception, motor control or higher cognitive functions, which are thought to take place in the associative areas (**Fig. 1A**). Simultaneously with its high degree of specialization, it remains integrative. Interestingly, presumably unimodal primary sensory areas can demonstrate multisensory integration (Kayser et al., 2005). Being the site of significant evolutionary changes, the cerebral cortex must both preserve its stability and ensure sufficient flexibility of cortical circuits. One of the best understood proposed models of cortical circuitry is the whisker-related barrel column, which is the subject of this thesis's investigation. To probe the nature of cortical function, a traditional approach is to measure its responses to sensory stimulation since it permits tight experimental control. Classical electrophysiological methods tend to focus on the deeper layers since their spiking can be more quickly resolved. However, the advent of optical imaging techniques allows the focus on supragranular layers which will be further explored in this dissertation.

The vertical and horizontal structure of the cortex

The cortex is divided horizontally into six layers, which differ in density, cell type and connectivity (**Fig. 1B**). Layer 1 (the molecular layer) is the outermost, characterized by a paucity of interneuron cell bodies and a mesh of traversing axons and dendrites. It receives corticocortical feedback, and, among others, expresses dopamine, serotonin, and acetylcholine receptors. Thus, it can play a role in associative learning, such as fear conditioning (Letzkus et al., 2011). Layer 2 is called the external granular layer and is mainly composed of pyramidal and stellate neurons. Layer 3 is the external pyramidal layer, which

contains pyramidal cells and interneurons. Since layers 2 and 3 blend into each other, they are often termed as layer 2/3. Layer 2/3 contains intracortical afferents and efferents, either within the same hemisphere or commissural. Layer 4 is the internal granular layer, and the main site for thalamocortical connections and intra-hemispheric corticocortical afferents, containing a large proportion of stellate or granular cells. The internal pyramidal layer is layer 5, mainly composed of large pyramidal cells. It sends out subcortical efferents to the thalamus, striatum or brainstem, and is the site of interhemispheric connections. Lastly, the multiform layer 6 also has large pyramidal cells, and is also the origin of thalamocortical efferents. This distinctive organization of afferents, efferents, and intrinsic neurons across cortical layers seems to be a universal feature of the neocortex (Jones, 1999). A conventional simplified circuitry that appears to be operating in the cortex is that the thalamus projects to layer 4, then layer 4 → layer 2/3 → layer 5/6 (**Fig. 1C**) (Feldmeyer et al., 2002; Petersen and Crochet, 2013).

About 60 years ago, Mountcastle proposed that the cortex is a conglomeration of independent vertical cortical columns (Mountcastle et al., 1957). A cortical column is often considered a perpendicular structure, with a definite border containing cells with the same tuning for a certain salient receptive field characteristic. It has been proposed as the underlying structure in an attempt to explain cortical organization (Feldmeyer et al., 2013). Douglas and Martin suggested a major excitatory pathway as a canonical columnar microcircuit (Douglas and Martin, 2004). Even though there is no universal genetic mechanism of origin for the cortical column, nor a single structure (Feldmeyer et al., 2013), we could still define it as having a shared receptive field, and periodic intra-and-intercortical connections (Horton and Adams, 2005).

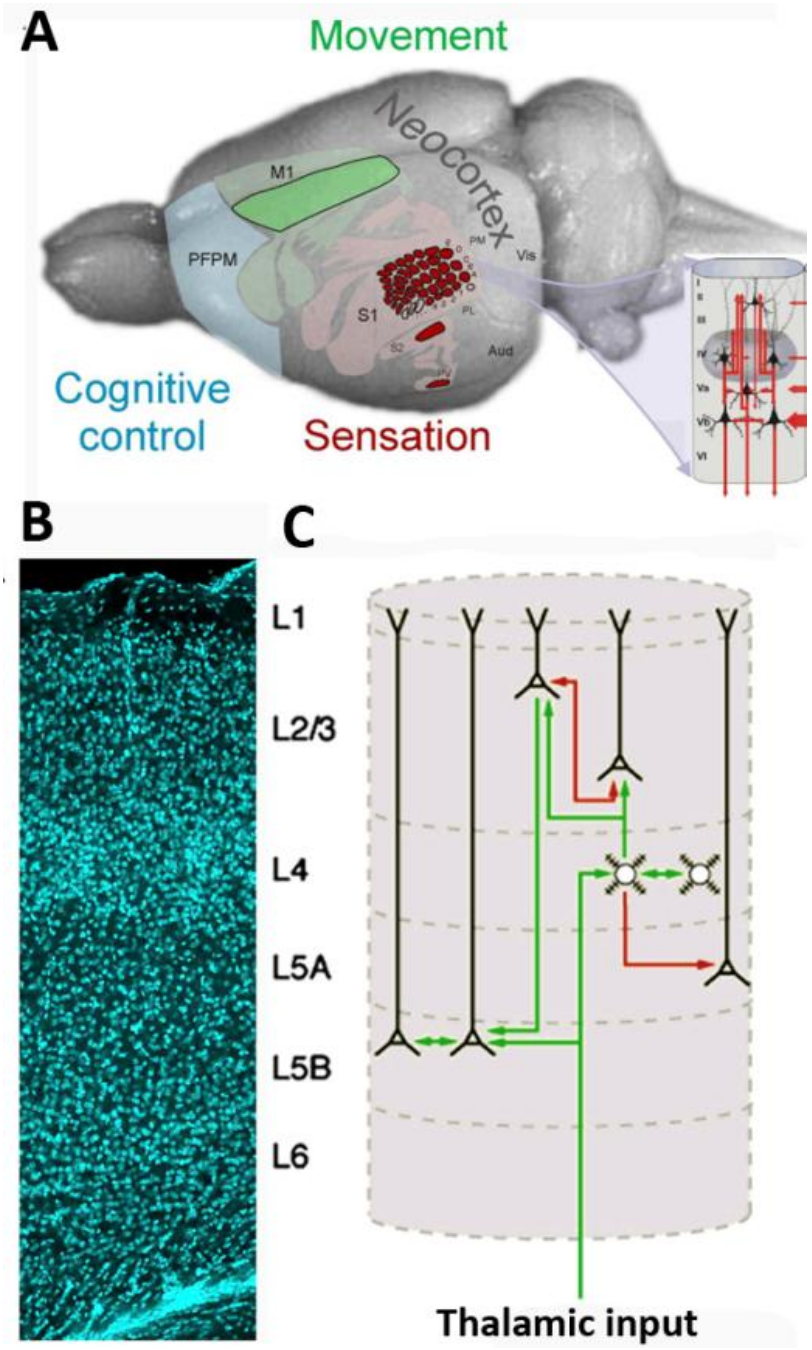

Figure 1. The organization of the cerebral cortex.

A. Location of somatosensory and motor cortex, and areas of higher cognitive control in the mouse brain, with an example of a cortical column (adapted from Feldmeyer et al., 2013). **B.** Confocal image of DAPI-stained nuclei (cyan) from a single plane in the C2 barrel column (adapted from Crochet and Petersen, 2013). C. Scheme of cortical circuitry (adapted from Feldmeyer et al., 2013).

3.2. Map plasticity in the barrel cortex

Neuronal plasticity and its mechanisms

The sensory cortices are dynamic constructs subject to plasticity events in response to behaviorally relevant experiences, which manifest as a modification in the neural responses to the same sensory stimulus (Blake et al., 2006). Indeed, it is known that changes in the use of different sensory inputs modify cortical maps (Glazewski and Barth, 2015). This includes the somatosensory cortex, where neuroplasticity has been demonstrated in a variety of experimental paradigms (Bieszczad et al., 2013; Buonomano and Merzenich, 1998; Galvez, 2006), or due to passive sensory experiences and even peripheral lesions (Hofer et al., 2009; Holtmaat and Svoboda, 2009; Trachtenberg et al., 2002). Plasticity events carry on into adulthood (Gilbert et al., 2001), along with changes in topographic maps (Ohl and Scheich, 2005; Sur, 2005). However, in adult animals, plasticity occurs predominately in layers 2/3 and 5 (Diamond et al., 1994; Stern et al., 2001).

Plasticity mechanisms tend to be defined as either following Hebbian plasticity rules (that tend to modify network properties) or homeostatic ones that tend to preserve system stability (Turrigiano and Nelson, 2000) (**Fig. 2A**). There are two mechanistically distinct processes of Hebbian plasticity. The first is the active process of a deprivation-induced weakening of layer 4 to layer 2/3 synapses, probably caused by spiking from competing inputs (Pologruto, 2004) with long-term depression (LTD) as a likely underlying physiological mechanism (Bender, 2006). The second independent process of Hebbian plasticity is the enhancement of the responses to the spared whisker, and a corresponding expansion of the respective cortical map (Maier et al., 2003), following the principle of “neurons that fire together, wire together.” A possible substrate for this form of plasticity is cortical long-term potentiation (LTP) (Bender, 2006). There are physiological substrates for cortical plasticity beyond LTP and LTD, such as the recruitment of a large pool of silent neurons characterized by very low firing rates (Margrie et al., 2002). Indeed, a weaker synapse is more likely to potentiate than an already strong synapse, given the natural neuronal dynamic range (Margolis et al., 2012).

However, certain forms of plasticity cannot be explained by Hebbian rules, such as non-competitive homeostatic regulation. Overall, a homeostasis of neuronal firing rates tends to be preserved. Otherwise, neuronal circuits would not be able to maintain their stability (Turrigiano and Nelson, 2000). Homeostatic cellular plasticity mechanisms occur in

parallel with Hebbian ones. For example, the reduction of responses of the high-responders and the increase of low-responders is in line with the non-competitive homeostatic regulation principle (Margolis et al., 2012). A homeostatic mechanism would also be the shrinkage of the cortical representation of the activated vibrissa after prolonged passive stimulation, with the goal reducing the neuronal responses to behaviorally irrelevant somatosensory inputs (Welker et al., 1992). Another form of non-Hebbian plasticity is the sharpening of receptive fields in layer 2/3 following exposure to enriched environments, during arousal, and acute exploration (Castro-Alamancos, 2004; Polley et al., 1999). Furthermore, excitatory synaptic strength can be scaled, so that the relative strengths remain constant while preserving activity within a functional range (Turrigiano, 2008). In addition, fear conditioning enhances the responses in primary sensory cortices by accentuating sparse population coding and reducing total network activity (Gdalyahu et al., 2012). In summary, there is a variety of both Hebbian and non-Hebbian plasticity mechanisms that occur synchronously and have yet to be fully elucidated.

Perceptual learning in primary sensory cortex

Context-appropriate behavioral adaptation to an ever-changing environment helps to ensure survival and is achieved through continuous learning. Thus, learning can be defined as the ability to predict the consequences of behavior and depends on the extent to which these predictions are erroneous, ending when outcomes become entirely predictable (Hollerman and Schultz, 1998). Plastic modifications of synaptic functioning and/or neuronal pathways are thought to be the neuronal mechanisms underlying learning (Crist et al., 2001; Rosselet et al., 2011). Hence, generating a behaviorally useful representation of the external world requires an interaction of sensory activation and cortical plasticity, which follows network-level rules (Kilgard et al., 2002). Here, we will focus on perceptual learning, which are improvements in the organism's perceptual acuity through training, causing long-term modifications in the nervous system to adapt better to the requirements of the external world. Perceptual learning consists of extracting previously unused information and evolves in four stages: attention weighting, imprinting, differentiation, and unitization (Goldstone, 1998). In attention weighting, perception becomes attuned to the critical dimensions of the relevant stimuli. In imprinting, specialized receptors are developed for the specific stimuli, or for some of their characteristics. During differentiation, previously indistinguishable stimuli

become separated. Finally, in unitization, the organism can detect a complex construct as a single feature (Goldstone, 1998).

Memory in the primary sensory cortex

Until recently, little research has been done on the ability of the primary sensory cortex to store memory (Weinberger, 2004), as it was widely viewed solely as a relay of sensory information. To prove that memory formation has taken place, there should be a neural change that correlates with the behavioral parameters of learning. Indeed, mounting evidence shows that primary sensory cortices can acquire and store memories of behaviorally relevant sensory stimuli. Furthermore, remodeling in the primary sensory cortex is sufficient to form distinct behavioral memories (Bieszczad et al., 2013). This form of plasticity has the characteristics of associative memory. It is rapidly acquired, consolidates, and endures for longer periods. Importantly, these experience-dependent changes in primary cortical areas are specific to the characteristics of the salient sensory stimulus used in a task (Kilgard et al., 2002), and this learning is not transferable to other parameters of stimuli (Ahissar and Hochstein, 1993; Karni and Sagi, 1991). It is important here to emphasize that plasticity in the sensory system developed during learning does not confirm actual learning and memorization have taken place (Weinberger, 2004).

Cortical maps and learning

Primary sensory cortex receptive fields can be altered by learning experiences in a rapid manner (Siucinska and Kossut, 1996), with the enlarged region corresponding precisely to the trained sensory input (Bieszczad and Weinberger, 2010a; Roelfsema et al., 2010). In reverse, cortical map plasticity enhances perceptual learning (Reed et al., 2011). The extent of topographic map plasticity correlates with the degree of sensory-driven acuity and learning (Polley, 2006; Recanzone et al., 1993), even though some studies failed to find a proportional relationship between increasing performance and sensory maps (Molina-Luna et al., 2008; Yotsumoto et al., 2008). The enhancement is transient, since after the initial receptive field expansion, there is a shrinkage and refinement by selecting the most efficient neuronal networks needed to complete the task (Gdalyahu et al., 2012; Takahashi et al., 2011). However, this subsequent fading of cortical map plasticity does not impair performance on sensory-driven tasks. Rather, it is no longer needed to sustain successful

behavior (Reed et al., 2011). In summary, map plasticity seems to be transiently functionally relevant for learning during its early stages.

Is plasticity regulated by top-down or bottom-up signals?

A crucial question is whether primary sensory cortex plasticity is determined by bottom-up or top-down influences. The barrel cortex is a very suitable system to study sensory-guided learning since it lies at the confluence of both bottom-up sensory inputs from the vibrissae, and top-down inputs from brain areas involved in cognitive functions. Adult animals passively exposed to sensory stimuli do not develop receptive field plasticity (Polley, 2006). Equally, plasticity also does not take place if internal signals, such as electrical stimulation or neuromodulatory release, are not temporally paired to sensory stimuli. Indeed, it has been shown that task demands influence responses already at the level of the primary sensory cortex (Ahissar et al., 1992; Crist et al., 2001). Furthermore, tasks that require attending to a different characteristic of the same stimuli will result in different specificities of plastic changes, thus indicating a mutual interaction of top-down and bottom-up influences (Ahissar and Hochstein, 1993; Fritz, 2005; Polley, 2006). The role of the task-specific top-down inputs might be to modify the representation of a single feature in a way that does not disturb other feature representations already embedded within the same neuronal network (Polley, 2006).

The influence of neuromodulation on learning

Cortical neuroplasticity seems to be gated by the behavioral state of the animal, which in turn is affected by the release of several neuromodulators (Ahissar and Hochstein, 1993; Recanzone et al., 1993). Indeed, it has been shown that neuromodulators play a significant role in shaping cortical maps upon behavior in sensory-driven tasks, by signaling the internal state and the relevance of external stimuli (**Fig. 2B**). For example, dopamine is released when the timing or occurrence of a reward are unexpected (Hollerman and Schultz, 1998), thus contributing to reward-related learning. The release of acetylcholine is needed for the induction and expression cortical map plasticity (Ji et al., 2001; Shulz et al., 2003; Yan and Zhang, 2005) and plays a role in determining its degree and direction (Kilgard et al., 2001). Furthermore, attentional gating via the neuromodulator acetylcholine is known to

play a role in receptive field plasticity (Shulz et al., 2003). Indeed, the cholinergic antagonist can block both learning and map expansion (Conner et al., 2005). Plasticity changes induced by noradrenaline have been shown to cause changes in sensory responses and improve long-term sensory perception (Martins and Froemke, 2015). In summary, neuromodulators are a crucial component of cortical plasticity events.

The role of layer 2/3 in sensory-driven learning

Sparse coding in supragranular layers of the barrel cortex provides an excellent framework for associative learning, since their simple coding scheme is easily interpreted by other brain functions, and they receive a wealth of subthreshold synaptic inputs (Petersen and Crochet, 2013). Neurons in layer 2/3 are particularly well suited to study the interplay of neuroplasticity and sensory processing since their functional properties are strongly regulated by the behavioral state of the animal (Kato et al., 2015; Petersen and Crochet, 2013). Even very brief periods of activity in a few supragranular cortical pyramidal neurons can drive perceptual decisions and learning (Huber et al., 2008).

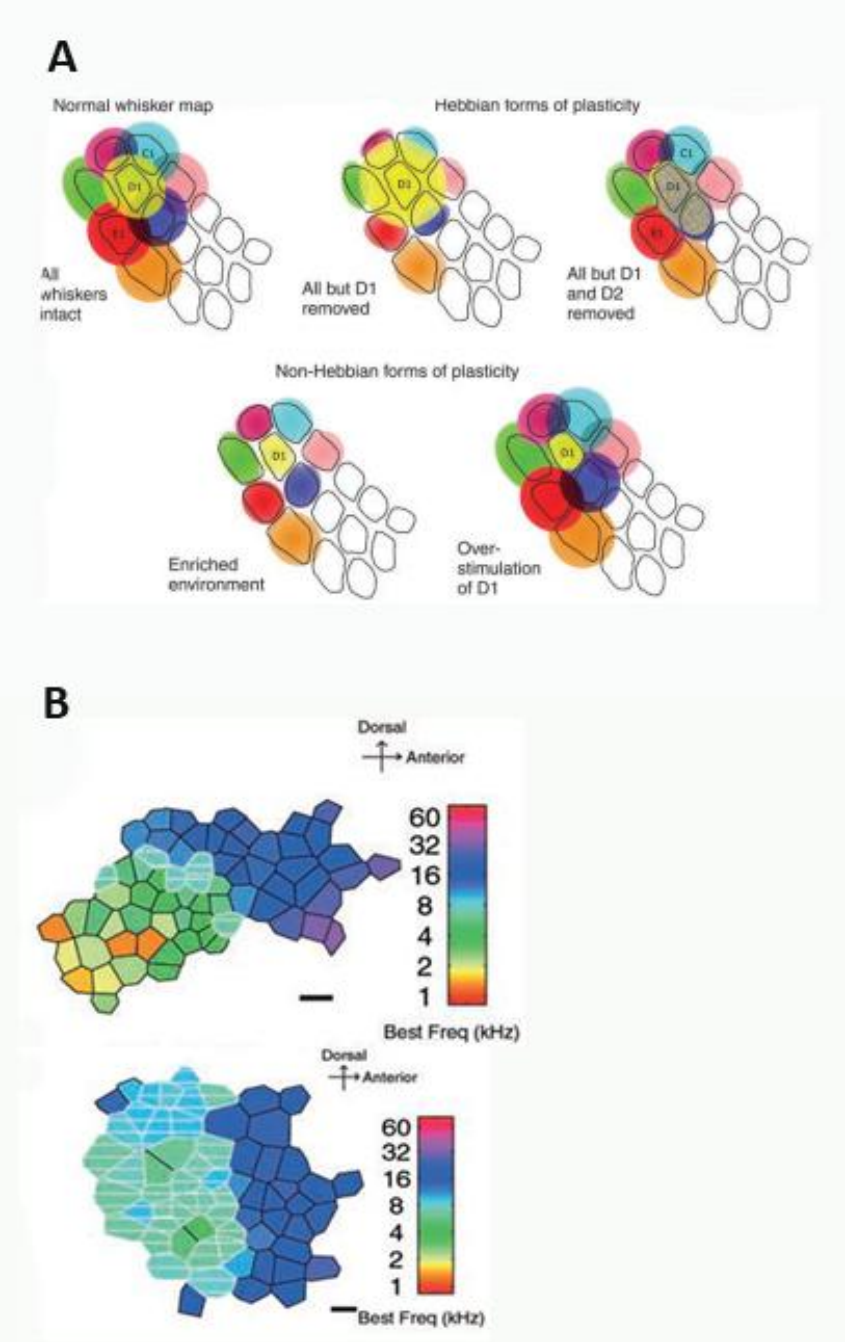

Figure 2. Plasticity of cortical maps.

A. Examples of Hebbian and non-Hebbian plasticity in the barrel cortex (adapted from Feldman and Brecht, Science 2005). **B.** An example of map reconfiguration through tone pairing with neuromodulator release (adapted from Kilgard et al. 2002).

3.3. Signal processing in the barrel cortex

The barrel cortex

Rodents use their vibrissae as an important channel to collect information about their surroundings, assisting survival (Diamond and Arabzadeh, 2013). The usage of their whiskers has been employed in a variety of experimental sensory-guided tasks, such as texture discrimination, frequency discrimination, judging distances or widths of apertures, surface orientations, position of objects, and so on (Adibi et al., 2012; Diamond and Arabzadeh, 2013; Knutsen, 2006; Mayrhofer et al., 2013). Even one whisker is enough to identify the location of an object by combining touch and movement (Mehta et al., 2007). Removal of whiskers, or even whisker trimming, causes results in diminished equilibrium, locomotion, and discrimination of surfaces (Simons, 1978). In the rodent, the whiskers are both sensors and effectors (Mehta et al., 2007). Perception mediated through whiskers can arise either from the rodent actively moving its whiskers forward and backward to seek contact with objects (generative mode), or the rodent immobilizing its whiskers to collect signals (receptive mode) (Diamond and Arabzadeh, 2013). If a whisker is deflected by the experimenter during quiet wakefulness, there is a strong cortical response, as opposed to a weak response obtained during active whisking (Hentschke, 2005; Petersen, 2007).

The somatosensory cortex has excellent functional capacities, and an anatomic and physiological organization for examining how stimuli are encoded (Arabzadeh et al., 2003). This is due to its distinct structural organization, where each region (or “barrel”) visualized in layer 4 by cytochrome oxidase activity, corresponds to sensory input from a single vibrissa, with the arrangement of the whiskers corresponding one-to-one with the arrangement of the barrels, thus forming a precise map (**Fig. 3A** and **B**).

Sensory information guides behavior, serving a starting point for motor control and the planning of future action (Petersen, 2007). The motor and somatosensory systems are tightly interwoven in rodents at the levels of the brainstem, thalamus, and cortex, in a nested series of loops (Kinnischtzke et al., 2013; Mehta et al., 2007). Sensorimotor integration takes place on all these three levels, with the primary motor and somatosensory cortex being reciprocally connected (Kinnischtzke et al., 2013). When the motor cortex is activated, substantial inhibition and excitation arise in the somatosensory cortex that in turn influences state-dependent changes in the somatosensory cortex (Kinnischtzke et al., 2013).

Sparse coding and layer 2/3

Sensory information tends to be processed by a small number of active neurons in a large neuronal population (sparse coding), because a small subset of excitatory neurons fire the majority of action potentials, while the remaining neuronal population remains silent (Hromádka et al., 2008; Kerr et al., 2005; O'Connor et al., 2010; Yassin et al., 2010). This way of processing sensory information offers several advantages. First, it saves energy by decreasing spiking, which has a high metabolic load (Attwell and Laughlin, 2001; Gdalyahu et al., 2012; Lennie, 2003). Second, it maximizes the capacity to form associative memories because of less potential cross-talk between firing patterns, thus offering a plausible substrate for the expression of Hebbian learning rules (Palm, 2013). Third, it allows complex data to be represented in an easier read-out for higher-up cortical areas (Olshausen and Field, 2004).

Even though most layer 2/3 excitatory neurons receive synaptic input, they still fire in a sparse manner (**Fig. 3C** and **D**). A variety of different methods have shown that spiking frequencies among layer 2/3 neurons tend to be consistently low in various brain areas. Juxta-cellular recordings in the barrel cortex of head-fixed rats have an average spiking rate of 0.28 Hz (De Kock et al., 2007; de Kock and Sakmann, 2009). Whole-cell recordings in the mouse barrel cortex displayed an average spiking rate of 0.61 Hz (Poulet and Petersen, 2008). Two-photon imaging in the rat visual cortex resulted in an average firing rate of 0.44 Hz (Greenberg et al., 2008). Lastly, whole-cell recordings from the hindlimb motor cortex of freely moving rats displayed spiking rates of 0.3 Hz (Lee et al., 2006). This is in part due to state-dependent activation of inhibitory neurons, since their silencing leads to increased firing (Atallah et al., 2012; Gentet et al., 2010) and they incite competition among excitatory neurons (Mateo et al., 2011). It is likely that this is due to the high neuronal activity of parvalbumin inhibitory interneurons (Petersen and Crochet, 2013). A partial contribution to sparse coding in this layer could be that the cells have a more hyperpolarized resting potential, due to a feed forward input from L4 GABAergic neurons (Lefort et al., 2009). Interestingly, the sparseness is modulated by a variety of factors, such as the brain state, development, or experience (Gentet et al., 2010). For example, fear conditioning increases sparse coding (Gdalyahu et al., 2012).

Processing sensory signals in the barrel cortex

The same sensory stimulus can produce a variety of different neuronal responses, resulting in a trial-to-trial variability in the experimental setting that could be caused by stochastic meaningless intrinsic noise or meaningful signals from other brain regions (London et al., 2010). Regardless of the variety in the neuronal representation of sensory stimuli, rodents still rapidly and accurately recognize and discriminate objects, textures, locations, and other stimuli. In the neuronal representation of vibration, the most salient firing property is the firing rate, which makes it impossible for rodents to sense elemental stimulus features (Adibi et al., 2012). Hence, the animal will judge the frequency of a stimulus by the integrated number of spike counts per trial in the primary somatosensory cortex (Lak et al., 2010; London et al., 2010; Luna et al., 2005). In line with that is the animal's overestimation of the intensity of the stimulus if noise is added to it since it will result in an increase in firing rates (Adibi et al., 2012), (Lak et al., 2007, 2010). However, stimuli that are intensity matched cannot be discriminated (Gerdjikov et al., 2010). This is because sensory perception mediated by the whiskers encodes not frequency or amplitude, but the mean absolute velocity of the whisker motion, which is proportional to the product of amplitude and frequency (Adibi et al., 2012; Arabzadeh et al., 2003; Gerdjikov et al., 2010).

Inhibition and excitation in the cortex

A universal feature of neocortical microcircuits is that a dense matrix of inhibitory cells is extended onto local pyramidal cells (**Fig. 3E**) (Packer and Yuste, 2011). It is thought that inhibitory cells act locally (therefore called interneurons), whereas excitatory cells convey information to other brain areas (Lak et al., 2010). Even though GABAergic neocortical neurons represent only 15% of the neuronal population, they play a pivotal role in shaping neocortical activity. They fire an order of magnitude more than excitatory neurons and receive stronger synaptic input (Gentet et al., 2010; Mateo et al., 2011; Reyes-Puerta et al., 2014), which gives rise to a relatively equal total amount of spiking between excitatory and inhibitory neurons in layer 2/3 (Petersen and Crochet, 2013). Furthermore, in layer 2/3, excitatory cells receive synaptic input from around 30 other pyramidal cells. Those connections are weak, while the connections between excitatory and inhibitory cells tend to be ten times more numerous and their interactions are stronger (Avermann et al., 2012;

Holmgren et al., 2003).These strong connections between excitatory and inhibitory neurons probably help to balance cortical excitation and inhibition (Mateo et al., 2011). This balance seems to be achieved by synchronizing their activities and maintaining a correlation in strength (Okun and Lampl, 2008).

Interhemispheric communication and ipsilateral responses

Rodents need to integrate bilateral information from the vibrissae to continuously compare distances, the width of apertures, etc. (Shuler et al., 2001). Since subcortical pathways are kept separate from the periphery to the primary sensory cortex, the comparison of bilateral sensory inputs occurs in S1 (Chiaia et al., 1991; Krupa et al., 2001; Li, 2005; Shuler et al., 2001) (**Fig. 3F**). In the neocortex interhemispheric communication is achieved via the corpus callosum that is composed of axonal fibers from layers 2/3, 5 and 6 (Li, 2005; Palmer et al., 2012; Ramos et al., 2008) and projects mainly to a topographic brain area (Cauller et al., 1998; Zhou et al., 2013). In addition, it has been suggested that callosal inputs are separated from thalamic inputs in the primary sensory cortex (Li, 2005). It is thought that transcallosal fibers mediate interhemispheric inhibition, which influences fine motor control, bilateral dexterity, visuospatial attention, somatosensory processing and cortical rivalry (Palmer et al., 2012). Interestingly, learning is transferred to the homotopic region of the other hemisphere (Harris and Diamond, 2000). Barrel neurons respond best to simulations of the contralateral whiskers, but they show responses to ipsilateral whisker stimulation, whose signals pass through the corpus callosum (Shuler et al., 2001). Ipsilateral responses, so far, have been recorded as evoked local field potential (LFP) and spiking in layer 5 (Li, 2005), (Shuler et al., 2001).

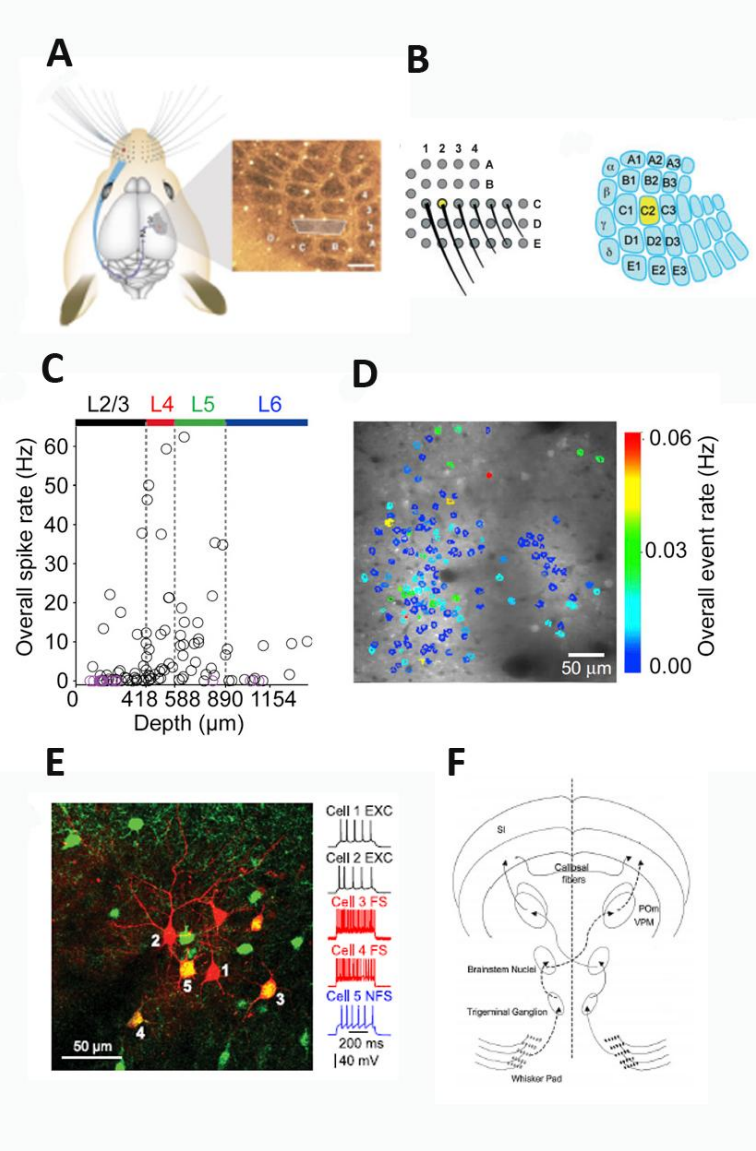

Figure 3. Signal processing in the barrel cortex.

A. Schematic drawing of the rodent brain with the neuronal pathways from the whiskers to the contralateral barrel cortex with an image of the barrel field (adapted from Knott et al., 2002). **B.** The whisker arrangement is reflected in the organization of the barrel cortex (adapted from Aronoff et al. 2010). **C.** The depth of cortical layers with their overall spike rate (adapted from Petersen and Crochet, 2013). **D**. Two-photon calcium imaging of the L2/3 barrel cortex. The colors of neurons correspond to their mean activity (event rate) (adapted from Petersen and Crochet, 2013). **E. A** two-photon image stack showing 2 excitatory cells (EXC) and 3 inhibitory cells (FS, NFS) (adapted from Avermann et al. 2011). **F.** A schematic drawing of synaptic connections from the whisker pad, through the trigeminal ganglion, brainstem nuclei, and thalamus, arriving at the primary somatosensory cortex (S1)

and the callosal connections between the two hemispheres (adapted from Shuler et al., 2001).

3.4. Behavior

The two-alternative forced choice paradigm

The Go-NoGo paradigm is often used in head-fixed rodents (Stüttgen and Schwarz, 2008). However, the two-alternative forced choice (2-AFC) paradigm offers several advantages in comparison. It can distinguish three behavioral response categories: namely “correct”, “error”, and “miss”. By responding, it can make a correct or incorrect (“error”) choice, and it can also withhold a response (“miss”), showing disengagement in the task. In contrast, in the Go-NoGo task, the animal is presented with either a positively reinforced stimulus, where it must respond, or a negatively reinforced stimulus, where it must withhold a response. Therefore, in the Go-NoGo task, one cannot distinguish a lack of motivation or lapses of attention from false and correct rejections. In contrast, the 2-AFC task can make a distinction between disengagement in the task from an incorrect response. A further advantage of a two-alternative forced choice discrimination task over a Go-NoGo task is that the animal does not judge a single stimulus, but has to identify which of the two stimuli is the target, therefore treating the stimuli as events in external space (Diamond and Arabzadeh, 2013). It has been suggested that rats can perform Go-NoGo tasks even without a cortex since information is transferred directly from subcortical sensory to motor areas.

In contrast, a two-alternative forced choice task is more likely to engage the cortex (Diamond and Arabzadeh, 2013). A Go-NoGo task is more likely to rely on habitual reflexive licking behavior and impulsivity, even more so, since deprived animals are more prone to impulsive behavior. In contrast, a two-alternative forced choice task probably involves goal-directed sensory decisions (Diamond and Arabzadeh, 2013), and the animal can obtain the reward in each trial, which cannot happen in the Go-NoGo task. In our experiments, the training of mice and rats in the 2-AFC behavioral task took on average 14 days until a high level of performance in the detection task was reached. This is roughly twice as long as it takes animals to learn to detect a Go/NoGo paradigm (Huber et al., 2008; Sachidhanandam et al., 2013). This prolongation of the learning phase can be explained by the fact that it

takes longer for the animal to make an association with a stimulus side to licking one of the two available spouts in the 2AFC task. Hence, the complexity of the task prolongs the learning process. Animals can develop a response bias in both paradigms (for review of different task strategies see (Stüttgen, 2011)). However, this can be easily corrected in the 2AFC task by implementing a bias correction algorithm (Knutsen, 2006). In summary, the 2-AFC paradigm offers several advantages for investigating behavioral state-dependent neuronal processing.

Detection and discrimination in the primary sensory cortex

It has been demonstrated that the primary sensory cortex has a causal role in both detection (Sachidhanandam et al., 2013) and discrimination tasks (Krupa et al., 2001). Interestingly, even in the case in which detection and discrimination have the same difference in amplitude, rodents are better at discrimination (Adibi and Arabzadeh, 2010). The available sensory information, and thus psychophysical performance, is limited by the sensitivity of individual neurons in a given population by the noise correlations between them and the amount of noise in the decision stages (Cohen and Newsome, 2009). If there is uncertainty about the spatial location, frequency or timing of the stimulus, psychophysical performance is impaired (Stüttgen and Schwarz, 2008). Interestingly, single neurons can perform better at the task than the behaving animal. However, the perception of sensory events could be based on the occurrence of spiking in four to five neurons (Stüttgen and Schwarz, 2008). It is important to accentuate that the relationship between neuronal sensitivity and psychophysical performance can be different in different kinds of discrimination tasks (Britten et al., 1992; Cohen and Newsome, 2009; Purushothaman and Bradley, 2005) and/or in different sensory modalities (Matsumora et al., 2008; Stüttgen and Schwarz, 2008).

The time window for evaluating sensory stimuli has to be very short (in the range of tens of milliseconds) since there is an evolutionary pressure to respond fast to prevent potential danger (Stüttgen and Schwarz, 2008). For examples, monkeys only take a few hundred milliseconds to decide on a psychophysical task (Cohen and Newsome, 2009). The time needed for the rat to integrate information obtained from whisker motion can be as short as just 25 milliseconds (Stuttgen and Schwarz, 2010). However, performance increased

with the length of the experiment, suggesting that information can be accumulated over time (Stuttgen and Schwarz, 2010).

3.5. Two-photon imaging

Two-photon imaging of calcium signals in neurons

Two-photon imaging revolutionized since it allows for cellular resolution optical imaging of both the structure and function of neuronal populations (Denk et al., 1990). It is most often performed in the supragranular cortical layers since imaging below 400 µm presents a technical challenge (Mittmann et al., 2011). Neurons use calcium as an important intracellular messenger. Upon cell activation, the internal calcium concentration rises from 50100nM to up to a hundred times more (Grienberger and Konnerth, 2012). This entry of calcium triggers exocytosis of synaptic vesicles harboring neurotransmitters, and therefore plays a role in activity-dependent synaptic plasticity. Voltage-gated calcium channels are responsible for rapid changes in calcium concentration and therefore serve as an approximation of neuronal spiking activity (Grewe et al., 2011; Kerr et al., 2007). If the firing rates are low, the calcium signal presumably increases linearly with spiking, but as the firing rates increase; the calcium rise can drive indicators to saturation (Lütcke et al., 2013a). An important technical breakthrough in the field of two-photon imaging came from the laboratory of Roger Tsien with the discovery of genetically encoded calcium indicators (GECIs) (Miyawaki et al. 1997). GECIs are composed of either one or two fluorophores, and in the case of two take advantage of the fluorescence resonance energy transfer (FRET) mechanism to signal changes in calcium levels (**Fig. 4A**). They produce a ratiometric signal that measures the relative change between the acceptor and donor signal, and therefore is less susceptible to motion artifacts (Yassin et al., 2010). Since GECIs enable functional imaging over months, the chronic cranial window preparation established itself as a means to perform long-term imaging (**Fig. 4B** and **C**) (Holtmaat and Svoboda, 2009).

Calcium imaging in awake animals

Several recording techniques have been successfully adapted to awake rodents, such as extracellular unit recordings, whole-cell recordings, voltage-sensitive dye imaging, and two-photon microscopy (Petersen, 2007). Two-photon imaging is a relatively non-invasive

technique, and in combination with calcium indicators, it has become one of the standard tools in monitoring neuronal activity (Helmchen and Denk, 2005; Svoboda and Yasuda, 2006). The development of the head-fixed preparation, followed by habituation to the head-restraint, allowed for imaging in awake behaving rodents, and has been successfully adapted to a variety of paradigms (**Fig. 4D** and **E**) (Andermann, 2010a; Dombeck et al., 2007; Huber et al., 2012; Komiyama et al., 2010). Importantly, this method avoids the sampling bias since it images all neurons in a respective imaging field, instead of sampling neurons based on their activity as in electrophysiology (Gerhard et al., 2011). It is possible to assign each neuronal signal to its corresponding neuron since this method provides spatial information, thus allowing the measurement of spatial distances and the analysis of activity patterns (Andermann, 2010a; Lütcke et al., 2013a; Margolis et al., 2012). The same population of neurons can be imaged over months to study plasticity and/or stability (Huber et al., 2012; Margolis et al., 2012; Mayrhofer et al., 2015a) since changes on the level of individual neurons can be followed over days (Lütcke et al., 2013b). The spatiotemporal information that this method provides offers invaluable insights into cortical microcircuits in the awake animal (Kerr et al., 2005). Equally, two-photon imaging allows for greater statistical power, since one can perform long-term measurements from the exact same neuronal population, giving rise to more trials per neuron (Andermann, 2010a; Lütcke et al., 2013b; Margolis et al., 2012).

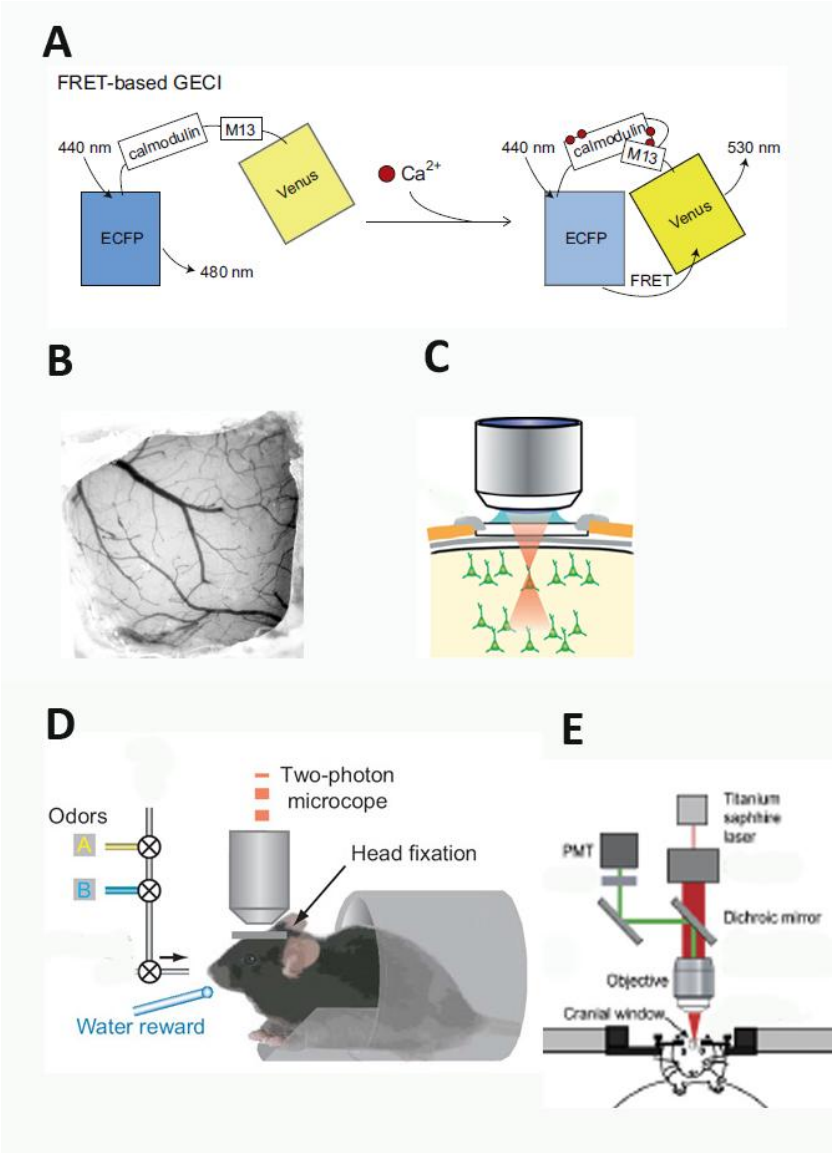

Figure 4. Two-photon calcium imaging in awake behaving animals.

A. Scheme of a FRET mechanism in a GECI (adapted from Grienberg et al. 2012) **B.** Image of a cranial window from animal m2. **C.** Scheme of tow-photon excitation via a cranial window (adapted from Lütcke et al. 2013). **D.** An example of two-photon imaging in awake behaving animals (adapted from Komiyama et al. 2010). **E.** An example of two-photon imaging in awake behaving animals (adapted from Dombeck et al. 2007).

4. Project 1: Novel two-alternative forced choice paradigm for bilateral vibrotactile whisker frequency discrimination in head-fixed mice and rats

This work was published as an original paper: Johannes M. Mayrhofer, Vida Skreb, Wolfger von der Behrens, Simon Musall, Bruno Weber, Florent Haiss (2013). Novel two-alternative forced choice paradigm for bilateral vibrotactile whisker frequency discrimination in head-fixed mice and rats. Journal of Neurophysiology 109(1), 273-284.

Author contributions
Johannes Mayrhofer and Vida Skreb act as shared first authors. Vida Skreb contributed to the conception and design of the research, performed a large part of the experiments in mice and rats. She also contributed to writing and editing the manuscript.

1.1. Abstract

Rats and mice receive a constant bilateral stream of tactile information with their large mystacial vibrissae when navigating in their environment. In a two-alternative forced choice paradigm (2-AFC), head-fixed rats and mice learned to discriminate vibrotactile frequencies applied simultaneously to individual whiskers on the left and right sides of the snout. Mice and rats discriminated 90 Hz pulsatile stimuli from pulsatile stimuli with lower repetition frequencies (10–80 Hz) but with identical kinematic properties in each pulse. Psychometric curves displayed an average perceptual threshold of 50.6 Hz and 53.0 Hz frequency difference corresponding to Weber fractions of 0.56 and 0.58 in mice and rats, respectively. Both species performed >400 trials a day (>200 trials per session, 2 sessions/day), with a peak performance of >90% correct responses. In general, rats and mice trained in the identical tasks showed comparable psychometric curves. Behavioral readouts, such as reaction times, learning rates, trial omissions, and impulsivity, were also very similar in the two species. Furthermore, whisking of the animals before stimulus presentation reduced task performance. This behavioral paradigm, combined with whisker position tracking, allows precise stimulus control in the 2-AFC task for head-fixed rodents. It is compatible with state-of-the-art neurophysiological recording techniques, such as electrophysiology and two-photon imaging, and therefore represents a valuable framework for neurophysiological investigations of perceptual decision-making.

1.2. Introduction

Rats and mice are nocturnal animals that use their array of movable whiskers to explore and navigate the environment. These tactile sensors enable rodents to acquire sensory information about the surrounding world. Several studies, mostly performed in rats, have reported that rodents are able to discriminate different textures (Carvell and Simons, 1990; Morita et al., 2011), the size of apertures (Krupa et al., 2001), gap size (Jenkinson and Glickstein, 2000), and the position of objects (Mehta et al., 2007). More recent work has shown that psychophysical measurements can be acquired during active palpation (Carvell and Simons, 1990; Knutsen, 2006; Morita et al., 2011; Prigg et al., 2002) or during the passive deflections of individual stationary whiskers (Gerdjikov et al., 2010; Stüttgen and Schwarz, 2008). Most of these studies employed paradigms in which the animals could move freely in the experimental arena. However, head-fixed paradigms are becoming increasingly popular, as they allow precise stimulus presentation and monitoring of whisker motion (Hentschke, 2005). Furthermore, fixing the animal's head is a requirement for several neuroscientific methods.

To investigate the neuronal code underlying perception and cognitive functions, it is necessary to combine behavioral measurements with recordings from the individual neuronal elements involved in these processes. Simultaneous acquisition of psychophysical and neural data is one of the gold standards in cognitive neuroscience (Parker and Newsome, 1998; Stuttgen, 2010). The current knowledge in this field has been obtained mainly from the head-fixed nonhuman primate preparation (Wurtz et al., 1968). Although recent developments in head-fixed rodent Go-NoGo paradigms allow single neurons to be recorded concomitantly with psychophysics, these complex head-fixed paradigms are still rare for rats and especially for mice. On the other hand, the mouse is the major mammalian genetic model that allows targeting of specific cell types with genetically encoded proteins. These proteins can be used to manipulate and visualize neural activity in subsets of neurons. Combining such specific manipulations and measurements with behavioral paradigms will allow us to pinpoint the contribution of individual cell types to perception and decision-making processes (O'Connor et al., 2009). We, therefore, developed a two-alternative forced choice (2-AFC) task for mice and rats, allowing us to report psychophysical metrics for both species. We have chosen a 2-AFC paradigm because it has clear advantages over Go-NoGo paradigms since it allows a cleaner classification of behavior into correct rejections and

omitted trials on a single-trial basis. Go-NoGo paradigms are more susceptible to biases due to fluctuations of motivation compared with 2-AFC tasks (for review, see (Stüttgen, 2011)).

We found that mice and rats learned to discriminate frequencies that were simultaneously applied to single whiskers on the left and right sides of the muzzle in the head-fixed situation. Furthermore, mice and rats showed similar psychometric curves. Other behavioral readouts, such as reaction times, learning rates, trial omissions, and impulsivity, were also very similar in the two species. Reaction times did not depend on the level of difficulty but were in general higher for error trials. Prior whisking of the animal before stimulus onset decreased the task performance significantly. To our knowledge, this is the first description of a 2-AFC task in head-fixed mice and rats. This paradigm allows precise behavioral control and readouts, which can be combined with techniques that take advantage of genetic tools available in the mouse and starting to become available in rats.

1.3. Methods

Animals

All experimental and surgical procedures were approved by the local veterinary authorities, conforming to the guidelines of the Swiss Animal Protection Law, Veterinary Office, Canton Zürich (Act of Animal Protection 16 December 2005 and Animal Protection Ordinance 23 April 2008). In total, six female adult Sprague-Dawley rats (r1, r2, r3, r4, r5, r6; 250–350 g) and one male and two female adult C57BL/6J mice (m1, m2, m3; 20–26 g) were trained in a 2-AFC task. The animals had to discriminate between two simultaneously presented vibrotactile stimuli in a head-fixed situation. The age of the animals on the day of headpost implantation was 10–15 weeks. The rats were housed in groups of two with food ad libitum, whereas the mice were housed individually with food ad libitum. The animals were subjected to water deprivation for 5 days/wk during the behavioral training. Body weight was monitored prior to each of the two daily training sessions, during which water acted exclusively as a reward. When body weight dropped below 90% of the initial weight, additional water was given after the training session. The animals were housed under an inverted 12:12-h light-dark regime such that they were trained during their dark cycle when they are active.

Surgical procedure

The animals were anesthetized with isoflurane (1–3%; Abbott, North Chicago, IL). The depth of the anesthesia was monitored by both hind paw withdrawal and corneal reflexes. The animal's temperature was monitored with a rectal temperature probe and maintained at 37°C by a feedback-controlled heating pad (Harvard Apparatus, Holliston, MA). The head was fixed in a stereotaxic apparatus, and a local anesthetic (Bucain, 5 mg/ml; Actavis, Steinhausen, Switzerland) was given subcutaneously preceding the scalp incision. Eyes were protected with ointment (vitamin A eye cream; Bausch & Lomb, Zug, Switzerland). For rats, nine titanium cortical screws (Modus 1.5, 3-mm length; Medartis, Basel, Switzerland) were inserted into the cleared skull, acting as anchors for the headcap. The exact positions of these screws have previously been described (Schwarz et al., 2010). Cortical screws were not used in mice. A bonding agent (Gluma Comfort Bond; Heraeus Kulzer, Hanau, Germany) was applied to the cleaned skull and was polymerized with a handheld blue light source (600 mW/cm^2; Demetron LC, Bioggio, Switzerland). The headcap was formed with layers of transparent light-curing dental cement (Tetric EvoFlow; Ivoclar Vivadent, Schaan, Liechtenstein) applied on top of the bonding layer. A screw (M5x15) turned head-down was cemented into the headcap at the midline (2 mm caudal to lambda), and subsequently acted as the post for rat head fixation. In mice, a custom-made aluminum headpost was placed at the same position and connected with dental cement to the underlying bonding layer. After the wound was rinsed with saline, an antibiotic ointment was applied (Cicatrex; Janssen-Cilag, Baar, Switzerland). The open skin was sutured and attached to the implant with acrylic glue (Histoacryl; Braun, Tuttlingen, Germany). After surgery, the animals were kept warm and provided with analgesics (Novaminsulfon, 50%; Sintetica, Mendrisio, Switzerland). In the first week of recovery an antibiotic was added to the drinking water [Baytril (enrofloxacin), 200 mg/l drinking water; Bayer, Leverkusen, Germany].

Behavioral apparatus

In the 2-AFC task used in this study, head-fixed animals had to discriminate between pairs of simultaneously presented vibrotactile single-whisker stimuli (**Fig. 5A**). A custom-made head fixation box was built for this purpose (**Fig. 5B**). The animal was fixed to head rotation mechanics (**Fig. 5A**), which allowed movement in a defined way (maximum ±30° from its initial central head position) when a mechanical brake was released (see **Fig. 5B**,

inset). The head rotation mechanics consist of a brake (**Fig. 5B**, blue), which was moved by a DC motor with a motion controller (rat box: 3564K024B CS, Faulhaber, Schönaich, Germany; mouse box: DC motor 1628T024B and motion controller MCBL-3006-S, Faulhaber) and the help of a knee lever (**Fig. 5B**, green). The headpost holder (**Fig. 5B**, red) is pivoted by a ball bearing. For the prompting procedure, the headpost holder was directly connected to the motor through an additional lever (lever not shown; note: knee lever was detached in this case). This allowed direct setting of the head rotation angle. The tactile stimulus consisted of single whisker deflections generated by a piezo bending actuator (T223-H4CL-303X; Piezo Systems, Woburn, MA). A single whisker was plugged into a glass capillary, which was mounted on the piezo actuator (**Fig. 5A**). The control voltage driving the piezo actuator was generated by a custom-written LabVIEW program (National Instruments, Austin, TX) using a multifunctional data acquisition card (PCI-6259; National Instruments) and was amplified by a piezo controller (MDT693A; Thorlabs, Newton, NJ). The stimulator system was attached to an articulated arm (Baitella, Zürich, Switzerland) to allow precise and rapid positioning of the stimulator. Movement of the stimulator was calibrated with a laser displacement sensor (0.1-µm resolution at 2.5-k Hz sampling rate, ILD17002; Micro-Epsilon, Ortenburg, Germany) and strain gauge sensors mounted directly on the piezo element. The vibrotactile stimulus consisted of a series of deflections to a single whisker on the animal's left and right whisker pads. The C1 whisker was stimulated in all animals except for m2, in which the gamma whisker was stimulated. The peak velocity of a prototype pulse (taken from a single-period 120 Hz cosine wave) was kept constant, and the repetition rate of pulses was varied randomly from 10 to 80 Hz in steps of 10 Hz for the distractor stimulus (unrewarded side) and kept constant at 90 Hz for the target stimulus (rewarded side) (**Fig. 5C**). The stimulus duration was 1 s. The peak velocity was 1,296°/s for both rats and mice. The stimulator was placed 10 mm away from the whisker pad for the rats and 4 away for the mice. In the beginning, training sessions were done without whisker trimming. Subsequently, only the stimulated whisker on each side was kept untrimmed. At least once every 2 weeks, the animals were lightly anesthetized (isoflurane) to trim down the whiskers that were not stimulated (to a length of 15 mm for the rats, and 5 mm for the mice). Additionally, in four animals (r1, r2, r3, and r4) the left C2 whisker was elongated with a light polyimide tube (diameter: 250 µm; length: 2–2.5 cm; weight: ~0.7 mg) such that it covered the hair 3–5 mm from its origin to its free end. The C2 whisker position was quantitatively recorded with a

laser curtain and a linear CCD array (RX 03; Metralight, San Mateo, CA) with a resolution of 3.5 µm in space and a 2.5-k Hz sampling rate (Hentschke, 2005). The behavioral apparatus was placed in a light- and soundproof box.

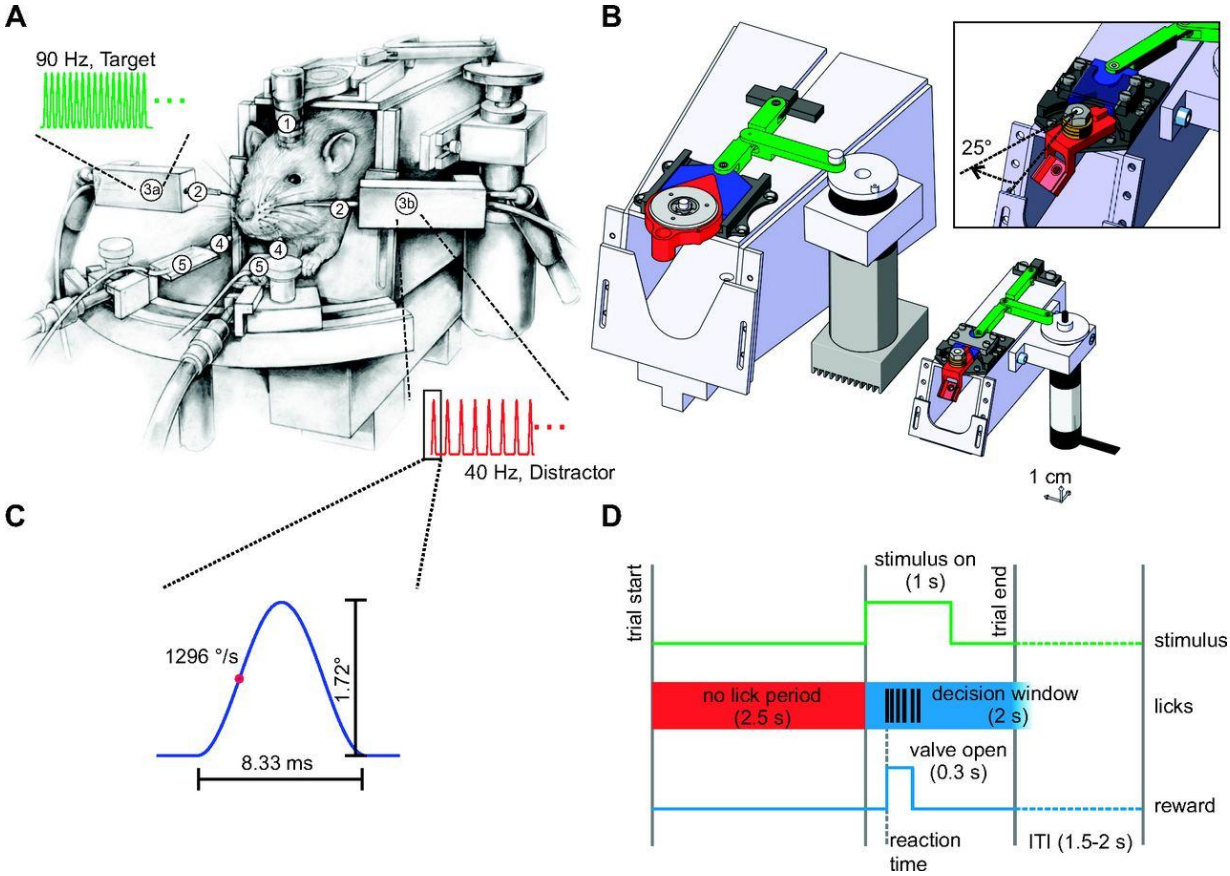

Figure 5. Setup, paradigm, head rotation mechanics, and stimulus.

A. Schematic representation of a rat in the behavioral apparatus that is connected to the rotation mechanics via an implanted headpost (1). A single whisker is inserted into a glass tube (2) that is glued to a piezo actuator (3a, 3b) used to simultaneously deliver the vibration stimuli, e.g., 90 Hz (3a) as target and 40 Hz (3b) as a distractor. The water reward is delivered with 2 waterspouts (4), which are mounted on a semicircular rail in front of the animal and equipped with piezo lick sensors (5). **B.** CAD renderings of the rat (left) and the mouse (right) behavioral apparatus. Inset: mouse apparatus with an opened head rotation brake. The head rotation mechanics consist of a brake (blue part), which is moved by a DC motor with the help of a knee lever (green part). The headpost holder (red part) is pivoted by a ball bearing. For the prompting procedure, the headpost holder was directly connected to the motor through an additional lever (lever not shown; note: knee lever was detached in this case). This allowed direct setting of the rotation angle. **C., D**.: Schematic representation of a single stimulus pulse (**C**) and the time sequence of an individual trial (**D**).

Auditory masking noise (80dB white noise) was presented with a loudspeaker located 10 cm above the animal's head to prevent auditory cues. CMOS cameras with infrared illumination were used to monitor the animal's whiskers to ensure that they stayed in the glass capillary of the stimulator for the entire session. Two drinking spouts (**Fig. 5A**) were placed on the left and right sides of the animal's head in a way that they could only be reached while the head rotation brake was released. After 5–10 weeks of initial training, the angle of the two spouts was gradually reduced such that the animals could reach them from a fixed center position. Licking was detected with piezo sensors (**Fig. 5A**) mounted on the waterspouts (LDT0028K; Measurement Specialties, Hampton, VA). Two solenoid valves (Bürkert, Ingelfingen, Germany) were used to control the water delivery to the drinking spouts. All the components of the behavioral apparatus were controlled and monitored with millisecond temporal precision by a custom-written LabVIEW program (National Instruments) running on personal computers using multifunctional data acquisition cards (PCI-6259; National Instruments).

Behavioral paradigm

Handling of the animals started after 2 weeks of recovery from the headcap implantation (**Fig. 6**). The animals were water deprived 24 h before the head fixation training started. Animals were slowly familiarized with the experimenter in two or three daily sessions lasting roughly 10 min for 1–2 weeks. In the following 2–3 weeks, the animals were trained to tolerate head fixation. Water was given manually from a syringe in the head fixation training. As soon as the animal tolerated the head-fixed situation for up to 10 min without any signs of stress, the animal was placed into the behavior setup. A drinking spout was placed in front of the animal's snout. In the first three sessions, water was given every 5–6 s. Later, the animal had to first lick once and then a couple of water drops were delivered through the drinking spout (referred to as the “reward on lick” mode). In the next step, the procedural training started (Schwarz et al., 2010). The rodents were subjected to a prompting procedure (6–15 sessions) to establish an association of the vibrotactile stimulus location with the reward location. The 90 Hz target stimulus was presented without a distractor stimulus, and the animal's head was gently turned by the motorized system to the

stimulus side, where water was delivered via the spout. After about two sessions, the "reward on lick" mode was turned on as soon as the animal started licking without waiting to sense water coming from the correct spout. Next, actual behavior measurements started and the animal's performance was recorded. The animal had to turn its head to reach the reward location. First, rats and mice had to detect the side of the 90 Hz target stimulus. When they reached a stable performance (rats: ∼18 sessions; mice: ∼11 sessions), gradually more difficult distractor stimuli (10 to 80 Hz pulse trains in steps of 10 Hz) were introduced, and they had to discriminate the higher frequency (90 Hz pulse train target stimulus) from the lower frequency. The distractor and the rewarded target stimuli were presented simultaneously on both sides (**Fig. 5D**). To preserve the animal's motivation, more difficult distractor stimuli (40–80 Hz) were always intermingled with less difficult ones (10–30 Hz). In the initial training phase, the head rotation brake was released 0–0.2 s after stimulus onset. After an additional waiting time of 0–0.2 s, the animal was given a 2-s-long window of opportunity (**Fig. 5D**) to respond with a lick at one of the two waterspouts. The animal could turn its head to the left and right sides, reaching the drinking spout with its tongue to report the perceived target stimulus side. Correct choices led to water delivery (rats: 20–50 µl/trial; mice: 5–20 µl/trial). During the aforementioned window of opportunity, a lick at the incorrect waterspout (distractor side; not rewarded) or no-lick response for 2 s after stimulus onset led to a closure of the head rotation mechanics, bringing the rodent back to the center position. Initiation of the next trial was preceded by a randomly varied intertrial interval (ITI, 1.5 ± 0.3 s; **Fig. 5D**). Lick events in a 2.5-s-long prestimulus time window (no-lick period; **Fig. 5D**) were punished with a temporal delay (1–2.5 s) of the stimulus presentation. A temporal jitter of maximal ±30% was added to the no-lick period to avoid prediction of the stimulus onset. In the learning phase, a bias correction algorithm was used to avoid stereotypical response biases (Knutsen, 2006), thus preventing the animals from developing a preference to one side and acting against stereotypic licking such as left-right alternation. When the animals reached a stable performance and unimpulsive behavior, both the head rotation angle and the angle of the waterspouts were gradually narrowed until the brake remained closed (time span over 1–2 week(s)). The rats performed up to 400 trials per session, and the mice up to 380 trials per session. Two sessions per day were conducted, one in the morning and one in the evening.

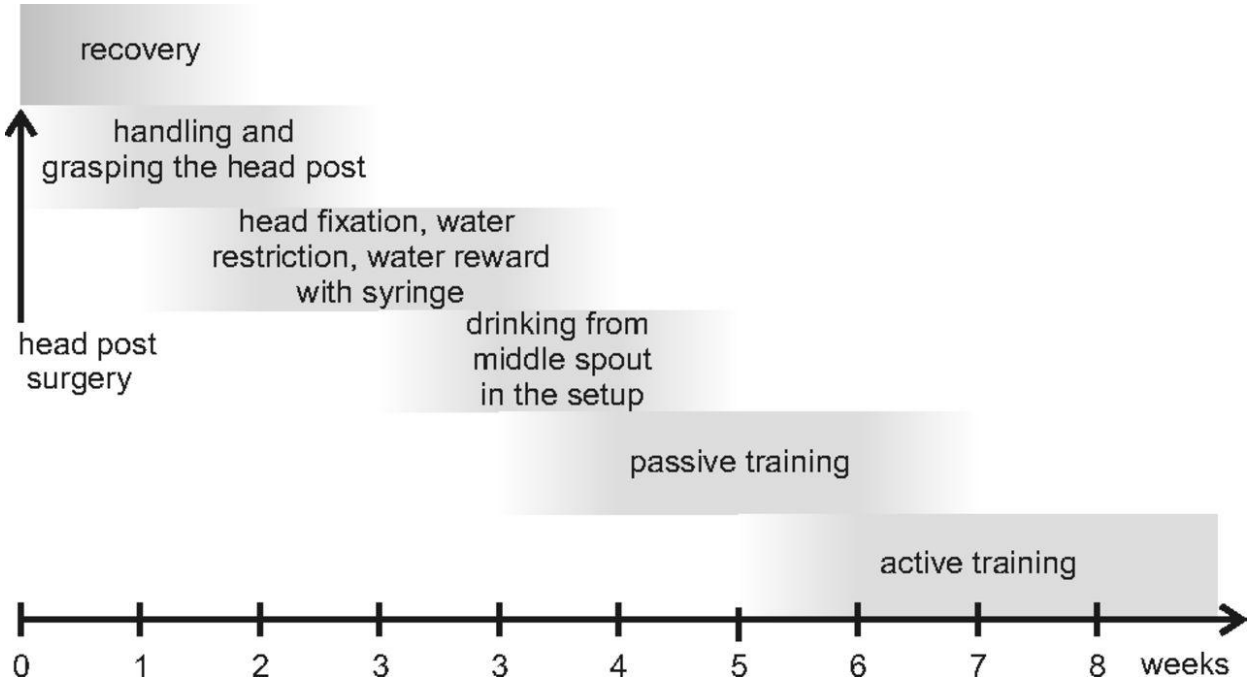

Figure 6. Training procedure.

The different training phases are shown, starting with the headpost surgery through to the acquisition of the psychometric curves. Gray shadings indicate that the duration of the individual phases adapted for each animal.

Data analysis

The data set consisted of behavioral recordings from six rats (r1, r2, r3, r4, r5, r6) and three mice (m1, m2, m3). There was no significant difference in performance between the morning and evening sessions (data not shown). A trial was counted as a correct response when the animal licked at the rewarded spout first. An error was counted when the animal licked at the unrewarded spout first. A no-lick response within the 2 s time window after the start of the decision period was classified as a missed trial. To compute the performance, only trials with a behavioral response were taken into account (correct response and error): correct responses/(correct responses + errors). To analyze whisker position traces, whisker velocity was computed by taking the first derivative of the low-pass filtered (Butterworth 4th order, cutoff frequency 200 Hz) whisker movement recording. For each trial, the root mean square (RMS) velocity was computed in the prestimulus period from −200ms to stimulus onset. If prestimulus RMS velocity exceeded a threshold of 0.02 m/s, the trial was classified

as a movement trial; otherwise, it was classified as a non-movement trial (as in (Hentschke, 2005)). To test whether behavioral performance was different in movement versus non-movement trials, a fourfold χ^2-test was done. All data analysis was performed with MATLAB (MathWorks, Natick, MA).

Psychophysics

A psychometric curve was obtained by computing the performance for each stimulus pair and plotting it against the difference between distractor and rewarded frequency. The confidence intervals were calculated based on a binomial distribution with a confidence level of 95%. Psychometric functions were fitted with the software package psignifit (version 2.5.6; see http://bootstrap-software.org/psignifit/), which implements the maximum-likelihood method described by (Wichmann and Hill, 2001). A logistic function

$$\Psi(x;\alpha,\beta,\gamma,\lambda)=\gamma+(1-\gamma-\lambda)F(x;\alpha,\beta)$$

where

$$F(x;\alpha,\beta)=1/(1+\exp[(\alpha-x)/\beta]$$

was fitted (fit parameters: α, β, γ, λ; γ fixed to 0.5 and λ constrained between [0 0.2]) to the data points and used to obtain the discrimination threshold and slopes. The discrimination threshold (DTh) was defined as the frequency difference between distractor and target frequency at which the logistic fit reached 50% of its cumulative value. This value was used to compute an additional measure of sensitivity, the Weber fraction: DTh/90 Hz. For the psychometric curves, only the last 270–300 trials (20–40 sessions) in each category were considered. For r5, r6, r1, r3, m1, and m2, the frequency range from 10 to 80 Hz in steps of 10 Hz was sampled. A reduced set of distractor frequencies was presented to r2, r4, and m3 (r2 and r4: 0 Hz, 10 Hz, 40 Hz, 60 Hz, and 80 Hz; m3: 0 Hz, 10 Hz, 20 Hz, 40 Hz, and 60 Hz). Peak performance of each animal was determined at a 10 Hz distractor frequency and with no distractor present. The learning curves were generated and quantified by analyzing the performance over sessions in trials with no distractor frequency. A cumulative Weibull function was fitted to the mean performance over sessions (first 60 sessions, r1, r2, r3, r4, m1, m2) except for m3, as this mouse reached stable performance within the first session after the prompting procedure. The dynamic phase of learning was defined as the range between the first and ninth decile ordinate values of the fitted cumulative Weibull function. The performance stability was computed by taking the standard deviation of the session

performance during detection (0 Hz distractor frequency) over the last 60 sessions. Reaction times were defined as the time span between stimulus onset and first lick response and were estimated by the median of the first lick latencies of the trials (same data set as for the psychophysics). Latencies were measured in 10 ms bins and used to construct cumulative plots on a probit scale with a reciprocal time axis (Carpenter and Williams, 1995). The median first lick latency was the interception of the 50% ordinate value with the cumulative lick count distribution. The relative reaction time difference between error trial ($time_{error}$) and correct trial ($time_{correct}$) was computed per session (i = 1, 2, 3, … N) and averaged over sessions:

$$\text{reaction time} = 2/N \sum i(\text{timeerror}(i) - \text{timecorrect}(i))/(\text{timeerror}(i) + \text{timecorrect}(i)).$$

This relative value was computed to compensate for session-to-session variability over weeks. In addition, only trials with a first lick emission 200ms after stimulus onset were considered. The influence of session number on the reaction time was tested with the Kruskal-Wallis test. The significance of a behavioral response was tested by the Wilcoxon signed-rank test. The average number of trials in which an early lick was detected served as a measure for impulsivity and represented the average number of trials in which a lick was emitted within the no-lick period. This value was taken as zero when there were no early licks before the stimulus onset. A value of 10% denoted that the animal did an early lick on average every tenth trial. For each frequency, the percentage of missed trials was computed and statistically tested with the Kruskal-Wallis test. To facilitate the comparison between different animals, the curves were normalized to mean value over all stimulus categories. A control session for each of the animals was performed to rule out the use of auditory cues in the discrimination task. In the first half of the session, the animal had to discriminate between 90 Hz and no distractor frequency or an 80 Hz frequency difference between the distractor and the target frequency. In the second half of the session. the whiskers on both sides were unplugged from the whisker stimulator, and the animal had to continue without mechanical stimulation. It was ensured that the stimulators were as close to the head as in the normal stimulus situation but without touching any whisker. The influence of the bias correction was measured by comparing the percentage correct of the left and right sides with each other, |% correct left side − % correct right side|/(% correct left side + % correct right side), for each session, and testing the first 15 sessions against the last 15 sessions with bias correction switched on.

Statistics

Statistical errors are SE of the mean unless noted otherwise. For binary values a binomial distribution was used to compute the 95% confidence intervals. The Kruskal-Wallis test, the Wilcoxon signed-rank test, and the χ^2-test (MATLAB implementations) were used for statistical analyses.

1.4. Results

Training procedure

All animals entering procedural training reached the frequency discrimination training after 7–10 weeks of training with two daily sessions (**Fig. 6**). Slow adaptation to the head fixation and regular daily training (5 days/wk) were essential for good performance (data not shown; see (Schwarz et al., 2010)). The criterion to enter discriminative training was that the animals accepted drinking water from a syringe in the head-fixed condition. The animals that required more handling sessions to reach this criterion did not perform worse than the animals that adapted more rapidly (e.g., m1 9.7week: 96% and 222 trials/session compared with m2 7.5week: 93% and 228 trials/session). The mice adapted to the head fixation and behavioral apparatus in a time frame similar to the rats [rats (r1, r2, r3, r4): 3week; mice (m1, m2, m3): 2.5week].

Discriminative training

The discriminative training started with a prompting procedure, in which the animal's head was gently turned to the side where the stimulus was presented (passive training; **Fig. 6**). The motorized head rotation mechanics allowed well-controlled direction of the animal's head to the rewarded waterspout during the presentation of the vibrotactile stimulus. This helps the animal to establish an association between stimulus and reward location, but may not be necessary for the animal to learn the task. The rewarded frequency (90 Hz pulse train, 1-s duration; **Fig. 5C**) without a distractor was presented (detection paradigm). The rats only needed six sessions (~500 trials) to establish an association between stimulus and reward location. A lick response to the side of the target stimulus presentation was taken as a criterion for the association. The mice needed 11 sessions for this step (~1,600 trials). After the passive training, the animals had to indicate their decision by turning the head to the

reward location to collect the water. In the first sessions, water was given automatically without an initial lick to the spout. During the early phase of training, the animals performed a detection task without any distractor stimulus. After the animals had reached a stable performance in the detection paradigm (rats: ∼18 sessions, mice: ∼11 sessions of active training), task complexity was increased by introducing distractor frequencies in the paradigm. The animals were trained to discriminate between the rewarded 90 Hz stimulus and the simultaneously presented unrewarded distractors ranging from a 10 to 80 Hz (in 10 Hz steps) frequency difference. The animals performed several hundred trials per session, twice a day. The average median number of trials per session was 202 ± 18 (rats) and 231 ± 6 (mice).

Psychophysics

Fig. 7 shows the psychometric curves computed from 20–40 sessions for each of the nine animals. For each stimulus category, only the last 270–300 presented trials were considered, thus excluding the initial learning phase (**Fig. 7, A–E**). For each animal, a logistic function was fitted to the stimulus pair performance values to obtain the thresholds and slopes in the transition region of the psychometric curve (see methods). The best-performing rat (r6, not shown separately) had a discriminative threshold of 42.0 Hz frequency difference [95% confidence interval (CI95): 38.8–45.1 Hz] and a slope of 2.32 ± 0.50%/ Hz. The highest threshold for the rats (r4) was 71.9- Hz frequency difference (CI95: 69.5–76.7 Hz). The population mean of the thresholds of all six rats was 53.0 ± 4.4- Hz frequency difference. Peak performance in one animal (rat r3; **Fig. 7B**) for the least difficult discriminative category (80 Hz distractor to target frequency difference) went up to 93.0% (CI95: 90.3–96.0%) (group mean: 84.1 ± 2.5%) and for the detection up to 97.3% (CI95: 95.3–99.0%) (group mean: 93.0 ± 1.2%). In the three mice, the psychometric curves showed similar characteristics. Peak performance for discriminating a distractor to target frequency with a difference of 80 Hz reached 93.0% (CI95: 90.0–95.7%) for the first mouse (m1; **Fig. 7C**) and 85.0% (CI95: 81.0–89.0%) for the second (m2; **Fig. 7D**). The mean for three mice was 85.0 ± 5.6%. In the detection task, a performance of 96.0% (CI95: 98.0–93.7%) for the first mouse (m1) and 87.7% (CI95: 84.0–91.4%) for the second mouse (m2) was reached (group mean: 89.7 ± 3.2%). The discriminative threshold was 49.4- Hz frequency difference (CI95: 48.1–51.9 Hz) for m1 and 48.5- Hz frequency difference (CI95: 42.5–56.2 Hz) for m2 (group

mean: 50.6 ± 1.7 Hz frequency difference). In summary, rats and mice displayed very similar psychometric measures. The discrimination threshold averaged over three mice was 50.6 ± 1.7 Hz frequency difference compared with a mean of 53.0 ± 4.4 Hz frequency difference for all six rats. These values correspond to Weber fractions of 0.56 ± 0.02 and 0.58 ± 0.04, respectively. The peak performance for the detection task was 93.0 ± 1.2% for the rats and 89.7 ± 3.2% for the mice. The slope of the psychometric curve in the transition regime, which captures the sensitivity fluctuation of the sensory process, was 2.00 ± 0.25%/ Hz and 1.82 ± 0.36%/ Hz for rats and mice, respectively. Note that an ideal sensory process would have a step function as a psychometric curve and therefore a high slope value at the threshold, e.g., 5%/ Hz and above. For each animal, at least one control session was recorded to ensure that the animal was exclusively using the vibrotactile whisker stimulus for making the decision (**Fig. 7F**). In the first half of the control session, the animal was in the normal situation with a single whisker stimulated on each side. In the second half of the session, the whiskers were unplugged from the stimulator. The stimulator was placed as close as possible to the animal's head without touching the whiskers. All the animals performed above chance level in the first half of the control session [binomial test of performance against chance level, P value < 0.01 for all rats (n = 6) and mice (n = 3)]. As soon as the stimulators were detached from the whiskers, the performance dropped to chance level (binomial test of performance against chance level, P value > 0.05 for all animals).

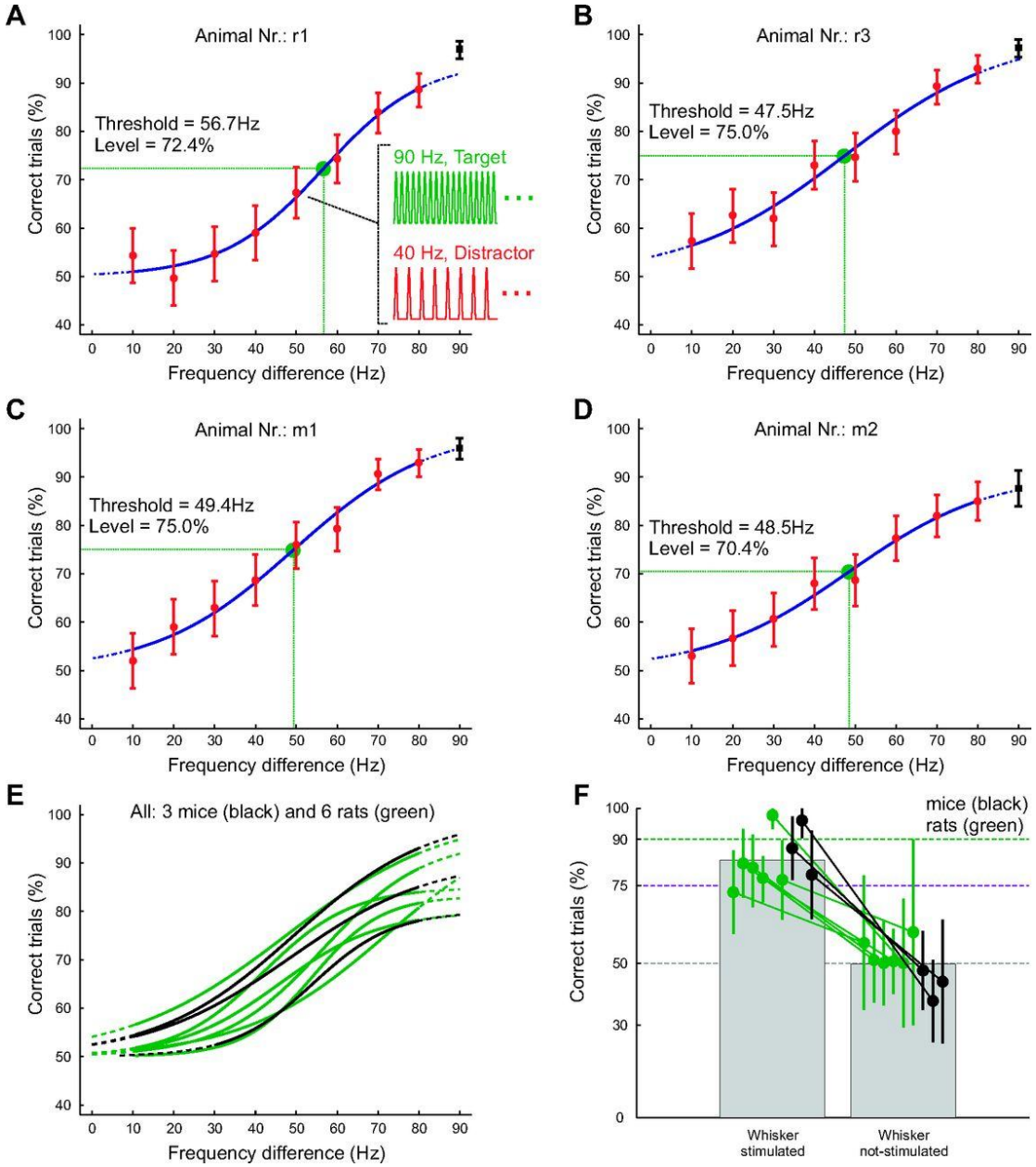

Figure 7. Psychophysical performance—performance over the difference between distractor and target frequency (90 Hz).

A–D. Psychometric curves of single animals (rats r1, r3; mice m1, m2) with logistic fits (blue) and thresholds (green). The detection performance is shown as a black square symbol at a 90 Hz difference, and was not used for the fitting procedure. Inset in A shows the stimulus pair close to the threshold regime for the 50 Hz frequency difference data point (90 Hz target and 40 Hz distractor). **E.** Psychometric curve fits from all animals. **F**. Control session for all 9 animals. The first half of the training session was performed with normal stimulation (whisker attached to the piezo stimulator), where all animals performed above chance (P <

0.05). In the second half of the training session, the stimulators were retracted from the whiskers (no mechanical contact). The performance of correct trials dropped to the chance level for all animals when the stimulators were retracted ($P < 0.05$). Error bars are plotted as 95% confidence intervals.

Learning and behavioral performance stability

To characterize the learning phase, a cumulative Weibull function was fitted to the mean performance of the detection paradigm over sessions (**Fig. 8**). The dynamic range where most of the performance change was observed was characterized as the range between the first and the ninth decile of a fitted cumulative Weibull function (**Fig. 8**, insets). The first session after the dynamic learning phase was chosen as a criterion for reaching stable performance. Rats r1, r2, r3, and r4 could perform the detection task (90 Hz target frequency and no distractor frequency) within 18.2 ± 9.0 sessions (2,256 ± 1,373 trials, 1.8 weeks; **Fig. 8**. **A** and **B**), while the mice needed 16.5 ± 10.8 sessions (1,312 ± 835 trials, 1.7 weeks; **Fig. 8**. **C** and **D**) to reach the criterion. The dynamic learning phase varied across the animals and was 30.9 sessions (mouse m1), 1.2 sessions (mouse m2), 12.2 sessions (rat r1), and 11.0 sessions (rat r3) long. The animals showed session-to-session variability but never dropped to chance level after the dynamic learning phase. To quantify the performance stability over days, the standard deviation was computed over the last 60 sessions of the data set shown. The mean variability was 5.6 ± 0.25% for the rats (r1, r2, r3, r4) and 3.9 ± 0.26% for the mice (m1, m2, m3), demonstrating that rats and mice had comparable levels of performance variability in the 2-AFC discrimination task.

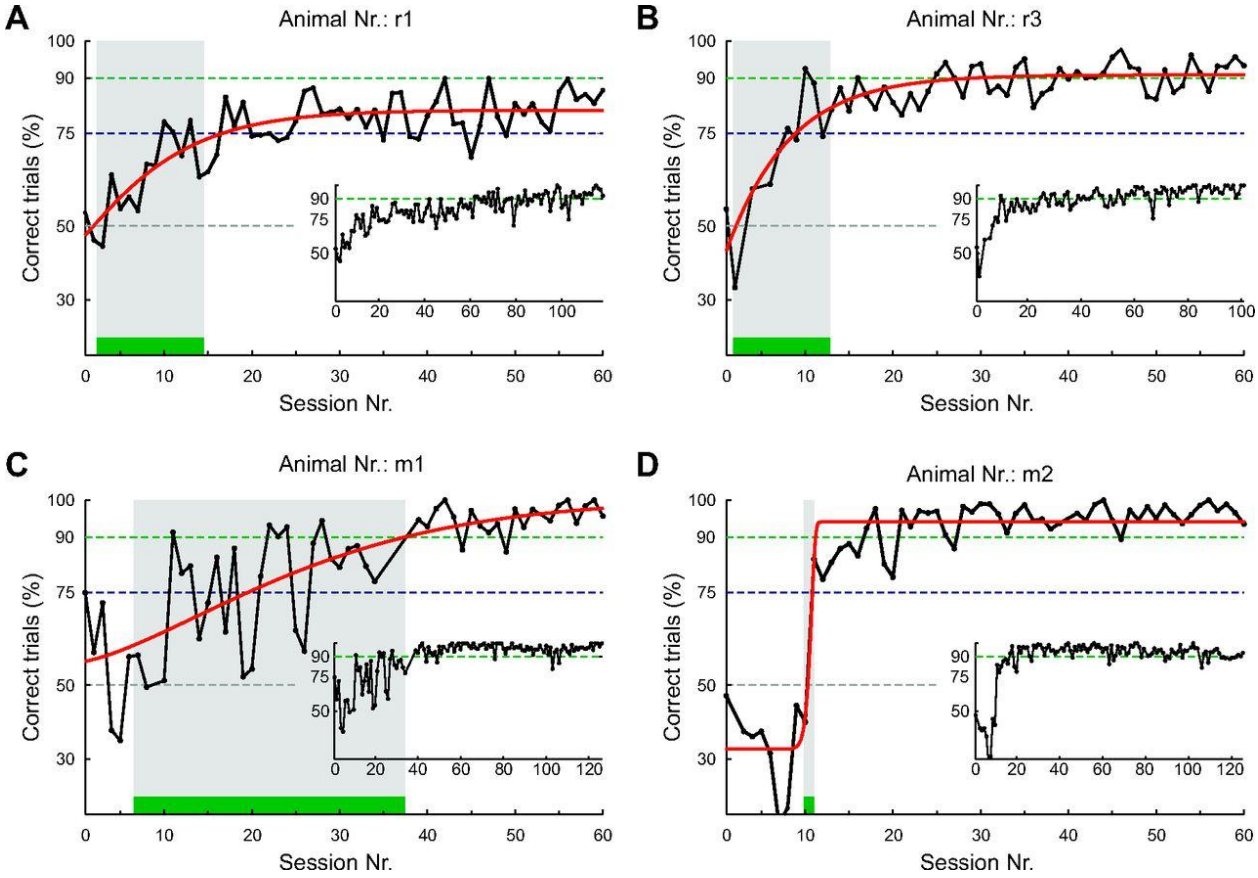

Figure 8. Learning and stability—performance in detection paradigm over initial learning phase and period of stable behavioral performance.

A–D. Performance over time for the detection stimuli for 4 of the animals (rats r1, r3; mice m1, m2). Insets show the initial learning phase, which was fitted with a Weibull function. Gray-shaded areas show the dynamic learning phase.

Reaction times

In **Fig. 9** the distribution and analysis of the first lick latencies for behavioral (error and correct) and different stimulus (easy and difficult) categories are shown. The time span between the stimulus onset and the first lick detected was used to compute the reaction time of the animals. These measurements were performed when the animals were not allowed to rotate their heads. The head rotation mechanism brake was kept closed during the whole session, and the rodents solely indicated their decision by licking one of the two reachable waterspouts. To depict the stochastic distribution of the reaction times (first lick event), the cumulative probability is plotted on a probit scale as a function of reciprocal

latency (reciprobit lick histogram in **Fig. 9A**) (Carpenter and Williams, 1995). The median first lick latency is the interception of the 50% ordinate value with the cumulative lick count distribution. The shortest median reaction time was 232 ± 3ms for the rats and 337 ± 3ms for the mice. The average of all rats was 334 ± 49ms and for all mice was 486 ± 120ms. A straight line in this type of diagram denotes that the underlying distribution has a Gaussian-like shape. All the curves are composed of two almost linear components, one with a shallow inclination and the other with a steep inclination. The reaction time curves, shown in **Fig. 9A,** have a similar form to saccadic eye latency distributions, where subjects had to do a saccade from a central fixation point to a target on the left or right (Carpenter and Williams, 1995). Note **Fig. 9**, inset, where similar numbers of counts in the correct and error conditions occurred in the early phase and the form of correct and error distributions in the late phase look similar, suggesting two underlying processes for the observed distribution. Nevertheless, all the animals except one showed a significantly longer reaction times for error trials compared with correct trials (Wilcoxon signed-rank test P values < 0.05 for 6 rats and 2 mice; **Fig. 9B**). The reaction time difference between the error and correct trials was computed for each session and averaged over sessions (**Fig. 9B**). This step was necessary to compensate for session-to-session variability (Kruskal-Wallis test, $P < 0.001$, indicating session dependence). **Fig. 9B**, inset, shows example raw reaction times for the error and correct conditions and the resulting relative reaction time over sessions. Except for one animal, we did not observe a significant difference in reaction times depending on the level of difficulty (i.e., distractor frequency).

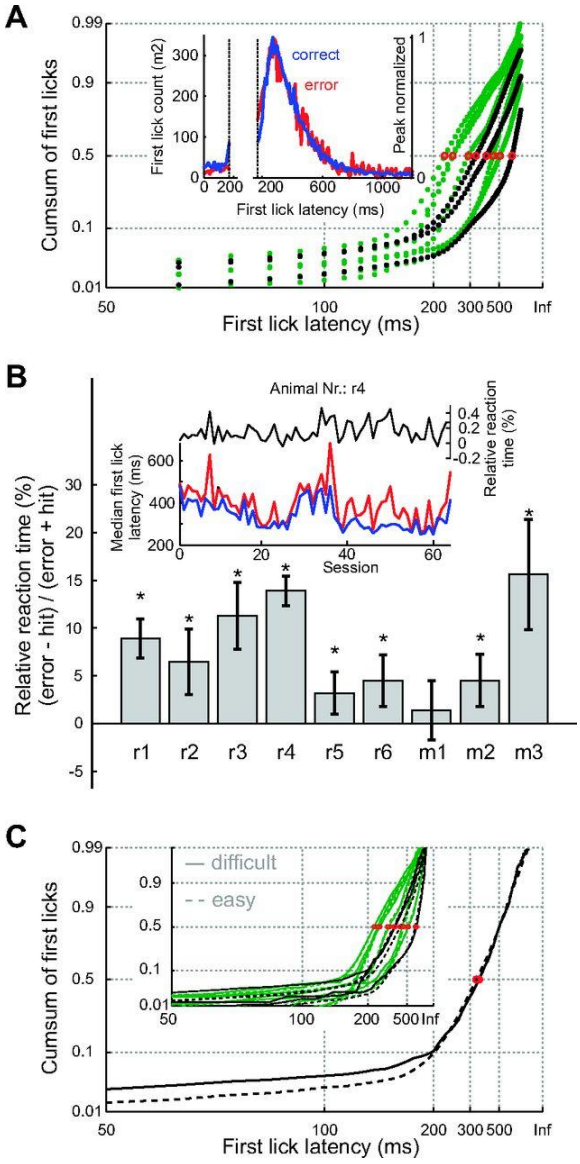

Figure 9. Reaction times—distribution and analysis of the first lick latencies for behavioral (error and correct) and different stimulus categories (easy and difficult) for all animals.

A. Cumulative first lick latency count for the different animals (rats r5, r6, r1, r2, r3, r4 in green; mice m1, m2, m3 in black) with a probit scale as a function of reciprocal latency. Red dots depict the median first lick latency, corresponding to the interceptions of the 50% ordinate value with the cumulative lick count distributions. The inset shows the first lick histogram for m2 for correct and error trials. The second part (>180ms) was normalized to the peak of the histograms to highlight the similar form of the distributions. **B**. % of the median reaction time of error trials relative to correct trials. *Significance level $P < 0.05$ ($n = 9$). The inset shows raw median reaction times for error and correct trials and the resulting relative reaction times over sessions. **C**. Same plot as in A but split into easy (0–40 Hz

distractor) and more difficult (50–80 Hz distractor) stimulus pairs for mouse m2. The inset shows an overview of all animals (mice in black and rats in green). Solid lines correspond to the difficult category and dashed lines to the easy category.

The comparison of difficult (50 to 80 Hz distractor frequency) to less difficult (0 to 40 Hz distractor frequency) stimulus pairs in the first part of the reciprobit lick histogram (20–100ms; **Fig. 9C**) for correct trials revealed no significant differences in the distribution in all but one animal (Kolmogorov-Smirnov test, $P < 0.01$ for 1 rat). This finding suggests that the underlying process for the lick responses in the 20–100ms time window is independent of the level of difficulty, and may reflect impulsive behavior. Analyzing only those trials in which the animal responded in the 20–100ms time window after stimulus onset showed that, except for two animals, the performance of correct trials never exceeded chance level (binomial test, $P < 0.05$ for 1 rat and 1 mouse).

Impulsive behavior and motivation

To address the questions of how much impulsive behavior and motivation vary over different animals or species, the percentage of early licks and misses are plotted in **Fig. 10**. One of the major advantages of a 2-AFC paradigm is that correct rejections can be distinguished from omitted trials (e.g., lack of motivation) on a single-trial basis in contrast to a Go-NoGo paradigm. However, it is essential that the animals do not develop a response bias in the 2-AFC task (e.g., positional bias). This can be avoided by training the animals with a bias correction algorithm in the learning phase (see methods). Comparing the early phase with the late phase of the training with bias correction switched on, four of nine animals had significantly less response bias to one side (see methods, Kruskal-Wallis test, $P < 0.05$). The response bias was quantized as the absolute value of % correct on the left side minus % correct on the right side divided by the sum of both (r1 from 0.144 ± 0.044 to 0.052 ± 0.008, r2 from 0.138 ± 0.028 to 0.052 ± 0.014, r3 from 0.226 ± 0.069 to 0.076 ± 0.011, r4 from 0.087 ± 0.017 to 0.083 ± 0.015, r5 from 0.035 ± 0.006 to 0.048 ± 0.011, r6 from 0.048 ± 0.010 to 0.036 ± 0.007, m1 from 0.131 ± 0.023 to 0.065 ± 0.0151, m2 from 0.214 ± 0.052 to 0.050 ± 0.01, m3 from 0.053 ± 0.011 to 0.049 ± 0.009). To characterize the impulsive behavior, the licks before stimulus presentations were measured and classified as early licks in the situation where the animals were not allowed to rotate their heads and solely indicated their

decision by licking one of the two waterspouts. This impulsive licking behavior can be completely abolished if the head rotation brake is released and the animal can only reach the waterspouts by rotating its head. Nevertheless, impulsive behavior could be quite different across species. Thus, licking behavior where the head rotation brake was closed was measured. The early lick count represents the average number of trials in which a lick occurred before the actual stimulus presentation (**Fig. 10A**). Note that in the case of an early lick, the stimulus presentation was shifted backward, so that each stimulus was preceded by a "lick-free" period (**Fig. 5D**). The average value number of trials with early licks over the last sessions (same data set as for the psychophysics) was 19.3 ± 2.5% for rats and 22.1 ± 7.7% for mice. These almost identical early lick counts for rats and mice indicate that the species are highly comparable in terms of impulsivity. It is worth mentioning that the task design allowed chance performance only if the animal licked irrespective of the stimulus side. As shown in the reciprobit plots in **Fig. 9A**, only a small fraction of licks occurred at very short latencies (<100ms), and these lick time points appear to originate from a different behavioral process reflected in a separate distribution compared with the majority of the responses (linear fits in **Fig. 9C**).

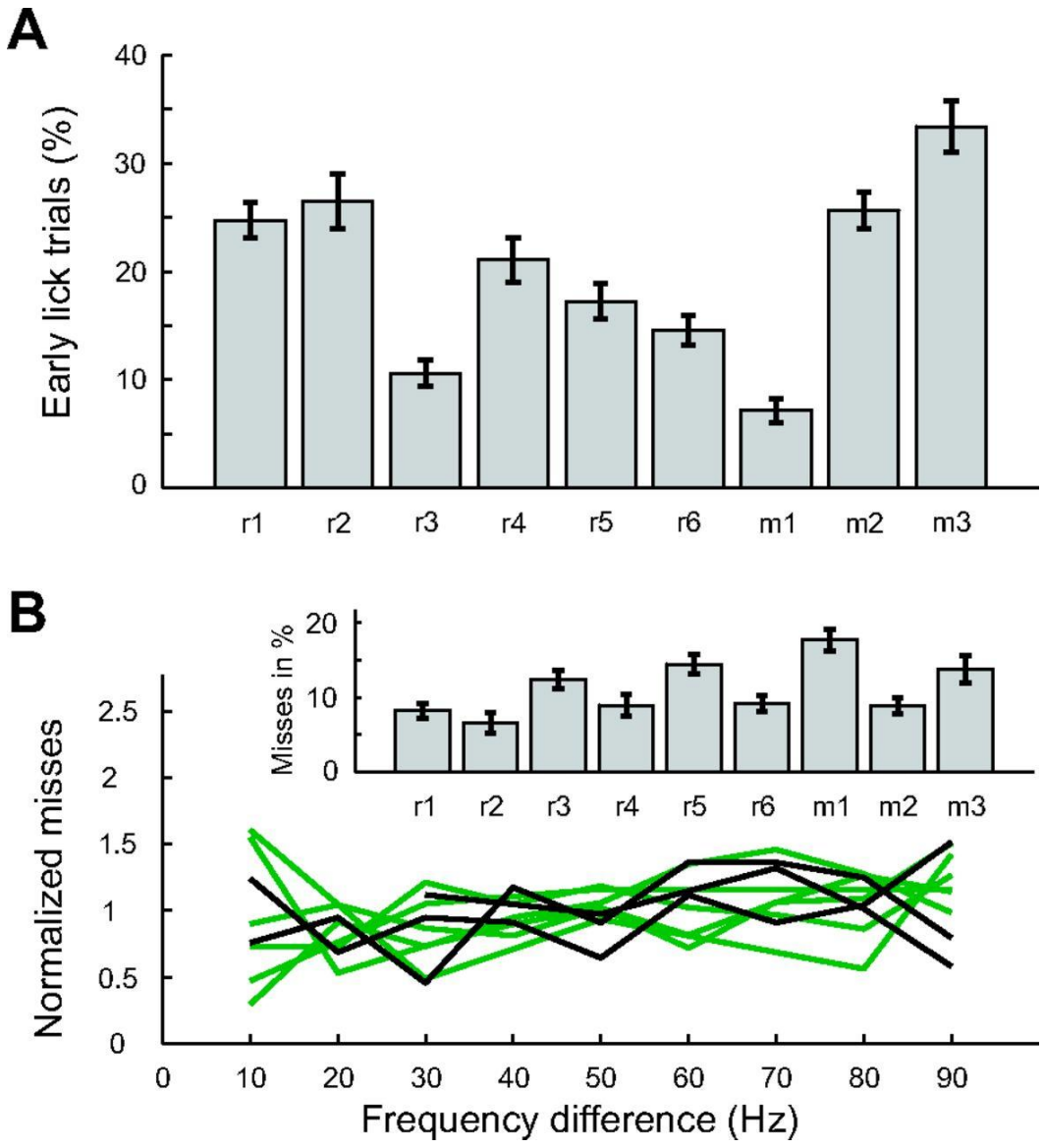

Figure 10. Impulsivity and missed trials—% of early lick trials and missed trials are similar for rats and mice.

A. The average number of early lick trials expressed in % for all animals (n = 9). **B**. % of missed trials over frequencies normalized to the mean over all frequencies (rats in green, mice in black). The inset shows the mean values for the corresponding animals (n = 9).

Does the level of difficulty influence the number of trials without a response? The average numbers of omitted trials over all distractor frequencies are shown in **Fig. 10B**. To compare between animals, the values were normalized to the mean over all frequencies. Of each session, only the first 30 omitted trials were taken, thus avoiding a dominance of omitted trials usually occurring at the end of a session when the animal is not engaged in the

task anymore. The mean values for each animal are shown in **Fig. 10B**, inset. There was no significant effect of the distractor frequency on the number of omitted trials in eight animals (Kruskal-Wallis test P values: m1 0.080, m2 0.223, m3 0.429, r5 0.358, r6 0.063, r1 0.287, r2 0.455, r3 0.114, r4 0.016).

Whisker movements and behavioral performance

To clarify whether whisker motion has an impact on the psychometrics measured during the bilateral frequency discrimination paradigm, the position of one whisker (C2) was tracked with a linear CCD sensor (**Fig. 11A**) in four rats. The measured RMS velocity of this whisker was used for classifying trials in non-movement and movement trials (**Fig. 11B**). About 9% of all trials (r1: 15.44% of 3,095 trials; r2: 6.76% of 6,095 trials; r3: 10.68% of 7,807 trials; r4: 5.15% of 6,022 trials) were classified as movement trials. Comparing these two categories showed that trials with motion had a significantly reduced discrimination performance (χ^2-test, $P < 0.01$). The mean performance for all four animals was 70.01% (CI95: 67.88–72.09%) in movement trials and 73.93% (CI95: 73.28–74.59%) in non-movement trials. When only detection trials were considered, a larger effect was observed (movement: 71.79%, CI95: 61.53–82.05%; non-movement: 89.62%, CI95: 87.15–92.09%), which is in line with the study of (Ollerenshaw et al., 2012). At the discrimination threshold (50 Hz frequency difference) a similar trend was present, but no significance was reached (movement: 48.00%, CI95: 28.00–68.00%; non-movement: 59.29%, CI95: 52.65–65.93%; **Fig. 11C**).

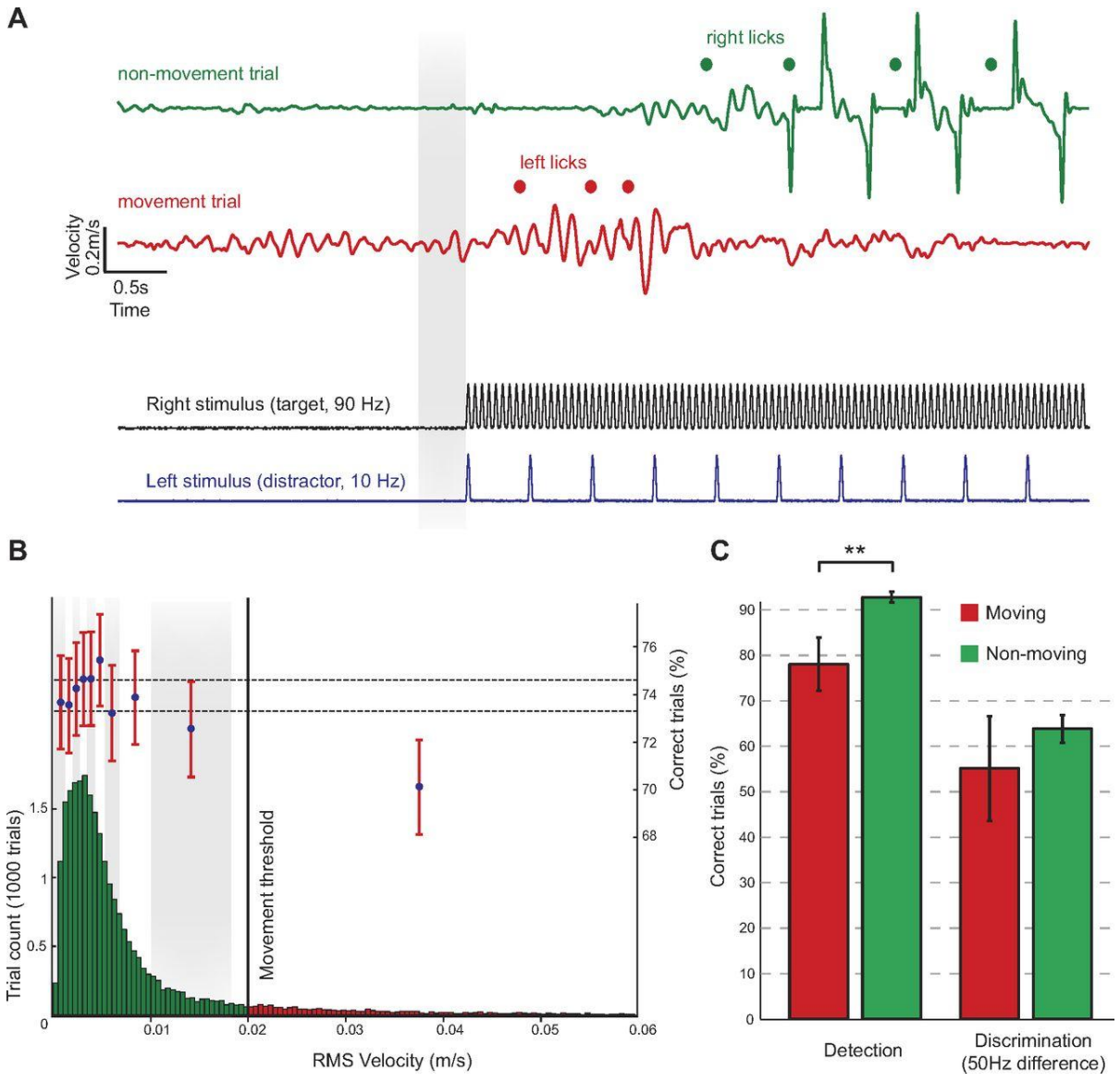

Figure 11. Whisker motion and behavioral performance — whisking prior stimulus presentation decreased task performance.

A. Example trials, demonstrating the presence or absence of whisker movements in the prestimulus phase of sensory stimulation (−200ms, gray shading). The top 2 traces show whisker velocity for a non-movement and a movement trial. Red and green dots indicate left and right licks, respectively. Bottom 2 traces show sensory stimuli as measured by a strain gauge sensor on each stimulator. Sensory stimulation was the same for both trials, with the target being presented on the right side. **B.** The histogram shows the distribution of prestimulus root mean square (RMS) velocity over all trials. The vertical black line indicates the RMS velocity threshold for the classification of movement trials. This was the case for

~9% of all trials (2,268 of 25,287 trials). To visualize the distribution of behavioral performance for different RMS velocities, trials were binned into 0.1-quantiles (gray shading), and behavioral performance was computed for each bin. Error bars represent 95% confidence intervals and horizontal lines the 95% confidence interval for all trials. **C**. Behavioral performance in trials without whisker movements is better than trials with whisker movements. Analyzing only detection trials led to a stronger and significant drop (χ^2-test, $P < 0.01$) compared with trials in the discrimination case (at the threshold, 50 Hz difference). **Significance level $P < 0.01$.

1.5. Discussion

In the present study, we describe a frequency discrimination paradigm for head-fixed rats and mice. Two vibrotactile frequencies were presented simultaneously to individual whiskers on the left and right sides of the animal's snout. The task was to report the presentation side of the target frequency by licking from one of two possible waterspouts. To our knowledge, this is the first bilateral frequency discrimination paradigm and the first description of a 2-AFC task in head-fixed rats and mice. We found that both the perceptual thresholds and the psychometric curves were very similar for rats and mice. Hence, our results show that mice can achieve complex discriminative behavior in a paradigm initially designed for rats in our laboratory. The average perceptual threshold was 50.6- Hz (Weber fraction of 0.56) and 53.0 Hz (Weber fraction of 0.58) frequency difference in mice and rats, respectively. The slopes of the psychometric curves of mice and rats were 1.82 and 2.00, respectively. Mice and rats performed on average >400 trials a day (>200 trials/session, 2 sessions/day), with a peak performance of >90% for the detection task in both species. The average reaction time was 334ms for rats and 486ms for mice and was longer for error trials compared with correct trials. Reaction time distributions found in this study were like previously reported tasks (Carpenter and Williams, 1995). Motivation and impulsivity varied over animals but were similar for the two species. Finally, we could demonstrate that trained animals rarely moved their whisker prior to stimulus presentation (9% of trials). In trials where whisker motion occurred, we observed a significant drop in discrimination performance. Response biases could successfully be reduced by using a previously published bias correction (Knutsen, 2006). Although the head rotation mechanics were closed for most of the data presented in this study, and it is not essential for the entire training procedure, it

is a valuable tool for prompting the animals and avoiding early lick events. Furthermore, it allows a simple implementation of a working memory task. Animals can be forced to wait after a stimulus offset by keeping the brake system closed for a variable delay period before a response is allowed by opening the brake. The fact that the animal can turn its head to retrieve a reward from two different locations would also allow one to study neuronal correlations with head orientation movements (Erlich et al., 2011; Taube et al., 1990) while keeping the advantages of the head-fixed preparation.

Frequency discrimination in different species

Frequency discrimination paradigms have been performed previously in rats, monkeys, and humans (Gerdjikov et al., 2010; LaMotte and Mountcastle, 1975; Mountcastle et al., 1990). The perceptual threshold for frequency differences, however, depends on the location and the timing of the stimuli. Many tasks published to date involved a working memory component. In these paradigms, frequencies were presented consecutively to the sensory organ, and thus the subject had to compare them in sequence (2-interval forced choice; see (Hernandez et al., 1997)). Our paradigm is different in that the simultaneously applied single-whisker stimuli had to be compared between the left and the right whisker pads while the stimuli were presented. The interhemispheric communication and the concomitant perception of two stimuli required to solve this task may involve neuronal processes that are distinct from those involved in a working memory task. Frequency thresholds and the resulting Weber fractions were higher as reported in working memory tasks in rats (Gerdjikov et al., 2010) and monkeys and humans (LaMotte and Mountcastle, 1975; Mountcastle et al., 1990). Additionally, it has been shown in human subjects that discrimination performance was more accurate when frequencies were applied sequentially to the same finger. Discrimination performance dropped when the frequencies were presented to corresponding fingers on both hands (Harris et al., 2001). However, vibrotactile input arriving simultaneously from both sides might be behaviorally relevant when rodents navigate in darkness in narrow environments. Whisker vibrations may be generated by the texture of walls and ground on both sides of the animal and lead to simultaneous inputs that can be used for orienting in these situations. Passive whisker vibrations (i.e., when the animal is not actively whisking) may be a common setting that rodents encounter in their natural environment. Previous work showed that freely moving rats were able to accurately

discriminate small variations of aperture sizes without the need of active whisker movements (Krupa et al., 2001). Furthermore, we observed lower discrimination performance when the animals moved their whiskers just before stimulus presentation. Active whisker movements are often observed when animals have to lean over a gap to discriminate different textures (Carvell and Simons, 1990; Cybulska-Klosowicz and Kossut, 2000; von Heimendahl et al., 2007; Morita et al., 2011), and therefore hamper the use of body movements to contact textures. However, whisker tracking data from freely moving animals discriminating wall properties in proximity are still lacking.

Mice and psychophysics

The question as to why there is a need to transfer a psychophysical task that has been developed for rats to mice requires addressing. The mechanical difficulties of downsizing the behavioral apparatus components and the potential problems of tracking the whisker motion of an animal about a tenth of the weight of a rat argue against such an endeavor. There are, however, several benefits, in particular with respect to the combination of state-of-the-art imaging and electrophysiology techniques that demand well-controlled behavioral paradigms for head-fixed mice. The mouse is currently the best developed mammalian genetic model organism, allowing cell type-specific readouts and manipulation of neuronal activity (Luo et al., 2008). The parallel acquisition of psychometric and neurometric curves is one of the gold standards in cognitive and systems neuroscience for understanding the role of individual neurons in behavior (Parker and Newsome, 1998). The psychophysics described here will, therefore, allow the expansion of these types of investigations to a cell type-specific level and shed light on the contribution of individual neuronal elements to perceptual decision-making processes. Here we demonstrate that mice can perform tasks that have long been a standard in head-fixed monkey behavior and neurophysiology (Wurtz et al., 1968). The animals were highly motivated at all levels of difficulty and performed several hundreds of trials per day with high maximum performance levels. In conclusion, we can report that the two species (rats and mice) have very similar capacities for frequency discriminations in the 2-AFC paradigm described here.

2-AFC paradigm vs. Go-NoGo paradigm

Several laboratories are currently using Go-NoGo paradigms to measure psychophysics in head-fixed rodents (Andermann, 2010b; Gerdjikov et al., 2010; O'Connor et al., 2009). These paradigms are well-suited to obtaining psychometric curves from head-fixed rodents performing sensory discrimination and detection tasks. In these tasks, animals are subjected to water deprivation for motivation. Deprived animals, however, are prone to impulsive behavior as the measured responses are tightly linked to the pressure of retrieving a reward. In a Go-NoGo paradigm, it is difficult to implement that the animal receives a reward in the Go condition and in the NoGo condition. This is more straightforward in 2-AFC tasks, as the animal can retrieve a reward in each trial. Another obstacle present in the Go-NoGo paradigm is that animals can contaminate the measured threshold by developing a strong response bias toward Go or NoGo stimuli (for review of different task strategies see (Stüttgen, 2011). Although animals did not show strong stereotypical response behavior (positional bias: left or right side preference, left/right switching behavior, etc.), this can be a problem in a 2-AFC task. Nevertheless, this kind of behavior can easily be inhibited by implementing a bias correction algorithm. In the Go-NoGo task, it is difficult to distinguish a lack of motivation or lapses of attention from false rejections or correct rejections. The 2-AFC paradigm is, therefore, ideal for investigations of behavioral state-dependent neuronal processing. The uncoupling of reward retrieval (i.e., licks) from the stimulus report action (i.e., the choice of 1 of 2 reward locations) allows a clear distinction of correct, incorrect, and missed trials. Furthermore, the task can easily be modified to accommodate a yes-no paradigm by providing only a single stimulus per trial.

Outlook

The presented apparatus and behavioral paradigm have been designed to combine two-photon imaging and electrophysiology with simultaneous psychophysical measurements. The dura mater of mice is transparent and therefore facilitates the use of high-resolution functional imaging such as two-photon imaging. The quality of two-photon images of neocortical neurons obtained in mice appears to be superior to those obtained in rats (our own observations and Helmchen F and Kampa BM, personal communication). Vessel density and size may play a role in the number of scattered photons that can be collected. Although it is possible to reduce these effects by blood exchange techniques in

anesthetized animals (Haiss et al., 2009), the long-term use of this technique in behaving animals seems not to be feasible in the near future. The mouse is, therefore, an excellent model organism that combines genetic tools and the feasibility of imaging large populations of neurons in behaving animals (Dombeck et al., 2010). In addition, the use of transgenic animals, such as Cre driver lines, permits the expression of functional indicators or markers in specific subsets of neurons (O'Connor et al., 2009; Zariwala et al., 2011). The head-fixed 2-AFC paradigm presented here, therefore, promises to be a valuable framework in which to conduct two-photon imaging in the mouse while measuring its psychophysics.

2. Project 2: Long-term evolution of neural responses in the barrel cortex during learning of a bilateral vibrotactile two-alternative forced choice task

Author contributions

Vida Skreb and Christoph Pokorny act as shared first authors. Vida Skreb completed all the experiments for the five animals expressing YC3.60 (surgery, behavioral training, two-photon imaging), analyzed and interpreted the data, prepared the figures, wrote the paper, and contributed to developing the experiment design.

5.1. Abstract

It has been shown that the primary somatosensory cortex (S1) exhibits experience-dependent plasticity. However, little is known about the long-term dynamics of neuronal responses in cortical layer 2/3 due to behavior in a sensory-guided task. To evaluate the impact of learning on somatosensory processing, we performed chronic two-photon calcium imaging in layer 2/3 in the awake mouse S1 during a sensory-guided bilateral two-alternative forced choice task. During ongoing performance, behavior in the task increased the amplitude of calcium transients, in comparison to trials without active participation in the task. Furthermore, we observed a rapid growth of calcium transients once a vibrotactile stimulus becomes behaviorally relevant to the animal, showing long-term modulation of tactile responses in S1. Recordings from the same mice under anesthesia showed that the progressive increase of calcium transient amplitude with increasing repetition rates of the vibrotactile stimulus was disrupted after long-term training in the task. In addition, we elucidated that contralateral stimuli evoked larger neuronal responses compared to moderate neuronal responses to ipsilateral stimuli in layer 2/3 of S1. In summary, the context of learning plays a distinct role in shaping the way somatosensory stimuli are represented in layer 2/3 at early stages of cortical processing. Our results contribute to a better understanding of the neuronal processing during learning of a complex whisker-dependent task.

5.2. Introduction

A crucial function of the nervous system is to adapt to an ever-changing environment behaviorally. This adaptation is achieved through continuous learning, which can be defined as the acquisition of context-appropriate action and prediction (Hollerman and Schultz, 1998). Neuroplasticity at the level of synapses and neuronal pathways is thought to underlie learning (Rosselet et al., 2011). Neuronal plasticity can occur when the brain modifies or creates new neuronal connections due to learning, but also in response to sensory experience (Hofer et al., 2009; Holtmaat and Svoboda, 2009; Trachtenberg et al., 2002). Interestingly, sensory cortical areas can exhibit neuroplasticity (Gilbert et al., 2001) and topographic map changes (Ohl and Scheich, 2005; Sur, 2005), not only during development but also during adulthood. It has been shown that when the sensory cortex undergoes plasticity, the neural response to the same sensory stimulus is altered (Blake et al., 2006).

In this study, we investigated the impact of behavior in a sensory-guided task on cortical layer 2/3 neurons in the primary sensory cortex (S1). S1 is well suited to study the link between neuroplasticity and learning since it receives both bottom-up sensory inputs from sensory receptors and top-down inputs from brain areas involved in cognitive functions, attention and behavioral reinforcement (Polley, 2006). In addition, the sensory cortex is highly malleable, and exhibits experience-dependent plasticity in a variety of paradigms (Bieszczad et al., 2013; Galvez, 2006). It also has a causal role in detection tasks (Sachidhanandam et al., 2013). In most mammals, the functional properties of layer 2/3 neurons are strongly regulated by the behavioral state of the animal (Kato et al., 2015; Petersen and Crochet, 2013), and are therefore particularly well suited to study the impact of neuroplasticity on sensory processing. However, how long-term changes in the responses of cortical layer 2/3 neurons in S1 are related to learning remains largely unknown. Two-photon microscopy allows for imaging of the cortical surface up to a few hundred micrometers in depth, which encompasses cortical layers 1 and 2/3 and hence is well suited to study learning in the cortex (Kerr et al., 2005; Ohki and Reid, 2014). Furthermore, it has been used to successfully image awake, behaving animals (Andermann, 2010a; Chen et al., 2013a; Huber et al., 2012; Komiyama et al., 2010). Here we take advantage of two-photon microscopy to image calcium transients in the primary somatosensory cortex of mice while learning a two-alternative forced choice (2-AFC) task over four months. During the 2-AFC task, the animal had to report the side of its snout where a single-whisker stimulus was

presented, and at a later stage to discriminate two simultaneously presented vibrotactile stimuli (Mayrhofer et al., 2013).

Here we report plasticity effects due to long-term behavior in the 2-AFC task and the impact of engagement on online sensory processing. In the awake animal, we show a rapid enhancement of the neuronal representation of the same vibrotactile stimuli, once they gained behavioral relevance in the sensory-guided task. Additionally, plasticity effects were visible under anesthesia. We report that the statistically significant trend of an increase in calcium transients with increasing repetition rates of the stimulus was abolished due to long-term training in a 2-AFC task. Furthermore, we explored the representation of different behavioral categories during ongoing behavior, showing that engagement in a sensory-guided task correlates with changes in the representation of vibrotactile stimuli.

While our core question concerned plasticity changes in neural function during learning, an additional question addressed in our paradigm was the cortical representation of contralateral versus ipsilateral stimuli. In the rodent whisker system, sensory information is completely lateralized subcortically until it reaches the S1 (Shuler et al., 2001). In the neocortex, interhemispheric communication is achieved through the corpus callosum, which is composed of axonal fibers from layers 2/3, 5 and 6 (Palmer et al., 2012; Ramos et al., 2008). Callosal axons project mainly to homotopic brain areas (Zhou et al., 2013). Even though barrel cortex neurons respond best to stimulation of the contralateral whiskers, they are also influenced by ipsilateral whisker stimulation, as shown by evoked local field potential and spiking activity in layer 5 (Li, 2005). However, it is still largely unknown whether layer 2/3 neurons respond to ipsilateral inputs. Here, we took advantage of our 2-AFC task to explore this question.

5.3. Methods

Animals

Subjects included six male C57BL/6 mice (m1, m2, m3, m4, m5, m6). All animals weighed approximately 25 grams and were older than 15 weeks at the time of the surgery. The mice were housed in an inverted 12-hour day/night cycle, and all handling, training, and imaging took place during the active phase. All experimental and surgical procedures were approved by the local veterinary authorities and are in conformity with the guidelines of the

Swiss Animal Protection Law, Veterinary Office, Kanton Zürich (Act of Animal Protection 16 December 2005 and Animal Protection Ordinance 23 April 2008).

Surgical procedures

All surgeries were performed under isofluorane anesthesia (1-3%), and the depth of anesthesia was checked by hindpaw withdrawal reflex. Body temperature was monitored via a rectal temperature probe and maintained at 37°C with a feedback-controlled heating pad (Harvard Apparatus, Holliston, MA, USA). The animals' heads were fixed in a stereotaxic apparatus, and a local aesthetic (Bucain) was injected subcutaneously preceding the scalp incision. Eyes were protected with vitamin A eye cream. After each surgery, the antibiotic ointment was applied to the wound (Cicatrex), which was then sutured and the skin attached to the head post with acrylic glue. Animals were given analgesics (Novaminsulfon, 50%; Sintetica, Switzerland) and recovered for one week. Antibiotics were provided (1 ml Enrofloxacin (Baytril)/500 ml drinking water; Bayer, Leverkusen, Germany) after each surgery.

Headpost implantation surgery

The skin was removed from the skull. The skull was cleaned with saline and allowed to dry, and the bone was thinned down with a dental drill above the left barrel cortex. After functionally identifying the barrel cortex with intrinsic optical imaging using 630nm illumination, we obtained a cortical map linking the position of the barrels corresponding to several whiskers. Then, a bonding agent (Gluma Comfort Bond; Heraeus Kulzer, Hanau, Germany) was applied. It was allowed to dry for 40 s, and was then polymerized with blue light (hand-held device; 600 mW/cm2; Demetron LC, Bioggio, Switzerland). On top of the polymerized bonding agent, layers of light-curing dental cement (Tetric EvoFlow; Ivoclar Vivadent AG) were applied, each layer polymerized for 40s with blue light before the subsequent one was applied to form a head-cap. A custom-made aluminum headpost was fixated onto the head-cap (3mm caudal from lambda), that served to head-fix the animal (Mayrhofer et al., 2013).

Virus injection and cranial window surgery

One week following the first surgery, the mice received another surgery to inject a recombinant adeno-associated virus (rAAV) that expresses the genetically-encoded fluorescent calcium indicator Yellow Cameleon 3.60 (YC3.60) (n=5) or GCaMP6f (AAV1.Syn.GCaMP6f.WPRE.SV40, n=1) (Chen et al., 2013b; Nagai et al., 2004), and to put the cranial window in place. In the surgery, the dental cement above the left barrel cortex was drilled down, the skull was removed, and 250 nl of rAAV (with the speed of 40 nl/min) carrying the YC3.60 or GCaMP6f construct were injected at approximately 300µm depth in layer 2/3, in the location identified with intrinsic optical. Selective expression in neurons of both AAV constructs (YC3.60 and GCaMP6f) was driven by a human synapsin promoter (Lütcke, 2010). The viruses were 1:1 diluted with mannitol (20%, B. Braun, Switzerland), to increase the infection area (Mastakov et al., 2001). They were delivered through a thin glass pipette by means of stereotaxic injection (Mayrhofer et al., 2015b) targeted at the chosen cortical area. A glass window (3 × 3mm; UQG Optics Ltd, UK) was placed over the barrel cortex and sealed with dental cement.

Experimental setup

Behavioral training was performed inside the two-photon imaging setup (**Fig. 12E**). The setup box was lightproof. Whisker stimuli were presented via a 15-mm long glass capillary GB 1208P; Science Products GmbH, Germany; the tip was melted to reduce dead space) mounted to a piezo bending actuator (T223-H4CL-303X; Piezo Systems, Woburn, MA, USA; 440 Hz resonant repetition rate of the piezo element), amplified by a piezo controller (MDT693A; Thorlabs, USA) and fixed on an articulated arm (Baitella, Zurich, Switzerland). A laser displacement sensor (0.1 µm resolution at 2.5 k Hz sampling rate, ILD17002; Micro-Epsilon, Ortenburg, Germany) was used to calibrate the movement of the stimulator and strain gauge sensors mounted directly on the piezo element (example recordings have been published in (Mayrhofer et al., 2013). In addition, 80 dB auditory white noise was played to mask the potential auditory cues from the piezo stimulator, thus preventing the animal from using these to solve the task. A single whisker on each side was placed in the glass capillary. The stimulus lasted 1 s, and consisted of a series of deflection in a rostro-caudal direction. The peak velocity of a prototype pulse (from a single period 120 Hz cosine wave) was constant; the repetition rate of the vibrotactile stimuli was 10, 40 or 90 Hz and the peak

amplitude 120 µm. The stimulator was at a 4mm distance from the whisker pad with a peak-to-peak amplitude of 1.72° and maximum velocity of 648°/s. Intertrial interval was kept constant at 9 s throughout the protocol. The setup was illuminated with infrared lights invisible to the animal, and a CMOS camera was used to monitor the whiskers to make sure it stayed in the glass capillaries. In front of the animal, two waterspouts were placed at about 15 degrees from the center position to the left and the right of the animal. Piezo sensors glued to the waterspouts measured licking activity (LDT0028K; Measurement Specialties, Hampton, VA, USA). Two solenoid valves (Bürkert, Ingelfingen, Germany) controlled water delivery to the drinking spouts. The entire behavioral apparatus was controlled with custom-written LabVIEW programs (National Instruments) using multifunctional data acquisition cards (PCI-6259; National Instruments).

Two-photon imaging and behavioral training

Following one week of recovery after the virus injection and cranial window placement surgery, the mice were handled 25 min daily, 5 days a week for 2 consecutive weeks. In each training session after the handling, we trained animals to tolerate head-fixation. We progressively increased the amount of time of head-fixation to allow them to become acclimated to it, such that they could tolerate head-fixation for 25 min without signs of stress.

Three weeks after virus injection surgery, we performed several imaging sessions for each mouse under anesthesia (isofluorane 0.9-1.3%)to find a neuronal population suitable for imaging. Intrinsic optical imaging maps were used to locate the cortical area corresponding to a particular whisker (**Fig. 12A**). The whisker we chose to stimulate in each animal was kept constant through the protocol and chosen based on the IOI map and the area of expression (**Fig. 12B**). We opted to image in the barrel next to the main barrel, based on indications from previous research (Margolis et al., 2012). The YC3.60 GECI showed stable expression throughout the whole duration of the imaging protocol with no signs of cytotoxicity since no nuclear filling could be observed (Packer et al., 2014). Each stimulus was 1 s long and always applied to the same whisker on each side of the mouse's snout in each imaging session, monitored with a CCD camera.

Baseline imaging sessions

Baseline imaging sessions were performed to characterize the evoked neuronal activity of single barrel cortex neurons to vibrotactile stimuli before any learning took place. Stimuli of various repetition rates were presented to a single whisker on either the left or the right side of the mouse's snout. In addition to unilateral stimuli, we also presented the animal with bilateral stimuli, where one repetition rate was presented on one side of the mouse's snout, and stimuli with the same duration but different repetition rates were applied simultaneously to the opposite side of its snout.

In these baseline imaging sessions, the animals were presented with 40 repetitions of each of the 7 following stimuli sets: 10 Hz contralateral, 40 Hz contralateral, 90 Hz contralateral, 10 Hz contralateral with 90 Hz ipsilateral, 40 Hz contralateral with 90 Hz ipsilateral, 90 Hz contralateral with 10 Hz ipsilateral, and 90 Hz contralateral with 40 Hz ipsilateral with respect to the imaging site. This set of randomly interleaved unilateral and bilateral stimuli formed a fixed set of 280 (7x40) stimuli that was presented to the animal during each baseline session.

Each of these baseline imaging sessions was performed first in the awake animal, trained to tolerate head-fixation in the two-photon microscope setup and immediately afterward under anesthesia (0.7% isofluorane in oxygen). This allowed us to analyze responses to the same stimuli in different brain states. Three animals had 10 baseline sessions (one session per day consisting of awake and anesthetized recordings for 5 days per week). Two animals had 15 sessions to control for effects due to long-term stimulus presentation versus learning. We recorded the activity of a neuronal population in layer 2/3 of the cortex corresponding to the neighboring barrel of the stimulated whisker.

Training animals in the 2-AFC task

To evaluate the impact of learning, we designed a 2-AFC task where water acted as a reward. We trained the head-fixed mice in this operant conditioning task in which they had to report the side where a 1s-long pulsatile vibrotactile stimulus was presented to a single whisker either on the left or the right side of the mouse's snout. Since water acted as a reward for the task, mice were put on a water restricted schedule after completion of the baseline imaging series. Body weight was measured before each behavioral session. If the

animal did not regain 90% of normal body weight during the training, water was afterward freely given to compensate for it. After the presentation of the stimulus, the animal had a 2s window of opportunity in which it could lick one of the two water spouts, located at its left and right side. Licking the spout that corresponded to the side where the stimulus was presented counted as a correctly solved task (referred to as "correct", **Fig. 17A**), and water was given to the animal as a reward. The water reward was 5 µl per trial. Licking the spout opposite the side where the stimulus was presented was counted as an error response (referred to as "error", **Fig. 17A**) and no water was given. The 2-AFC task allowed the animal to withhold a response, resulting in neither a correct or error response but a third category of responses of missed trials (referred to as "miss", **Fig. 17A**). The consequence of making an error response or missing a trial was that no water was given. The intertrial interval was 9 seconds.

Two-photon imaging of barrel cortex neurons was performed during every behavioral session that followed the baseline imaging sessions. The same population of neurons was imaged during baseline and learning. Each animal had one imaging session a day, 5 days a week. Anesthesia recordings during baseline were compared to anesthesia recordings after learning, and awake recordings during baseline were compared to awake recordings. In this way, the possible learning-related changes were compared within the same experimental setups (awake or anesthetized). Furthermore, we compared baseline recordings between the two conditions to detect possible differences in the two states.

The first phase of training in the 2-AFC task consisted of presenting the animal with a 90 Hz target stimulus on either the left or right side of the mouse's snout, and water was given automatically at the spout which corresponded to the side where the target stimulus was presented (on average 128 trials per session). The animal could retrieve the water reward by licking the spout where water was presented without having to solve the task, meaning without having to detect the side where the vibrotactile stimulus was presented. This stage of the protocol allowed the animal to establish the connection between the vibrotactile stimulus side and reward side. During this first phase, every 8–12 trials, a trial was presented during which the water was not given automatically. This was done to test if the animal could solve the task by first licking the correct spout to trigger a water reward ("probe" trials). If the animal reached a 75% correct performance, by only considering the responses to the probe trials in three consecutive sessions, it was put into the second phase

of training. The first phase lasted 10 to 20 sessions (behavioral performance for all animals is shown in **Supplementary Fig. 1**).

In the second phase of the training (detection phase), water was not given automatically. Licking the spout corresponding to the side where the stimulus was presented resulted in a correct response. This activated the detector vibrations sensor of the spout and caused the water valve to open and release the water reward. If the animal licked the spout of the side opposite the side where the stimulus was presented, this resulted in an error response. In this case, licking did not activate the spout and the water release. Hence, in this phase, it is only the animal's behavioral response that can cause the reward to be given.

The third phase (the discrimination phase) of the training consisted of introducing a simultaneously presented stimulus of a lower repetition rate (distractor stimulus) than the target stimulus contralateral to the target presentation side. In the last 3-6 behavioral sessions (after 12±6 sessions in the detection phase), the 10 Hz distractor repetition rate was introduced in 30% of the trials. The animal had to discriminate the 90 Hz target stimulus from the 10 Hz distractor stimulus, and lick the spout on the side where the target 90 Hz stimulus was presented.

After each 5-10 imaging sessions, we performed a session under anesthesia with the same set of stimuli that was presented during the baseline imaging sessions. This served as a control to monitor possible plasticity effects that could be visible during anesthesia. After the training in the 2-AFC task was completed, the animals had 5 sessions in the anesthetized state, only with the same set of stimuli as in the baseline recordings.

Two-photon imaging

All imaging was done with a custom-made two-photon laser scanning microscope as previously described (Mayrhofer et al., 2015a). The YC3.60 virus expression in the neuronal cell was excited with a Ti:sapphire laser (870 nm, Chameleon Ultra II; Coherent, Santa Clara, CA, USA). Light emitted from the fluorescent calcium indicator YC3.60 was detected with two GaAsP photomultiplier modules (H10770PA-40; Hamamatsu Photonics, Japan) with the following filters: dichroic mirror 515 DCXR, bandpass filter BrightLine HC 542/50 (yellow channel) and bandpass filter BrightLine HC 475/64 (blue channel) (Semrock, Rochester, NY, USA). For scan mirror control and photomultiplier data acquisition, Scanimage (Janelia Farm Research Campus (Pologruto et al., 2003)) was used, running on personal computers using

multifunctional data acquisition cards from National Instruments. Imaging was at a 128x128 resolution for the functional signal, acquired at a 15 Hz repetition rate. Anatomical images were acquired with a 256x256 resolution. The same neuronal population was traced over days in each animal and in all imaging sessions. In all animals, we imaged in cortical layer 2/3. In animals with YC3.60 (n=5), we imaged a total of 206 neurons and with GCaMP6f (n=1) 86 neurons (for data in **Fig. 14E**), and 56 neurons (for data in **Fig. 17D** and **E**). For each awake imaging session, whisker motion was recorded with a CCD camera (Pixelfly, PCO, Germany) and infrared illumination (850nm) was used for the entire length of the session. All whiskers were trimmed regularly (only at the tip), except the row of whiskers where the stimulated whisker was.

Data analysis

Data analysis of calcium imaging was performed with Matlab (MathWorks, USA) and ImageJ (ImageJ, U.S. National Institutes of Health, USA, http://imagej.nih.gov/ij/). Regions of interest (ROIs) were selected manually for each imaging session in ImageJ, both for cell bodies of neurons and the neuropil. Pixel values for each ROI were separately summed for the two photomultiplier channels (yellow fluorescent protein (YFP) and cyan fluorescent protein (CFP)). For each of the two channels, we subtracted the background, by finding the minimum pixel value for each imaging movie and then subtracted it from all pixels of the movie. The ratio time series (R) was obtained by dividing the YFP by the CFP photomultiplier channel values for each of the selected ROIs. The mean R value from the 1s time window before stimulus onset was taken as the baseline activity (R_0) and individual traces were computed according to the formula $\Delta R/R0 = (R-R0)/R0$. The imaging movies were aligned over trials by maximizing the correlations through xy-rigid shifts of the frames. Movies with motion in the z or xy direction were excluded based on following criteria: the correlation value of each ROI in each frame of a particular trial was larger than the median correlation value minus twice the standard deviation of the correlation value of all trials in a session. This correlation threshold was computed for each session separately. If the calcium transient of a neuron crossed a threshold of one standard deviation for the entire trial in two out of three frames, it was classified as a neuronal event. If the repetition rate of these neuronal events of a cell was larger than one standard deviation of the rate of neuronal events in the baseline imaging, then this cell was classified as stimulus-responsive. To compute calcium

transients for each neuron, the ΔR/R0 from 0ms to 1000ms relative to stimulus onset was integrated for each trial (∫ΔR/R0dt: area under Ca2+ transient in %s). Previous publications have shown that the Ca2+ response is approximately linearly proportional to the firing of action potentials for moderate firing (Lütcke et al., 2013). Single-cell neuronal activities from all six animals (m1, m2, m3, m4, m5, m6) were normalized to each animal's median activity across all target frequencies and cells and were pooled together for subsequent data analysis.

Since different categories of responses had different trial numbers, we normalized the trial numbers in each category by random selection. We separated the overall pool of neurons into three distinct categories (depending on the magnitude of their responses) into "low", "mid", and "high" (**Fig. 13G** and **H**). The categories were assigned based on whether the activity levels were in the lowest (under 50%), medium (50–90%), or highest (90–100%) percentiles rank from the overall pool of neurons (**Fig. 13G** and **H**).

We applied a non-linear support vector machine (SVM) classifier with a radial basis function (RBF) kernel to obtain single-trial classification results for individual animals by using the activity of single neurons that were common in all the sessions (**Table 1.**, all applied parameters are in **Supplementary Table 1.**). The SVM hyperparameters (c, sigma) were determined with a grid search (an 11x11 exponential grid), and, based on those hyper-parameters, the classification results were computed. Only trials with a 90 Hz target repetition rate and no distractor were selected to have exactly the same conditions throughout all classes. A fivefold cross-validation was repeated five times (5x5) to avoid overfitting of classification results. For computational reasons, a maximum of 250 trials was taken from each class by means of random subsampling to perform the classification. For each repetition of the classification procedure, another subset of the 250 trials was randomly selected. If the classes were unbalanced, to take them into account "balanced accuracy" was used to measure performance. Balanced accuracy was calculated as the mean of the true positive rates (TPR) of all classes.

The classification results for selecting the most or least active cells were merged across animals by normalizing the x-axis ranging from 0100% of the total number of cells in the respective animals and then interpolating and averaging the performance curves. The 80% threshold was the chosen as the 80% difference between the theoretical chance level and maximum value according to the equation "threshold = chance_level +

0.8*(maximum_value - chance_level)“. The grid search was performed only once for each condition and animal when all cells were selected and used the same hyper-parameters (c, sigma) (**Table 1.**, all applied parameters are in **Supplementary Table 1.**) for all subsequent classification tasks using subsets when selecting k<N most/lest active cells.

Whisker motion was analyzed with a custom-made Matlab program and software for fully automated vibrissae tracking (Clack et al., 2012). If whisker movement for a trial crossed a chosen threshold (angular velocity higher than 1.2 degrees per 100ms for 20% of frames in a trial, 1s contains 10 frames) for angle deflection inside the 1s stimulation time window, it was considered movement (degrees per frame), and it was discarded from the analysis (**Fig. 12F**).

Statistical analyses were conducted in R (version 3.2.2, R Core Team, 2015), using linear mixed effects models (Bates et al., 2014). While conventional analysis (e.g. t-tests, ANOVA) can inflate the probability of type I errors when applied to nested data (i.e. repeated measures from the same animal, field, of view, neuron, etc.), linear mixed effects models account for the hierarchical nature of such data (Aarts et al., 2014). For each analysis, we specified intercepts for each mouse, imaging session, and neuron as random effects, and fixed effects according to the data (e.g. stimulus frequency, time point, etc.). Visual inspection of the residual plots revealed no obvious deviations from homoscedasticity and/or normality. P-values for the overall significance of an effect were determined by likelihood ratio tests of the full model with the effect(s) in question against a model without the effect(s) in question. P-values for differences between the effects were obtained posthoc using the Tukey correction for multiple comparisons (Hothorn et al., 2008).

5.4. Results

Calcium transients in barrel cortex evoked by single vibrissa stimulation

We performed long-term two-photon imaging in layer 2/3 of the mouse barrel cortex. To achieve this goal, we cortically injected a viral vector to induce expression of the ratiometric genetically encoded fluorescent calcium indicator YC3.60 (n=5) or GCaMP6f (n=1) (**Fig. 12A**). The GECIs and our chronic cranial window preparation allowed us to image calcium transients for up to 13±3.5 weeks. To follow the same population of neurons for the entire duration of the imaging protocol we chose a single barrel for imaging in each animal

(**Fig. 12A**). Our imaging field of view captured a surface area of 200 µm x 200 µm and was centered on the barrel, with virus expression labeling the cytosol and sparing the nucleus (example for YC3.60 in **Fig. 12B**). The stimulated single vibrissa on each side of the mouse's snout corresponded to the barrel adjacent to the imaged barrel. The adjacent barrel was chosen based on indications from a previous study showing that plasticity events were larger there (Margolis et al., 2012) and the choice of several possible adjacent barrels depended on expression levels and neuronal activity. The single vibrissae on each side of the mouse's snout were stimulated with a 1s long vibrotactile pulse sequence, with repetition rates spanning from 10 to 90 Hz evoking calcium transients in a subset of the imaged neurons (**Fig. 12C**), in accordance with the sparse coding principle (Crochet et al., 2011). The entire protocol, consisting of imaging before, during, and after learning, was performed inside our two-photon imaging setup, which was adapted to the behavioral task. We stimulated the same whisker both on the contralateral side (**Fig. 12D,** whisker and neuronal connections colored red) and on the ipsilateral side (**Fig. 12D**, whisker and neuronal connections colored green) of the imaged barrel while tracking whisker movement (**Fig. 12D**). Analyzing whisker movement (**Fig. 12E**) allowed us to exclude trials where the animal was whisking from the analysis since whisker movement is known to produce self-generated tactile inputs that interfere with performance (Ollerenshaw et al., 2012). Following surgeries and habituation to head-fixation, baseline imaging sessions were performed in both awake and anesthetized states to measure responses to vibrotactile stimuli before behavior took place (**Fig. 12F**). Three animals had 10 baseline imaging sessions, and two had 5 more to control for effects due to long-term passive whisker stimulation in comparison to learning. We then proceeded with the 2-AFC detection, and afterward discrimination task, with an anesthesia session repeated after each set of 10 consecutive behavioral imaging sessions (**Fig. 12F**) (for details regarding the protocol see *Methods*). Mice could lick during a 2s long decision window (schematic drawing of an example trial **Fig. 12G**).

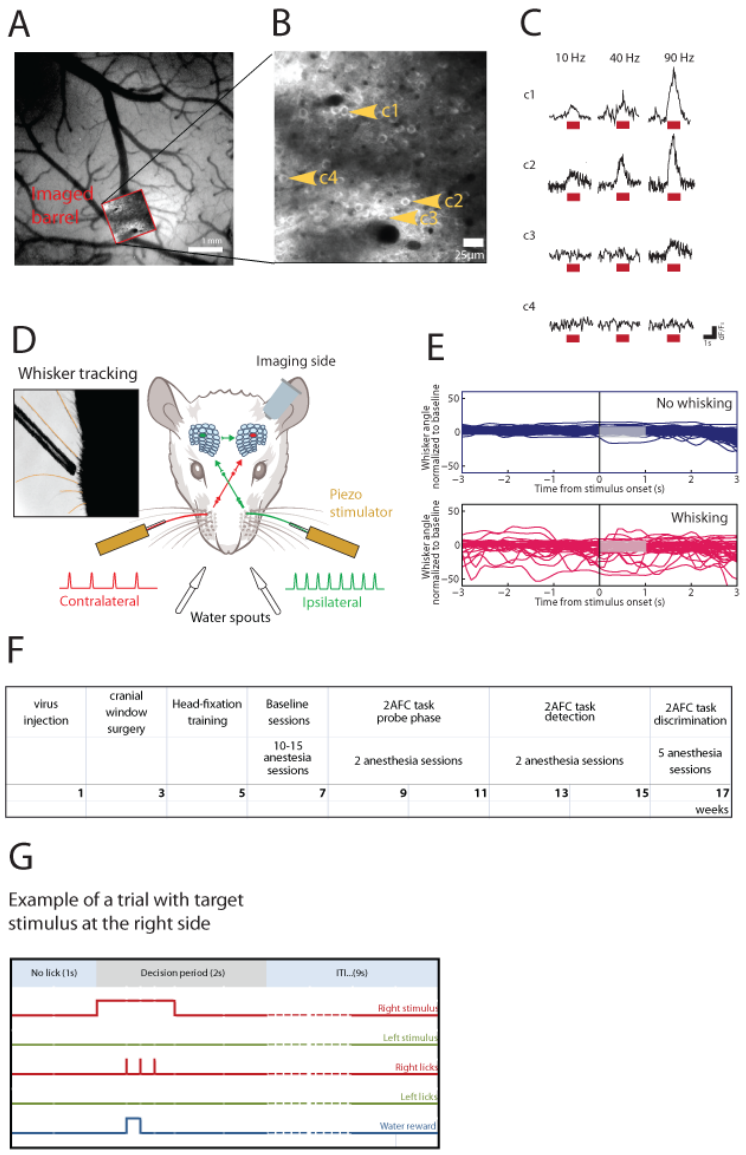

Figure 12. Two-photon imaging in the barrel cortex and long-term behavior in the 2-AFC task.

A. An example of a wide field fluorescent image of the expression area of YC3.60 with an overlay of a two-photon image onto the imaged cortical area. **B.** High resolution (256x256 pixels) two-photon image with example cells c1, c2, c3 and c4 marked. **C.** Example of calcium transients in awake animal using YC3.60 for contralateral single vibrissa stimulation (10, 40 and 90 Hz) in animal m2 for cells c1, c2, c3 and c4 shown in 1.B. **D.** Schematic drawing of a mouse performing the 2-AFC task, showing the stimulus presented on the contralateral and ipsilateral side projecting to their respective barrel cortices, with an image of whisker tracking. **E.** Whisker position traces of the whisking and non-whisking conditions. **F.** The entire imaging protocol, with average durations of each phase and the repetition rates used (see Methods). G. Schematic drawing of an example trial.

Calcium transients increase with higher repetition rates of whisker stimulation

We characterized the neuronal responses to vibrotactile stimuli of different repetition rates during baseline imaging sessions both in the awake and anesthetized states. We show calcium traces for stimuli of increasing repetition rates in a single neuronal cell (**Fig. 13A**) and in an averaged trace from an example animal in the awake state (**Fig. 13B**). Calcium responses to the 40 Hz stimulus were significantly higher than to the 10 Hz stimulus (**Fig. 13C**, number of neurons=206, number of animals=5, p=2e-16) and the calcium responses to the 90 Hz stimulus were significantly higher than to the 40 Hz stimulus (**Fig. 13C**, number of neurons=206, number of animals=5, p=2e-16). The same trend was observed in the anesthetized state (**Fig. 13D**; comparing 90 to 40 Hz, number of neurons=206, number of animals=5, p=2e-16; comparing 40 to 10 Hz, number of neurons=206, number of animals=5, p=2e-16). Hence, as the repetition rates of the 1s-long stimuli increased from 10 to 90 Hz, the magnitude of the corresponding calcium transient increased in both the awake (**Fig. 13C**) and anesthetized state (**Fig. 13D**) during baseline. We computed the histogram of calcium responses for stimuli of different repetition rates, and, again, higher repetition rates elicited higher calcium transients with a wider-spread probability distribution, compared to the single sharp peak of the probability responses to low repetition rates (awake animals shown in **Fig. 13E**, anesthetized animals in **Fig. 13F**). Since the average calcium responses were broadly distributed, we divided the neuronal population based on their activity levels into low (n=103), middle (n=82), and high (n=21) responding cells (designated as “Low”, “Mid” and “High”, respectively) to investigate whether the observed repetition rate representation was equally represented across neurons of different activity levels (for the criteria for the division see histogram in **Fig 13G** and **H**). Both in the awake (**Fig. 13G**) and anesthetized (**Fig. 13H**) state, neurons of all three levels of activity showed that stimuli of higher repetition rates evoked larger calcium transients. These results suggest that neurons of different activity levels show no preference for a particular repetition rate of whisker stimulation. Rather, we see a generalized feature of monotonic increase of neuronal response magnitude with increasing repetition rates of stimuli. Taken together, layer 2/3 barrel cortex neurons displayed a clear trend of increasing calcium transients with increasing repetition rates of vibrotactile stimuli in the cortical barrel neighboring the principal. This is consistent with a previous study in anesthetized animals in the principal barrel (Mayrhofer et al., 2015b).

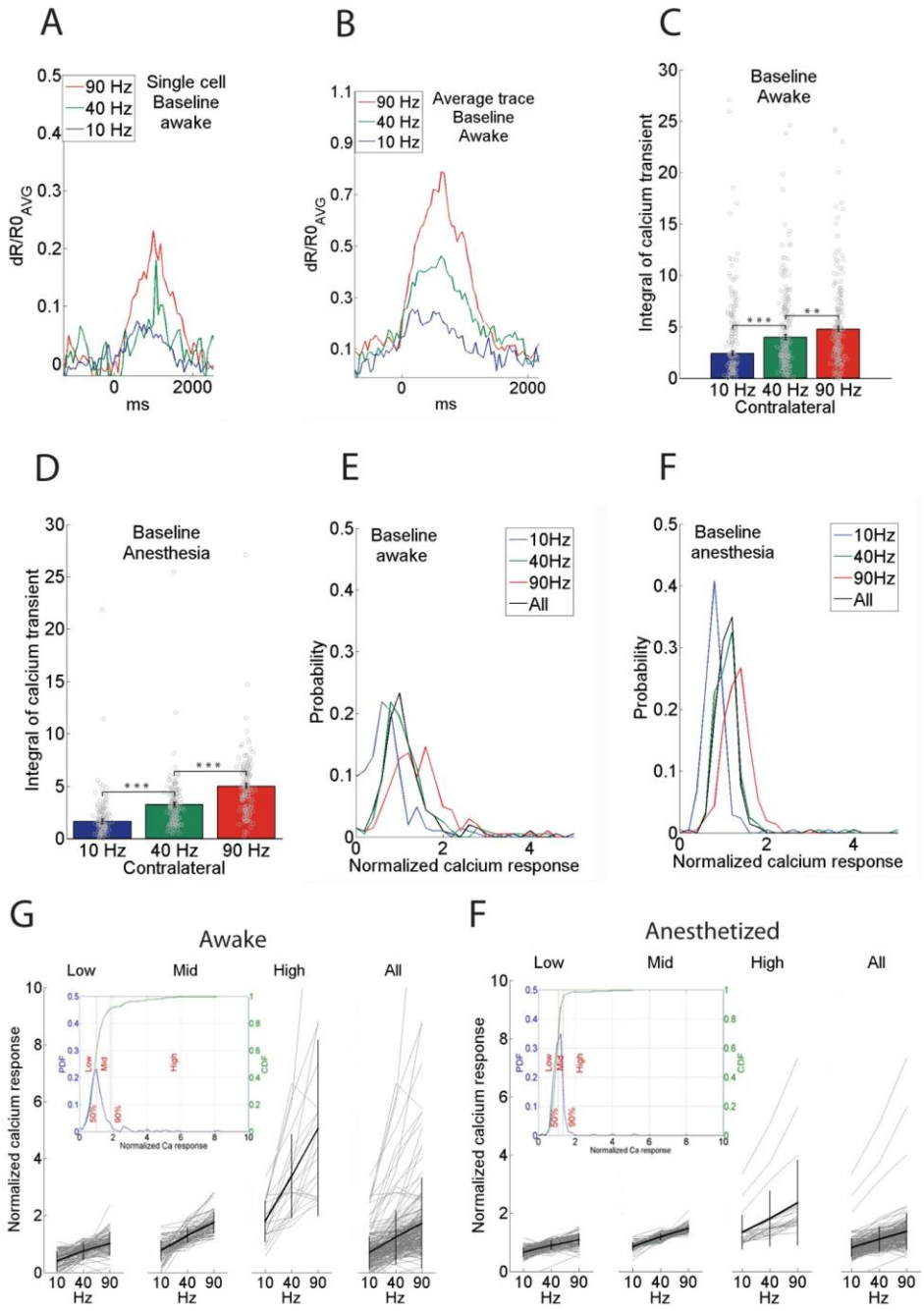

Figure 13. The neuronal representation of increasing whisker deflection repetition rates in S1.

A. Calcium responses of a single cell for stimuli of different repetition rates. **B**. Average calcium traces for animal m4 for stimuli of different repetition rates. **C-D.** Calcium transients for vibrotactile stimuli of different repetition rates presented on the contralateral side. **C.** Calcium transients in the awake animal; the response to the 40 Hz stimulus is larger than for the 10 Hz stimulus (number of neurons=206, number of animals=5, p=2e-16) and the 90 Hz is higher than the 40 Hz (number of neurons=206, number of animals=5, p=2e-16).

D. Calcium transient in the anesthetized state. The response to the 40 Hz stimulus is higher than for the 10 Hz stimulus (number of neurons=206, number of animals=5, p=2e-16, n=5) and the 90 Hz is higher than the 40 Hz (number of neurons=206, number of animals=5, p=2E-16). The grey circles represent the average of the calcium transients for an individual cell. **E-F.** Histograms of the normalized calcium responses for stimuli of different repetition rates. For each trial, the mean response was computed for the whole duration of the stimulus (1 s) and normalized by each animal's median activity level across all conditions. **E.** Distribution of stimulus responses in the awake state. **F.** Distribution of stimulus responses in an anesthetized state. **G.-H.** Calcium responses corresponding to neurons with the lowest (<50%), medium (50–90%), and highest (90–100%) activity across all target frequencies, respectively; and the responses of all neurons pooled (All). The inset shows the histogram of the mean response amplitude of all contralaterally presented stimuli of the individual neurons (PDF: probability density function; CDF: cumulative density function. **G.** Awake recordings with the histogram defining the three categories. **H.** Anesthesia recordings with the histogram defining the three categories. Grey lines and circles represent the average of the calcium transients for individual cells, and black lines represent mean +/-SEM. The used statistical method was linear mixed effects models. C.-G. Data is for mice with YC3.60. Significance legend: * = p<0.05, ** = p<0.01, *** = p<0.001.

Ipsilateral responses and ipsilateral modulation in layer 2/3 of the barrel cortex

We then asked how neurons in layer 2/3 of the primary sensory cortex represent ipsilateral and bilateral stimuli (**Fig. 14A**). As expected, the responses to vibrotactile stimuli on the contralateral side are greater than the responses on the ipsilateral side, reflected in traces of an example single cell (**Fig. 14B**), averaged trace (**Fig. 14C**), and in the pooled activity with both YC3.60 (**Fig. 3D**, number of neurons=206, number of animals=5, p=2e-16) and GCaMP6f (**Fig. 14E**, number of neurons=86, number of trials=208, p=2e-16). Similarly, under anesthesia, there was a strong increase in the magnitude of calcium responses to a 90 Hz stimulus on the contralateral side, compared to the same stimulus presented on the ipsilateral side (**Fig. 14F**, number of neurons=206, number of animals=5, p=2e-16). In summary, our results show that ipsilateral stimuli evoked much weaker neuronal responses than contralateral stimuli, thus corroborating an important and previously unclear aspect of stimulus representation in layer 2/3 of the mouse barrel cortex. We further explored

ipsilateral modulation by comparing the representation of unilateral and bilateral stimuli presented during the baseline sessions (**Fig. 14G**). In the awake baseline measurements, the simultaneous addition of a 10 Hz ipsilateral stimulus significantly increased the response to a 90 Hz contralateral stimulus (**Fig. 14G**, comparing 90 Hz with 90 Hz+10 Hz, number of neurons=206, number of animals=5, p=3.88e-06). Similarly, modulation of a 90 Hz contralateral stimulus by a 10 Hz simultaneous ipsilateral stimulus with a net excitatory effect was also present during anesthesia (**Fig. 14G** comparing 90 Hz with 90 Hz+10 Hz, number of neurons=206, number of animals=5, p=1e-06). These results support the notion that the presentation of a 10 Hz ipsilateral stimulus modulates the calcium responses to a 90 Hz contralateral stimulus with a net excitatory effect. In summary, ipsilateral stimuli are represented with considerably less neuronal activity than identical contralateral stimuli, but can still increase calcium transients of simultaneously presented contralateral stimuli.

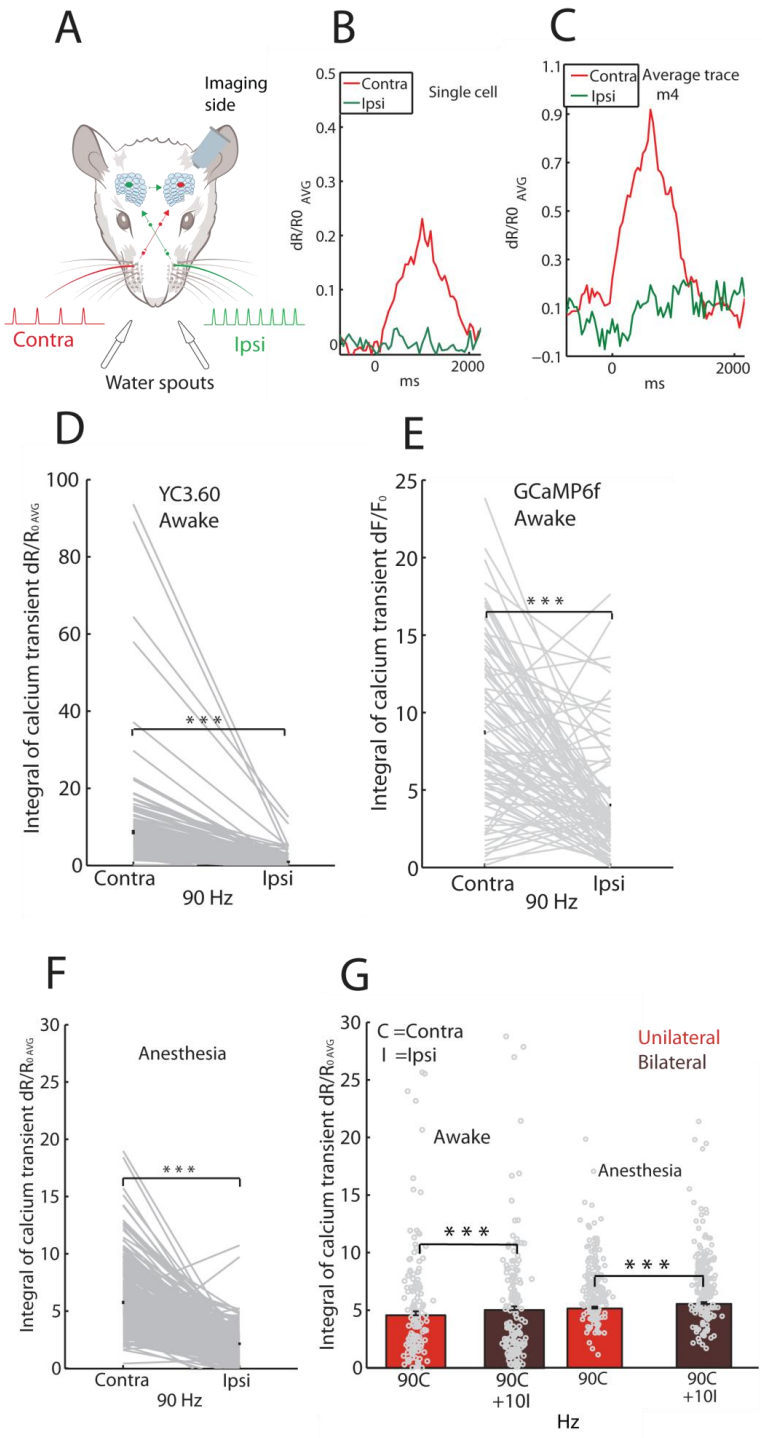

Figure 14. Ipsilateral stimulus representation and its modulation of contralateral stimulus representation in S1.

A. Schematic drawing illustrating the applied contralateral and ipsilateral stimulation. **B.** Calcium transients from a single neuron comparing the representation of 10 and 40 Hz. **C.** Average traces for contralateral and ipsilateral stimuli from animal m4 (with YC3.60). **D-E.** Comparison of contralateral and ipsilateral representation of the 90 Hz vibrotactile stimulus in the awake animal. **D.** YC3.60 (number of neurons=206, number of animals=5, p=2e-16). **E.**

GCaMP6f (number of neurons=86, number of animals=1, p=2e-16). **F.** Comparison of contralateral and ipsilateral representation of the 90 Hz vibrotactile stimulus anesthetized animal (number of neurons=206, number of animals=5, p=2e-16). **G.** Comparison of contralateral 90 Hz stimuli ("90C" red bars) with bilateral stimuli consisting of 90 Hz contralateral with 10 Hz ipsilateral ("90C+10I" brown bars) during baseline recordings. Awake state: 90C+10I is larger than 90C during the baseline (number of neurons=206, number of animals=5, p=3.88e-06). Anesthetized state: 90C+10I is higher than 90C before behavior (number of neurons=206, number of animals=5, p=1e-06). The gray circles represent the average of the calcium transients for individual cells. The used statistical method was linear mixed effects models. Significance legend: * = p<0.05, ** = p<0.01, *** = p<0.001.

Plasticity effects after long-term behavior in a sensory-guided task

Our main question was to investigate the effects of long-term behavior in a 2-AFC sensory-guided task on sensory processing. The first stage consisted of a detection paradigm, where the animal had to report the side of the mouse's snout at which a 90 Hz vibrotactile stimulus was presented (**Fig. 15A**). When comparing the representation of the 90 Hz contralateral stimulus at different stages of the protocol, we observed an increase in activity once the learning task commenced, i.e., once the stimulus gained behavioral significance for the animal (**Fig. 15B** comparing baseline to probe; number of neurons=206, number of animals=5, p=0.001998; comparing baseline to active, number of neurons=206, number of animals=5, p=0.000254). Furthermore, the increase in neuronal activity was also present for the bilateral stimulus combination of a 90 Hz contralateral with a 10 Hz ipsilateral (**Fig. 15C**, number of neurons=206, number of animals=5, p=0.000254). In addition, a non-linear support vector machine classification procedure was used to identify whether trials could be distinguished before and after learning, based on their neuronal activity. In all five animals, there was a statistically significant difference during contralateral target stimulus presentation, and in four out of five animals during ipsilateral target stimulus presentation, meaning that the classifier could distinguish neuronal traces from before and after behavior in a sensory-guided task (**Table 1.,** all bolded figures show a statistically significant value above the 1% chance level; all applied parameters are in **Supplementary Table 1.**). Furthermore, classification accuracy analysis at an 80% accuracy level was distinguished

before and after learning (**Fig. 15D**). It took an average of 11 of the most active cells to differentiate between the two categories; 16 cells when picked randomly, and 30 cells when the least active were taken first (mean value across animals computed as the maximum of the curve for each individual animal). The increase of calcium transients during learning was not simply due to stimulus presentation over time, since the 3 animals that had the short baseline (10 sessions) had a statistically significant increase in calcium transients after they started learning (**Fig. 15E**, comparing baseline 1 with learning 2 in the “short baseline” group; number of neurons=119, number of animals=3, p=0.00464). The 2 animals with the long baseline (15 sessions) showed no such increase in the same number of imaging sessions (**Fig. 15E**, comparing baseline 1 with learning 1 in the “long baseline” group, orange, number of neurons=97, number of animals=2, p= 0.98087). These results indicate that neuronal responses in layer 2/3 of the barrel cortex increased when the animal was involved in a behavioral task and that a small subset of neurons were highly active. This result indicates cortical map expansion of the principal stimulated whisker onto the adjacent barrel and increased neuronal excitation as a response to behavior in a sensory decision-making task.

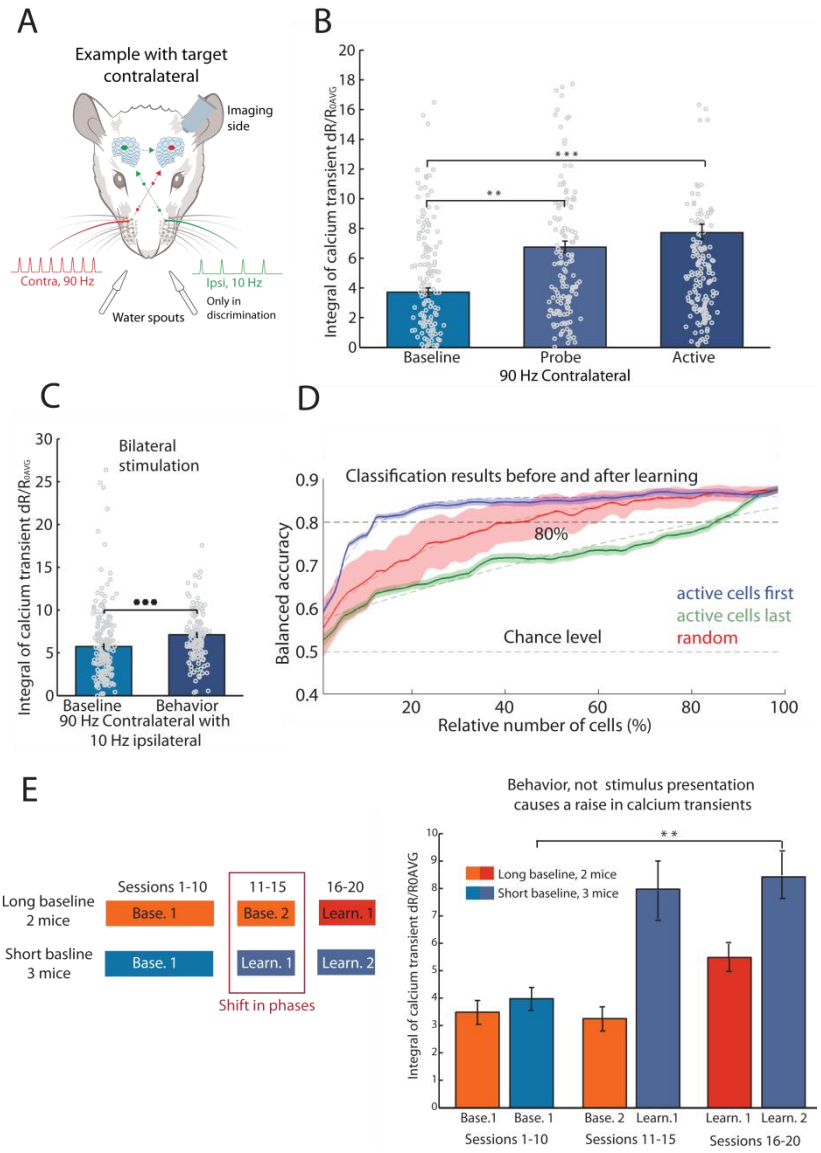

Figure 15. The modulation of the representation of vibrotactile stimuli in S1 depending on the behavioral relevance of the stimuli.

A. Schematic drawing of the relevant mouse in the 2-AFC paradigm. **B.** Calcium transient for the 90 Hz contralateral stimulus during the phases of the protocol (comparing baseline to probe; number of neurons=206, number of animals=5, p=0.001998; comparing baseline to active; number of neurons=206, number of animals=5, p=0.000254). **C.** Calcium transient for the bilateral stimulus combination before and during behavior (number of neurons=206, number of animals=5, p=0.000492). **D.** Classification accuracy for two classes: before and after learning over different population sizes when most active neurons were added first, least active neurons were added first, and a random selection of neurons. Lighter lines correspond to fits of the form: y(x) = A − B*exp (–x / C). **E.** Behavior (not long-term

stimulus presentation) causes an increase in calcium transients as shown by comparing data from 2 animals with a long baseline (15 sessions) with 3 animals that had a short baseline (10 sessions) (comparing base 1. and learn. 2 in animals with a short baseline; number of neurons=119, number of animals=3, p=0.00464). B.-E. Data is for mice with YC3.60 (n=5). Plots are mean ± SEM. The used statistical method was linear mixed effects models. Significance legend: * = p<0.05, ** = p<0.01, *** = p<0.001.

Effects of engaging in a vibrotactile stimulus-guided behavioral task on sensory processing during anesthesia

We investigated the sensory processing of stimuli in the anesthetized state following learning. The vibrotactile stimuli of various repetition rates (10, 40, and 90 Hz) were presented to the animal during anesthesia, both before and after learning. During behavior in the 2-AFC task, we applied a 90 Hz target stimulus and in the last several sessions, in 30% of the trials, a simultaneous 10 Hz distractor stimulus was added. The 40 Hz stimulus was only presented to the animal before and after learning. Hence, the stimulus repetition rates applied in the task were the target 90 Hz and the distractor 10 Hz stimulus. Our results show that, before learning, there is a monotonic increase in neuronal activity with increasing repetition rates of the 1s-long stimulus. The 40 Hz is represented with more neuronal activity than the 10 Hz, and the 90 Hz with more activity than the 40 Hz, reflected both in the averaged trace (**Fig. 16A**) and in the pooled activity (**Fig. 16B** and **16C,** 40 vs. 10 Hz number of neurons=206, number of animals=5, p=2e-16; 90 vs. 40 Hz, number of neurons=206, number of animals=5, p=2e-16, see also **Fig. 13D**). In contrast, after long-term behavior in the 2-AFC task, the monotonic increase in calcium transients with higher repetition rates was abolished (**Fig. 16D**) since the 40 Hz stimulus no longer evokes more activity than the 10 Hz stimulus (**Fig. 16E** and **F**). Hence, the vibrotactile stimuli applied during the task (10 and 90 Hz) were augmented with respect to the stimulus not presented during behavior (40 Hz), therefore disrupting the monotonic increase in response strength with increasing repetition rates. Thus, the monotonic relationship between stimulus repetition rate and neural response strength, which we have shown previously (Mayrhofer et al., 2015b), was extinguished after behavior in a sensory-guided task.

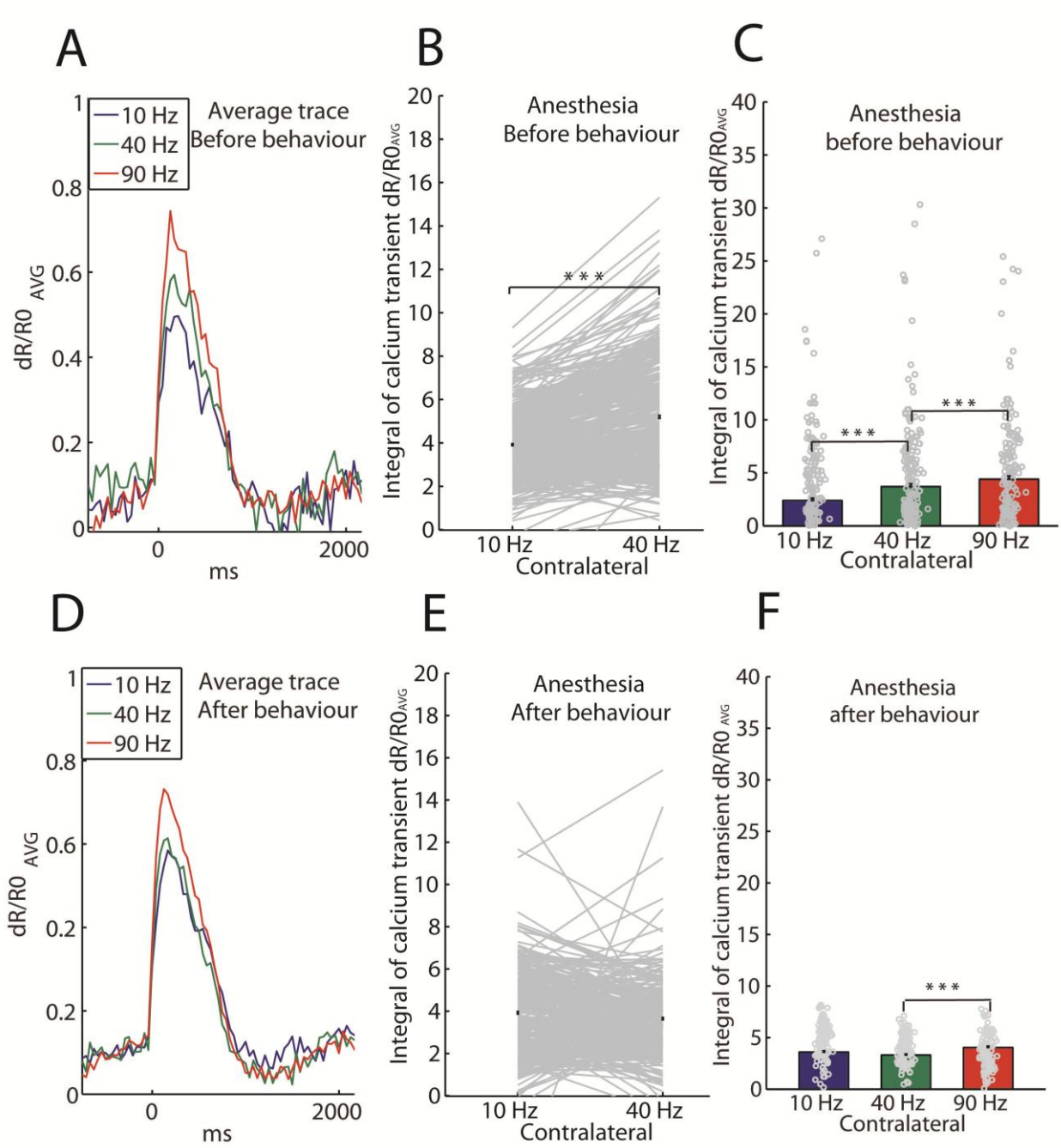

Figure 16. Disruption of the increase of calcium transient with increasing stimulus repetition rate during anesthesia due to behavior in a vibrotactile stimulus-guided task.

A.-C. Baseline (same as **Fig. 13D**). **A.** Average calcium traces for animal m2 for different stimuli. **B.** Calcium transients comparing the representation of 10 and 40 Hz (comparing 10 vs. 40 Hz, number of neurons=206, number of animals=5, p=2e-16). **C.** Responses to vibrotactile stimuli of various repetition rates: 10, 40 and 90 Hz presented on the contralateral side (comparing 10 vs. 40 Hz; number of neurons=206, number of animals=5, p=2e-16; comparing 40 vs 90 Hz; number of neurons=206, number of animals=5, p=2e-16,). **D.-F.** After behavior in the task. **D.** Average calcium

trace for animal m2 for different stimuli. **E.** Calcium transients comparing the representation of 10 and 40 Hz. **F.** Responses to vibrotactile stimuli of various repetition rates: 10, 40 and 90 Hz presented on the contralateral side (comparing 40 vs. 90 Hz, number of neurons=206, number of animals=5, p=1e-4). A.-F. Data is for mice with YC3.60. The gray circles represent the average of the calcium transients for individual cells. The used statistical method was linear mixed effects models. Significance legend: * = p<0.05, ** = p<0.01, *** = p<0.001.

Elevated neuronal activity in S1 during engagement in a tactile 2-AFC task

We investigated how engagement and disengagement in a behaviorally relevant task are reflected in the neuronal activity of layer 2/3 neurons in the primary somatosensory cortex. The distinct advantage of the 2-AFC task, as opposed to a commonly used Go-NoGo task (Yang et al., 2015), is that it can clearly differentiate between engagement and disengagement since it permits three possible behavioral outcomes (**Fig. 17A**). The first outcome occurs when the animal licks a water spout on the side where the stimulus was presented, and consequently retrieves a water reward ("correct"); second, when the animal licks the water spout on the opposite side to where the stimulus was presented ("error") with no water reward; and third when the animal withholds licking completely ("miss"), equally with no water reward (schematic drawings are shown in **Fig. 17A**; behavioral performance of animal m4 in **Fig. 17B;** behavioral data for all animals in **Supplementary Fig. 1**). Calcium traces of single cells (**Fig. 17C**) and averaged YC3.60 and GCamp6f calcium traces (**Fig. 17D**; data for all animals in **Supplementary Fig. 2**) show that all categories evoked robust activity. However, missed trials were represented with lower amplitude calcium transients compared to correct or error trials. We thus evaluated the impact of engagement by analyzing the engaged category, consisting of pooled correct and error trials versus the disengaged category, consisting of missed trials. We observed that the calcium transients are significantly larger during behavioral engagement in the 2-AFC task compared to the miss responses, where the animal received identical tactile stimulation without producing a behavioral response by licking one of the two waterspouts (disengaged category) (**Fig. 17E** left and **17F**, number of neurons=206, number of animals=5, p=2e-16) and **Fig. 17E** right GCaMP6f (right, number of neurons=56, number of animals=1, p=8.88e-16). We applied a non-linear support vector machine classification procedure to investigate whether a classifier could separate trials based solely on their calcium transients. We show that our classifier

could differentiate between the engaged and disengaged category in four out of five animals when the stimulus was presented on the contralateral side, and in three out of five animals when the target stimulus was presented on the ipsilateral side (**Table 1.,** all bolded values are statistically significant; all applied parameters are shown in **Supplementary Table 1.**). In addition, classification accuracy analysis at 80% of accuracy levels for engagement versus disengagement shows that it takes, on average, 13 of the most active cells from the entire neuronal population to distinguish the two categories; 23 cells when they are picked randomly, and 28 cells when the least active cells were taken first (**Fig. 17G**; mean value across animals computed as the maximum of the curve for each individual animal). Taken together, these results indicate that the primary sensory cortex represents sensory stimuli with more neuronal activity when the animal is actively engaged in a sensory-guided task than when it is disengaged, indicating a correlation between sensory cortex activity and perceptual choice.

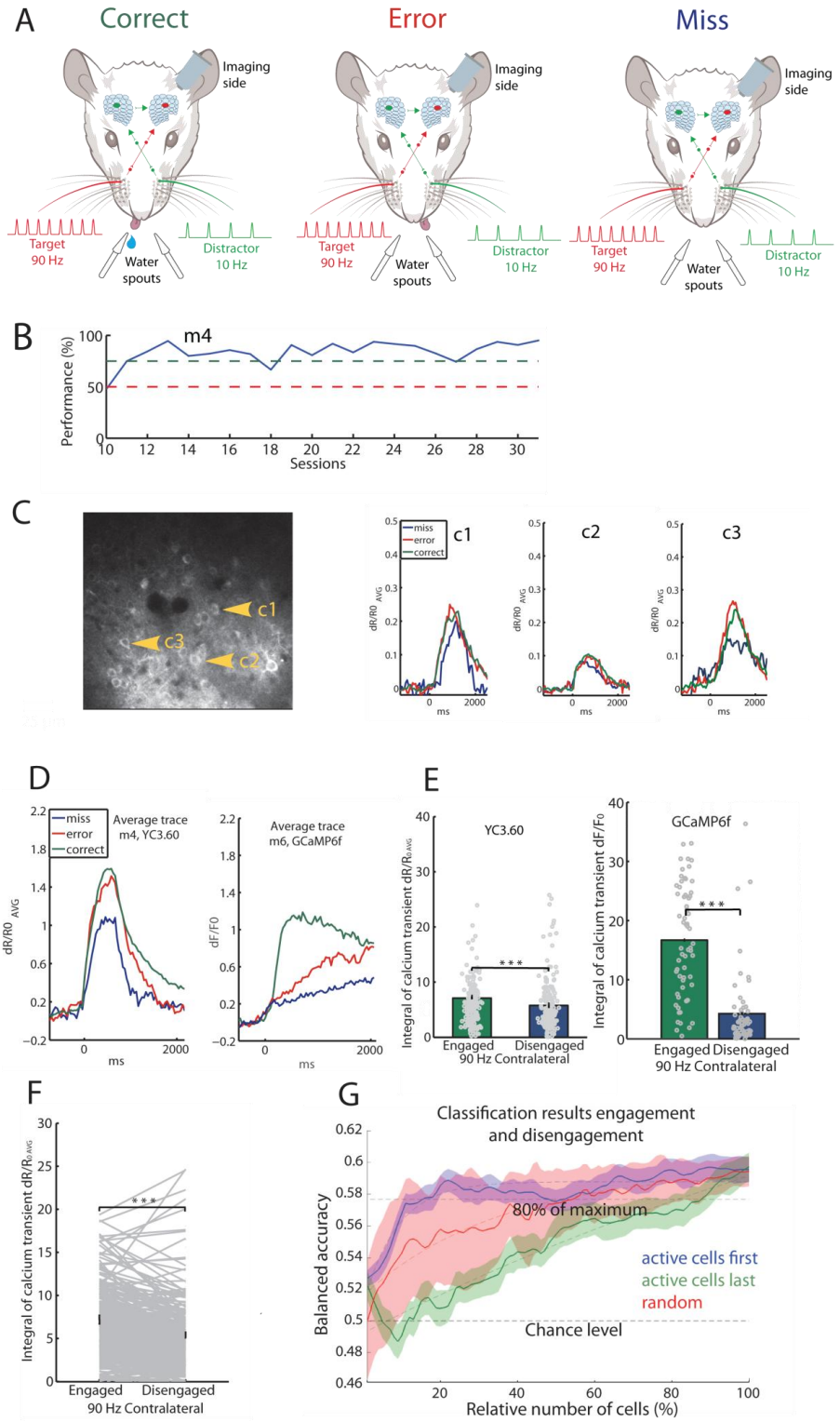

Figure 17. The excitatory effect of engagement in the 2-AFC task on neuronal activity during ongoing behavior.

A. Schematic drawing of three possible behavioral outcomes in the 2-AFC task; correct, error and miss. **B.** Behavioral performance of animal m4. **C.** An example of a two-photon imaging field (256x256 resolution) with calcium transients for 3 single cells (c1, c2,

and c3) in response to the 90 Hz contralateral target stimulus, for the behavioral categories correct, error and miss. **D.** Averaged calcium traces for an example animal with YC3.60 (m4) and GCaMP6f (m6) in response to the 90 Hz contralateral target stimulus for the behavioral categories: correct, error and miss. **E.** Pooled calcium transients in response 90 Hz contralateral target stimulus for the engaged (correct and error trials pooled) and disengaged categories (miss trials), for animals with YC3.60 (left, number of neurons=206, number of animals=5, p=2e-16) and GCaMP6f (right, number of neurons=56, number of animals=1, p=8.88e-16). **F.** Same as **6.E.** left. **G**. Classification accuracy for 2 classes (engaged versus disengaged) over different population size was tested when the most active neurons were added first, the least active neurons were added first, and neurons were randomly selected. Lighter lines correspond to fits of the form: $y(x) = A - B*\exp(-x / C)$. Plots are mean ± SEM. D. Left, E. left, F.-G. Data is for mice with YC3.60. D right and E. right is for a mouse with GCaMP6f. The used statistical method was linear mixed effects models. The gray circles represent the average of the calcium transients for individual cells. Significance legend: * = p<0.05, ** = p<0.01, *** = p<0.001.

Animal m1	**Before and after learning**		**Engagement and non-engagement**	
Target side	Contralateral	Ipsilateral	Contralateral	Ipsilateral
Balanced accuracy (%)	**73.2****	**62.1****	**62.5****	50.7
1% chance level estimation:	53.7	57.4	60.9	61.5

Animal m2	**Before and after learning**		**Engagement and non-engagement**	
Target side	Contralateral	Ipsilateral	Contralateral	Ipsilateral
Balanced accuracy (%)	**79.7****	57.6	53.1	56.2
1% Chance level estimation:	58.3	59.8	57.2	56.5

Animal m3	**Before and after learning**		**Engagement and non-engagement**	
Target side	Contralateral	Ipsilateral	Contralateral	Ipsilateral
Balanced accuracy (%)	**71.9****	**61.3****	**61.8****	**59.6****
1% Chance level estimation:	55.6	54.3	55.2	54.3

Animal m4	**Before and after learning**		**Engagement and non-engagement**	
Target side	Contralateral	Ipsilateral	Contralateral	Ipsilateral
Balanced accuracy (%)	**86.7****	**67.5****	**66.6****	**70.7****
1% chance level estimation:	54.5	54.4	55.0	54.0

Animal m5	**Before and after learning**		**Engagement and non-engagement**	
Target side	Contralateral	Ipsilateral	Contralateral	Ipsilateral
Balanced accuracy (%)	**87,4****	**75,5****	**62,4****	**60,7****
1% chance level estimation:	56,3	56,5	58,1	59,7

Table 1. Best single-trial classification results.

Bold, balanced accuracy values (Bacc) indicate results above the 1% chance level calculated as performance on the whole data set. The analyzed time window was 1000ms, and only unilateral 90 Hz stimuli were taken into consideration. “Before and after learning” compares data from before learning (baseline in the awake state) and after learning (after the animals reach a 75% threshold of performance). “Engagement” compared the engaged category (correct and error trials) versus the disengaged (missed trials) category. Data is for mice with YC3.60 (n=5), for 206 neurons Significance legend: ** = $p<0.01$.

5.5. Discussion

The main result of the present study is that neuronal coding of bilateral vibrotactile whisker stimuli in S1 is plastic during learning. We confirmed our previous results performed in anesthetized animals (Mayrhofer et al., 2015b): that stimulus-evoked activity increased for higher pulse repetition frequencies in awake animals that were not engaged in a task. Furthermore, we could show that interhemispheric interactions in layer 2/3 neurons of awake animals lead to increased calcium transient amplitude, where contralateral representations are enhanced by ipsilateral input from the other hemisphere. This is also in line with our previous report of stable long-term representation of the aforementioned aspects in anesthetized animals. These inter-hemispheric interactions are still poorly understood on a cellular level, and conflicting results concerning the sign (depressing or facilitating) of these interactions have been published in recent years (Palmer et al., 2012).

The highly stable representations of vibrotactile stimuli were subjected to plastic changes once the animal used these stimuli to solve a bilateral detection and discrimination task. Notably, the response amplitude of S1 neurons were increased once the animal was learning a discrimination task. This finding is in contrast to highly stable long-term neuronal representations of vibrotactile stimuli in anesthetized and awake mice not engaged in a task (Mayrhofer et al., 2015b). Both unilateral stimuli (used in the detection task) and bilateral stimuli (presented in the discrimination task) led to significantly increased responses during learning, compared to awake recordings in the same mice before task training began. In addition, we demonstrated that the typical stimulus frequency dependent increase in neuronal response amplitudes (Mayrhofer et al., 2015b) is disrupted after learning the task. Stimuli that were only presented in the anesthetized state (before and after the learning phase) did not elicit neuronal responses following the aforementioned rule after learning.

Specifically, we used a 40 Hz stimulus only in the anesthetized condition. Therefore, this stimulus was never presented and perceived by the animal in the behavioral task. These results hint to the fact that conscious perception of stimuli may be necessary to induce stimulus-specific learning-related plasticity.

On a shorter timescale, we observed trial-to-trial variations in neuronal response magnitude that were related to the engagement of the animal during the behavioral session. Trials where the mouse reported the perceived stimulus elicited larger responses to the tactile

stimulus in layer 2/3 neurons of S1, compared to the trials where the animal did not respond to the stimulus.

Inter-hemispheric processing of vibrotactile stimuli in layer 2/3 of S1

Electrophysiological studies have shown large responses to ipsilateral stimuli in the barrel cortex (Shuler et al., 2001; Wiest, 2005). However, one shortcoming of these studies is a lack of clear histological confirmation of the recording locations on the somatotopic map and cortical depth. In the current study, we were able to precisely target our imaging locations within the barrel cortex with the help of an intrinsic optical imaging mapping technique. Our imaging data from layer 2/3 neurons differed from these previous reports (Shuler et al., 2001; Wiest, 2005), as responses to ipsilateral stimuli were by far lower than the responses on the contralateral side. We investigated interhemispheric interactions in cortical layer 2/3 since it is still unknown how bilateral interactions take place in different cortical layers of S1 at a cellular level. Previous reports on layer 5 activity show an opposite effect; namely, a contralateral stimulus was inhibited due to an earlier ipsilateral stimulus (Shuler et al., 2001). Inhibition due to ipsilateral modulation was also identified in cortical layer 5 in the hindpaw region of the primary somatosensory cortex (Palmer et al., 2012). The discrepancy in these effects may stem from the differences in cortical layers observed and/or from different timings of the contra- and ipsilateral stimulus onset. We designed the behavioral paradigm in such a manner as to mimic a natural situation where the animals typically receive a constant stream of simultaneous bilateral tactile input while exploring their environment.

Plasticity effects due to learning of a sensory-guided behavioral task

In this study, we show that behavior in sensory-guided behavior evoked a substantial and long-term increase in calcium transient amplitudes of task-relevant stimuli. Hence, layer 2/3 neurons in S1 display flexible modulation depending on the behavioral relevance of the presented whisker stimuli. Our findings complement previous studies showing that learning a novel conditioning task reorganizes sensory-driven activity in the rodent somatosensory

cortex (Gdalyahu et al., 2012; Long and Carmena, 2013). Importantly, in addition to these previous investigations, we were able to follow the evolution of neuronal responses in defined neurons of a layer 2/3 population over an extended time span that covered anesthetized, awake and task learning phases. One possible mechanism for the learning-induced plasticity in S1 may be the selective plasticity of the inhibitory system gating cortical information flow based on the behavioral relevance of the stimulus. This form of selective cortical plasticity has been shown in layer 2/3 of the auditory cortex and was explained by a selective increase or decrease in the activity of local somatostatin interneurons (Kato et al., 2015). It also has been shown that the S1 GABAergic system is required for both the manifestation of functional cortical representation plasticity and for the development of a conditioned response (Posluszny et al., 2015). Future studies of learning-related plasticity of the somatosensory system will certainly benefit from the use of transgenic mouse lines with markers for different types of interneurons. The results of our study show that cells witness elevated levels of activity in the neighboring barrel after behavior in a sensory-guided task, suggesting an expansion of cortical representation of the main whisker that was used to solve the task. This effect has been described in the auditory system (Reed et al., 2011), with the magnitude of map expansion being proportional to the animal's level of motivation in a behaviorally-relevant paradigm (Rutkowski and Weinberger, 2005). However, it remains an open question how these plastic effects evolve in single cells over extended periods, when the animals are confronted with multiple novel behaviorally relevant scenarios. Taken together, we show that a behaviorally-relevant context of learning plays a distinctive role in shaping sensory representation in layer 2/3 at early stages of cortical processing. Modulation of sensory processing due to behavior in a sensory-guided behavioral task was also observed in recordings we performed under anesthesia. In the pre-learning phase, anesthetized animals show a monotonic increase in neuronal activity with increasing repetition rates of the stimulus (10, 40 and 90 Hz). After long-term behavior in the 2-AFC task, involving the highest (90 Hz) and lowest (10 Hz) frequency of the vibrotactile stimulus, the 40 Hz stimulus was no longer evoking larger calcium transients compared to the 10 Hz stimulus. Hence, the strong trend of monotonic increase with higher whisker deflection rate was abolished. Thus, behavior in a sensory-guided behavioral task modified stimulus processing as shown by the stimulus response of trained animals under anesthesia. Therefore, we conclude that stimuli with behavioral relevance showed larger neuronal activity after learning than stimuli without

task relevance. Taken together, we corroborate that the barrel cortex is highly plastic and adapts its coding strategies continuously to changes in the environment (Bekisz et al., 2010; Galvez, 2006; Gdalyahu et al., 2012; Kato et al., 2015; Kuhlman et al., 2014; Polley, 2006; Polley et al., 1999; Takahashi et al., 2011).

The impact of task engagement on cortical representation of vibrotactile stimuli

We addressed the issue of the impact of decision-related trial to trial variability in cortical responses in a sensory-guided behavioral task. We found that once the animal was engaged in the task, demonstrated as an engaged licking behavior, the cortical representation of identical sensory stimuli was enhanced compared to trials where the animal did not respond by licking (miss trials). Several potential mechanisms could explain these enhanced responses when the animal is actively involved in solving the task. Attention effects have been extensively studied in monkeys showing increased firing rates of cortical sensory neurons in receptive fields that were lying in the experimentally controlled spotlight of attention (Cohen and Maunsell, 2009; Steinmetz and Moore, 2014). Arousal and motivation of the animal may also explain our results that correct and incorrect response leads to higher response amplitudes compared to the trials where the animal did not respond to the stimulus presentation (miss condition). Neuromodulatory systems that are strongly linked to arousal and motivation states have been demonstrated to impact choice-related cortical activity (Constantinople and Bruno, 2011; Pinto et al., 2013). In a Go-NoGo task, it has recently been shown in mice that larger tactile responses were elicited in S1 for correct responses in comparison to missed trials, which is in agreement with our findings, confirming that responses in S1 predict perceptual choice (Kwon et al., 2016; Yang et al., 2015). One shortcoming of these studies is that the task design used may lead to the imprecise classification of the animal's choice. In the Go-NoGo task, it is difficult to distinguish a lack of motivation or lapses of attention from false rejections or correct rejections. The 2-AFC task design used in the present work has several advantages compared to Go-NoGo paradigms, as it allows a clear distinction between a lack of motivation/attention from correct and error responses. Therefore, it is ideally suited to study the impact of task engagement on state-dependent neuronal processing. Future

developments of highly complex attention paradigms in head fixed rodents will make it possible to dissect the involvement of arousal and attention mechanisms at a circuit level. However, it is still an open question if the required level of task complexity previously used in monkey paradigms can be reached in head-fixed rodents. A limitation of our work is that the two-photon imaging technique lacks the temporal resolution to disentangle the contribution of thalamocortical feed-forward and feedback influence of higher cortical areas onto the observed engagement modulated tactile responses. Future work using electrophysiological recordings paired with behavioral paradigms optimized to study decision and attention effects will be required to shed light on these state-dependent modulations of cortical network activity.

In summary, we have shown that the magnitude of neuronal responses in the primary sensory cortex is subject to variability predicted by the animal's engagement, indicating an allocation of perceptual resources adapted to the behavioral necessities.

3. General Discussion

3.1. The multiple roles of the primary sensory cortices

A long-held view in perceptual learning is that the primary sensory cortex serves merely as a relay in processing sensory information arriving from the thalamus, as a part of a hierarchical feed-forward network. From a computational point of view, it is hard to imagine that such a system would be able to recognize complex and changing patterns of sensory input (Gilbert et al., 2001). Indeed, there is accumulating evidence that the primary sensory cortex (S1) is involved in multiple functions. The long-range reciprocal connections are connected to a variety of other brain areas (secondary somatosensory cortex, motor cortex, perirhinal cortex, thalamus, thalamic reticular nucleus, zona incerta, anterior pretectal nucleus, superior colliculus, pons, spinal trigeminal brainstem nuclei, red nucleus, etc.) that support this notion (Aronoff et al., 2010). Deactivating the auditory cortex shows clear impairments in performing sound-guided behavioral tasks (Jaramillo and Zador, 2011). It has also been shown that the primary somatosensory cortex has a causal role in performing whisker-guided detections tasks (Sachidhanandam et al., 2013) with reliable behavior being optogenetically evoked by as little as 1% of barrel cortex neurons (Huber et al., 2008). Although S1 it is not necessarily needed for a Go-NoGo task, more complex behavior, such as a 2-AFC task, cannot be performed without its involvement (Diamond and Arabzadeh, 2013). Surprisingly, it has been shown that the primary auditory cortex encodes non-sensory variables (such as selection rules) as to what stimulus should be attended to (Rodgers and DeWeese, 2014). In addition, the retrieval of perceptual knowledge activates the corresponding primary sensory area (Goldberg, 2006). Furthermore, it can hold the working memory trace of a specific stimulus in tasks that require a brief memory detention (Harris et al., 2001) or even store long-term memory (Weinberger et al., 1993). This memory is characterized by being specific, rapidly created, and maintained for longer periods of time (Weinberger, 2007). The primary sensory cortex is also implicated in representing the timing of an expected reward (Gavornik et al., 2009; Pleger et al., 2008) which was previously thought to be reserved exclusively for higher cortical areas. In addition, the predictable timing of task-related sensory stimuli seems to ameliorate the speed and accuracy of

performance, by improving both sensory processing and motor preparedness (Jaramillo and Zador, 2011). Most importantly for this thesis, there is strong evidence that behavior in a sensory-guided conditioning tasks induces neuronal plasticity in primary sensory cortices (Butt et al., 2009; Gdalyahu et al., 2012; Long and Carmena, 2013; Polley, 2006; Recanzone et al., 1993; Weinberger, 2007; Weinberger et al., 1993). Hence, primary sensory cortices can perform a variety of tasks well beyond solely transferring sensory information. They are the locus of the interaction of top-down and bottom-up flows of information, dynamically adapting by performing different algorithms in response to different behavioral contexts (Fritz et al., 2007; Gilbert et al., 2001). Top-down influences include attention, expectations, priming, perceptual tasks, and hypothesis testing, showing a richness and complexity of internal representation. Attention as a top-down event is thought to activate the nucleus basalis, that in turn via the neuromodulator acetylcholine activates muscarinic receptors in the primary sensory cortex that are responsible for gating plasticity events (Fritz et al., 2007). Several other neuromodulators have been shown to shape brain states through both direct and indirect connections (Hurley et al., 2004). Thus, a hypothesis as to how cortical areas interact in perceptual learning is through the gating mechanisms of the specific brain state, which communicates how sensory inputs should be interpreted at all levels of processing through a mutual action of several brain states and feedback connections (Gilbert et al., 2001). This enables multiple functions of each cortical area, including the primary sensory cortices. In essence, cortical networks do more than signal processing. Rather, they generate goal-oriented behavior as a result of a joint context of internal and external signals (Feldmeyer et al., 2013).

3.2. How well do learning and map plasticity correlate?

It is generally considered that learning a sensory-guided behavioral task coincides with plasticity events (Froemke et al., 2012), or more specifically that plasticity is a neuronal substrate for learning to occur (Conner et al., 2003). In our results, a causal relationship between learning and plasticity cannot be concluded, since control experiments without learning were lacking, but rather a correlation with learning induced by repeated stimulus presentation. Conditioning tasks induced impressive changes in the responses of infragranular layers of the somatosensory cortex, such as an increased number of responsive neurons and the prolongation of responses (Wiest et al., 2010). These changes were specific

to the salient stimulus applied in the experimental paradigms (Kilgard et al., 2002). Several studies have shown that modifications to the response properties of the primary somatosensory cortex occur in concert with learning a novel conditioning task (Gdalyahu et al., 2012; Long and Carmena, 2013). Interestingly, map enlargement has been shown to increase proportionally with the degree of learning (Rutkowski and Weinberger, 2005). Even more so, preventing map expansion by blocking cholinergic modulation has been shown to impair learning (Conner et al., 2005; Miasnikov et al., 2001; Ramanathan et al., 2009). However, Peron et al. failed to find the expansion of the cortical representation of the spared vibrissa used in whisker-guided behavior (Peron et al., 2015). Indeed, cortical map expansion does not always correlate with learning (Reed et al., 2011), to the point of the absence of modifications of cortical topography, with only slight changes in response properties (Brown, 2004). It has been proven equally difficult to establish a causal connection between hippocampal LTP and learning (Buonomano and Merzenich, 1998). Yet, results from another set of studies demonstrate that map plasticity undergoes transient enlargement during learning, enhancing performance, and subsequently renormalizes following task mastery (Molina-Luna et al., 2008; Reed et al., 2011; Yotsumoto et al., 2008). The renormalization of cortical maps probably takes place once the minimum number of cells for successful task performance has been established (Gdalyahu et al., 2012). Furthermore, the degree of map expansion was correlated with the animal's motivation to perform (Reed et al., 2011). The mentioned discrepancies could be due to different recording methods and recording sites, different time-points of data acquisition with respect to the learning phase or even differences in the task design itself. Task design plays a crucial role since it has been shown that task strategy strongly determines map plasticity overriding the impact of motivation (Bieszczad and Weinberger, 2010b). It should be noted that only a subset of neurons are subject to plasticity changes to allow for the preservation of the stability of cortical networks (Fritz et al., 2007). This fact could add to explaining observed discrepancies in comparing results from different experiments.

3.3. Modulation of neuronal representation of stimuli

Passive exposure to repeated presentations of sensory stimuli leads to cortical habituation and reduction of neuronal responses (Kato et al., 2015). As the animal learns that a stimulus in not behaviorally relevant, the amount of dedicated cortical activity will be

reduced, likely since paying attention to it presents no evolutionary advantage. However, this process can be reversed once the stimulus gains behavioral significance. Indeed, a wealth of research has shown that neuronal activity in the primary sensory cortex can be rapidly reorganized through behaving in a sensory-guided task (Gdalyahu et al., 2012; Long and Carmena, 2013; Siucinska and Kossut, 1996). This flexible increase in activity could be regulated by the suppression of somatostatin-expressing (SOM) cortical interneurons and not by thalamic input since layer 4 cells do not show modifications in their activity (Kato et al., 2015). Indeed, it has been shown that a prerequisite for plasticity is a period of restricted inhibition (Froemke et al., 2012; Posluszny et al., 2015). One of the possible mediators of this shift in the balance between excitation and inhibition could be the cholinergic neuromodulatory system (Froemke et al., 2012; Pinto et al., 2013; Polack et al., 2013) which also drives activity in SOM-expressing cells (Chen et al., 2015). The excitatory drive from higher-up cortical areas could equally regulate the activity in SOM cells, or even their inhibitory neighboring neurons (Lee et al., 2013; Pfeffer et al., 2013; Pi et al., 2013). In the study presented in this thesis, we could not find specific neurons that were the carriers of the bidirectional modulation. Rather, the changes were reflected in the mean activity of the population, with variable activities of individual neurons as shown in studies monitoring long-term responsiveness of barrel cortex neurons (Lütcke et al., 2013b). It has been thought that attention gates plasticity events. Attentional shifts can occur as fast as 20ms after stimulus onset (Panteví et al., 1993), and plasticity modifications can last up to a lifetime, showing a difference in the timescales. Attention seems to be a precursor for plasticity changes, but to sustain these modifications, most likely non-attentional mechanisms take place (Fritz et al., 2007).

3.4. Engagement and state dependent cortical processing

Rodent behavioral engagement increases cortical neuronal responses to the same sensory stimulus, both in research presented in this thesis and in that of others (Fritz, 2005; Sachidhanandam et al., 2013; Yang et al., 2015). Engagement in a task is likely to involve higher level processing, such as sensorimotor integration, motivational impact, attention, the expectation of reward, associations between stimuli and rewards, etc., but their exact mechanisms of sensory processing are still unclear (Krupa et al., 2004). Krupa and colleagues have shown in the infragranular layers an earlier onset of responses in the engaged

condition due to top-down effects, possibly from the secondary somatosensory cortex, motor cortex, or contralateral S1 (Krupa et al., 2004). Furthermore, the fact that the animal is immobilized for long periods can have a negative impact on motivational levels. An increase in the number of missed trials is noticed as the behavioral session progresses most likely due to satiation leading to a reduced motivation to perform the task. In our behavioral paradigm, fluctuations in attention can be an additional factor explaining the missed or error trials. However, our paradigm cannot directly test the effects of attention on task performance. Another important factor in the animal's choices in performing the task is its previous decision history. According to Bayes' theorem the known probability of an event is constantly updated with incoming new information. Hence, the animal integrates the outcomes of its choices with previous decision history.

However, some studies suggested that behavior in a task does not affect evoked responses, but has an excitatory effect on thalamic activity (Otazu et al., 2009), or modulates spontaneous activity (Rodgers and DeWeese, 2014). Indeed, endogenously produced spontaneous patterns of activity interact with sensory input in primary sensory areas (Ringach, 2009). Nonetheless, a majority of studies show an increase in firing rates during task engagement that was explained in monkeys as enhanced attention (Cohen and Maunsell, 2009; Reynolds and Chelazzi, 2004; Steinmetz and Moore, 2014). Attention is likely to be a top-down effect, desynchronizing the cortical area that represents the attended object or feature (Chalk et al., 2010; Cohen and Maunsell, 2009; Mitchell et al., 2009). Interestingly, the elevation in activity during a behavioral output in the engaged condition, in comparison to passive stimulus exposure, is caused by a late depolarization starting at 50ms after stimulus onset (Sachidhanandam et al., 2013). Furthermore, this effect does not seem to arise from the thalamus or even mechanoreceptive neurons, but rather as a top-down effect from the secondary somatosensory cortex (Yang et al., 2015). This does not exclude the likely impact of the neuromodulatory systems, such as the cholinergic system, which has a causal role in regulating cortical activity and sensory processing (Butt et al., 2009; Pinto et al., 2013) or the noradrenergic system that regulates wakefulness (Constantinople and Bruno, 2011). Stimulating the reward system of the brain via VTA dopaminergic release stimulates the formation of stimulus-specific cortical map enlargement, demonstrating the involvement of primary sensory cortices in reward-

processing (Hui et al., 2009; Pantoja et al., 2007; Shuler and Bear, 2006). Interestingly, Otazu and colleagues have shown the exact opposite in their study done in the rat auditory cortex (Otazu et al., 2009). While the rat was engaged in a 2-AFC task, sound-evoked responses paradoxically witnessed a reduction in the primary auditory cortex as shown by electrophysiological recordings, possibly due to a depression at the thalamocortical synapses (Otazu et al., 2009). This discrepancy could be explained by recording performed in deeper layers. Also, their sensory stimulus was far from the threshold, and the observed reduction could have been for the irrelevant stimuli (Otazu et al., 2009).

Whisking behavior can also present an influence on sensory processing. Quiet immobility of the animal allows for optimal single-stimulus detection, whereas whisking facilitates the detection of multiple whisker stimuli (Fanselow and Nicolelis, 1999; Nicolelis and Fanselow, 2002). Thus, cortical resources dedicated to the processing of sensory signals appear to be allocated depending on the behavioral state of the animal (Fanselow and Nicolelis, 1999; Niell and Stryker, 2010; Zhou et al., 2014) and are continuously modified in response to external demands (Ulanovsky, 2004). Different cortical states were first observed via EEG measurements and span a large range from highly synchronized to highly desynchronized states, that in turn can have various amounts of gamma activity and/or activate different cell types (Harris and Thiele, 2011). It is important to note that the passive and awake state is not simply a point between the fully active engaged state and sleep, but that each state has a distinct and characteristic neuronal signature (Otazu et al., 2009). The organism shifts between different brain states via several different mechanisms. Activating the cholinergic systems plays a partial role in desynchronizing the brain state (Buzsáki et al., 1988; Mena-Segovia et al., 2008; Metherate et al., 1992). The serotonergic system can equally play a role in desynchronizing the brain independently of acetylcholine (Dringenberg et al., 2003), as can the noradrenergic system (Constantinople and Bruno, 2011). These neuromodulatory systems are activated via salient rewarding or punishing stimuli, external events, attention, and expectations on a moment-to-moment basis (Clayton, 2004; Lin and Nicolelis, 2008; Otazu et al., 2009; Ranade and Mainen, 2009; Richardson and DeLong, 1990). Besides the various neuromodulatory systems, thalamic glutamatergic neurons can cause cortical desynchronization by increasing their tonic firing rates (Bezdudnaya et al., 2006; Fanselow et al., 2001; Otazu et al., 2009). Both the thalamic relay cells and its reticular neurons are subject to cholinergic excitation and inhibition, respectively (Hirata, 2006). It is,

however, important to note that the mentioned glutamatergic and neuromodulatory systems have different effects on different neurons and synapses, and in different cortical areas (Dembrow et al., 2010; Kawaguchi and Shindou, 1998; Lawrence, 2008).

3.5. Where is the error signal encoded?

When behavior does not lead to the desired outcome in instrumental conditioning, the occurrence of a prediction error leads to behavioral readjustment, also explained as "causal learning". Both successes and failures offer valuable information with regards to optimizing task performance. Instead of evaluating all the incoming and outgoing information, the organism optimizes neuronal processing by comparing what is predicted with what occurs. This learning of adapting to outcomes lasts theoretically until the prediction errors are eliminated. In this thesis, it has been shown that correct and erroneous responses are represented with a similar, statistically indistinguishable amount of cortical activity in the primary somatosensory cortex. Indeed, errors are thought to be signaled in the prefrontal and cingulate cortex, with the construct and distribution of error signals arising from the dopaminergic system (Alexander and Brown, 2011; Frank et al., 2005; Matsumoto et al., 2007; Rushworth and Behrens, 2008; Schultz et al., 1997; Yuan et al., 2015). The cholinergic, as well as noradrenergic system, have also been implicated in coding unpredicted stimuli and rewards, rapidly shifting the animal's attentional and behavioral processing (Schultz and Dickinson, 2000). The integration of a neuronal error signal would involve Hebbian-learning rules (Schultz and Dickinson, 2000), with the responses shifting from the primary reward (unconditioned stimulus) to the predictive (conditioned) stimulus via the activity of dopaminergic and noradrenergic neurons (Aston-Jones et al., 1994). However, error-related activity has also been shown in the primary visual cortex, with the target stimulus receiving less activity than the distractor on erroneous trials, due to top-down influences from the prefrontal cortex transmitting the erroneous judgment to the primary area (Pooresmaeili et al., 2014). Another study explained the exact mechanism of this process in humans, showing that after an error the pMFC, via the activation of cholinergic projections, adjusts neuronal activity in task-relevant brain areas by increasing the representation of relevant stimuli and decreasing the activity or irrelevant stimuli (Danielmeier et al., 2015). Behavioral optimization after an error seems to depends on top-down influences for their detection and implementation.

3.6. Bilateral integration and ipsilateral stimuli

The rodent's cerebral cortex has to continually compare sensory information coming from vibrissae on both sides of the snout to navigate the environment (Shuler et al. 2002). Shuler et al. have shown with electrophysiological recordings that ipsilateral and contralateral responses in layer 5 are comparable in magnitude (Shuler et al., 2001). In contrast, our imaging data from layer 2/3 shows that ipsilateral responses are considerably smaller. This indicates potential discrepancies across cortical layers in representing sensory input from different hemispheres in the barrel cortex. Conflicting data also presents itself regarding interhemispheric interactions, which remains a poorly understood topic. Data presented in this thesis supports the notion that a simultaneously presented ipsilateral stimulus will strengthen the sensory representation of the contralateral stimulus in layer 2/3. In contrast, Shuler et al. have shown that a temporally preceding ipsilateral stimulus will inhibit a contralateral stimulus in layer 5 (Shuler et al., 2001). Inhibition in layer 5 due to pairing with an ipsilateral stimulus has also been shown in the hindpaw region (Palmer et al., 2012). Wiest and colleagues have shown that in awake animals, simultaneous bilateral stimulation shows strong interactions and heterogeneity of effects (Wiest, 2005). Since callosal fibers are predominantly excitatory in nature, inhibition could be due to local interneurons. The differences in effects in bilateral interactions could be due to differences in the respective timings of the stimulus occurrence and/or that they take place in different cortical layers, possibly via diverse mechanisms.

Interestingly, learning can be transferred across the hemisphere to the homologous barrel (Harris and Diamond, 2000). The transfer of learning is faster, the larger the shared cortical area (Harris et al., 1999). Another possible site for interhemispheric interaction is the secondary somatosensory cortex since it is reciprocally connected with the primary and secondary ipsilateral cortex, the thalamus and the contralateral primary cortex (Debowska et al., 2011). This area display a role in bilateral integration, yet remains still poorly understood (Debowska et al., 2011).

3.7. The complexities of researching learning

The scientific community has been investigating the neuronal underpinnings of learning for over a hundred years. The advancement of exciting new technologies opened

new windows for exploring brain function during learning. In spite of the wealth of research regarding this topic, the comparison is difficult due to differences in the task difficulty, task goals and motivation, species, duration of training, behavioral response, sensory modalities, etc. The environmental context, along with competing inputs, are not usually acknowledged in comparing various research, but they certainly impact results (Moucha et al., 2005). Learning is thought to entail an interaction between local circuits that contain contextual information and feedback connections (Gilbert et al., 2001). The operating principles guiding the restructuring of neuronal networks to adopt new behavior are not fully elucidated. What we do know is that plasticity changes are stimulus-specific (Kilgard et al., 2002), and that the neuromodulatory systems gate behavioral states, and with it experience-dependent plasticity (Ahissar and Hochstein, 1993; Recanzone et al., 1993). However, we do not know if plasticity is a consequence of learning, a homeostatic mechanism to accompany learning, or a mechanism that correlates with learning. Neither a potential causality of plasticity and learning has been elucidated, nor precise rules and mechanism that would explain a potential correlation of learning and plasticity. Furthermore, previous decision history needs to be taken into consideration. There is a prevalent inclination in learning research to focus on a reductionist analytical approach, rather than a synthetic one that calls for a careful all-encompassing integration of many levels occurring on various timescales and brain areas. To fully understand learning both approaches are necessary. For example, learning could entail a specific combination of changes on the intrinsic cellular level (oscillatory ionic conductances, spike initiation threshold, on the synaptic level (LTD, LTP that is explained elsewhere) or circuit-level changes in connectivity. Furthermore, it is important to underline the distinction between learning and performance. Learning is the organism's behavioral potential, by which permanent changes occur through experience, while performance is the displayed, and hence measurable, behavioral outcome (Shackleton-Jones, Gross, McIlveen,1999). Thus, what we are measuring is performance. Conditioning tasks are seen as a relatively simple and controlled paradigm and thus are very appealing to researchers. However, there are several caveats (Gallistel, 2003). Even simple Pavlovian conditioning can involve simultaneous learning of several conditions and related events, requiring the precise determination of the content of learning (Cahill et al., 2001). In fact, even Sir Charles Sherrington said that the rat limb spinal reflex arc was a "convenient fiction" (Cahill et al., 2001). In the seventies, several concepts regarding conditioning were discovered; it is not

the timing of the unconditioned and conditioned response that generates conditioning but their contingency. Conditioning to a new CS does not occur if the US was previously paired with another CS. If two CSs are present from the beginning, the responses to one of them will be much stronger, conditioning will happen with the more reliable of the two available CSs, and so-called “inhibitory conditioning” happens when the CS predicts the omission of a US (Gallistel, 2003). In short, all these discoveries reveal important facts about conditioning; namely, that temporal pairing is not necessary for this process to occur, which is a common misconception. Indeed, there is a lot of information processing that goes beyond mere temporal pairing. Furthermore, the reward is not the only factor guiding behavior. For example, a satiated rat might appear to have not learned the whereabouts of food when left to explore the environment, but when hungry it will find its way since latent learning occurs remaining unnoticeable before a motivator occurred (Tolman, 1932). Mice with a leasoned amygdala do not freeze at the occurrence of the conditioned fear stimulus. Surprisingly, it was discovered only later that when given a chance, they unexpectedly avoided the place of conditioning, and the amygdala lesion had actually impaired their unconditioned freezing ability (Vazdarjanova and McGaugh, 1998)! These examples call for a careful definition of what has actually been learned, in comparison to what is experimentally asked and measured to avoid oversimplification. Ideally, the experimental, theoretical and modeling approaches should work in concert to grant a deeper understanding of learning.

3.8. Methodological considerations and future directions

Plasticity in the adjacent barrel in layer 2/3

Single whisker stimulation is strongly represented in its corresponding barrel, but neighboring columns also respond with calcium transients (Kerr et al., 2007; Sato et al., 2007), given that short-range intracortical projections terminate in the neighboring barrel (Kim and Ebner, 1999). Since rodents use multiple whiskers in exploring their environment, sensory information could likely be stored in cortical areas that exceed the corresponding barrel (Chapin, 1984). Indeed, layer 2/3 neurons display weak whisker preferences (Brecht et al., 2003; Kerr et al., 2007; Margolis et al., 2012; Sato et al., 2007). Single unit recordings have shown that receptive fields of neurons in the rat barrel cortex layer 2/3 typically comprise two to six whiskers (Zhu and Connors, 1999), with the direction of the whisker deflection determining how the response will spread (Andermann and Moore, 2006). A

general characteristic of primary sensory cortices is that infra-and-supragranular layers have larger receptive fields than layer 4, and thus larger and more complex integrated receptive fields can be formed by receiving convergent information and diverging the information forward (Buonomano and Merzenich, 1998). Spatial analysis of plasticity in mouse layer 2/3 neurons showed even stronger effects in barrels adjacent to the principal barrel of the stimulated whisker (Glazewski and Fox, 1996; Margolis et al., 2012). Furthermore, layer 2/3 is a major site for adult neuroplasticity (Diamond et al., 1994). Interestingly, learning of a gap-crossing task can be transferred to the neighboring barrels (Harris and Diamond, 2000). Both exploring plastic changes in the principal and adjacent barrel offers useful information on sensory information processing and plasticity changes in layer 2/3.

Stimulus duration and comparing neurometric with psychometric data

A one-second-long vibrotactile single-whisker stimulus was used in the 2-AFC task in this thesis with repetition rates spanning from 10 to 90 Hz. Stüttgen and Schwarz have shown that detection does benefit from longer stimuli, albeit the improvement with longer stimuli is sublinear. Integration occurs in under 25ms. In this timeframe, neurometric data offer the best sensitivity and agrees with psychometric data (Stüttgen and Schwarz, 2008; Stuttgen and Schwarz, 2010). Indeed, rats display behavioral adaptation only after one brief surface encounter (Mitchinson et al., 2007). For future studies, a shorter stimulus could thus be an interesting avenue of exploration.

GECIs and two-photon calcium imaging

A potential problem with GECIs is their possible interference with normal cell physiology, and/or buffering calcium levels. However, both for GCaMP3 and YC3.60, there were no measurable signs of distortions of neuronal functioning (Huber et al., 2012; Margolis et al., 2012) still, damage cannot be fully excluded. The dynamic range of GECIs can be attenuated by both CaM and CaM-binding proteins present in the cell (Nagai et al., 2004). Since calcium is involved in several plasticity mechanisms, it was hypothesized that calcium indicators could impair plasticity. In recent studies in hippocampal brain slices (Huber et al., 2012) and the barrel cortex (Margolis et al., 2012) there were no noted adverse effects on plasticity due to GECIs. The AAV carrier used to deliver the GECIs labels preferentially excitatory cells, thus potentially causing a bias (Margolis et al., 2012). Another potential

problem with calcium imaging in interneurons is that they contain calcium-buffering proteins such as parvalbumin and calretinin (Barinka and Druga, 2010; Kwan and Dan, 2012; Langer and Helmchen, 2012). Although the number of action potentials can be calculated with a less than 100% success rate from the size of the calcium transient during low firing rates (Grewe et al., 2010; Kerr et al., 2007; Lütcke, 2010; Margolis et al., 2012), the millisecond-scale temporal resolution of action potentials in calcium imaging is not feasible. This is due to the slow decay of calcium removal from the cell, along with the slow rates of its dissociation from the dye (Grienberger and Konnerth, 2012; Helmchen et al., 1996). The two-photon imaging method is limited to the superficial layers, with cortical layer 5 being the limit of allowed depth to date (Mittmann et al., 2011). Red-shifted GECIs could present the possible solution to this shortcoming or imaging with a microprism (Chia and Levene, 2009). Another avenue for future research would be to expand our current imaging field of view by applying novel three-dimensional methods (Göbel et al., 2007) which would eventually allow the investigation of larger neuronal networks across cortical layers.

Novel technologies

Recent years have witnessed the development of exciting new methods for probing brain function and anatomy. Of great interest is the advancement of patch clamp recordings in awake animals, that, for example, led to discoveries regarding the influence of brain states on excitatory and inhibitory neurons (Crochet et al., 2011; Gentet et al., 2010, 2012; Poulet and Petersen, 2008). In freely moving animals, one can now combine optical stimulation with electrophysiological recordings through the advent of the optetrode (Anikeeva et al., 2011). Another technical innovation from the Deisseroth lab is the combination of optogenetic stimulation with fMRI measurements, which showed how global circuits are recruited by certain activity patterns. Fiber optics allows for both cell excitation and recordings in freely moving or anesthetized mice (Adelsberger et al., 2005), (Murayama and Larkum, 2009). These techniques can be combined with powerful genetic tools, which are discussed in the following paragraph. Local connectivity assessments in slices have been performed even with six simultaneous whole-cell recordings (Lefort et al., 2009). The Deisseroth lab and others introduced optimized tissue clearance methods that clear lipids from tissue, yet leaving the proteins, nucleids and all the fine structures intact (Chung and

Deisseroth, 2013). With these methods, histological investigations could be done on very large cortical and subcortical networks to elucidate the system's full connectivity.

Investigating causal roles of neuronal subtypes in plasticity and learning

The research presented in this thesis has shown that mice are equally capable as rats to learn complex tasks. One of the advantages of the mouse as a model organism is that it offers a plethora of transgenic lines, creating unprecedented avenues of research. For example, Cre-transgenic mouse driver lines allow for the identification of specific neuronal subtypes, thus permitting us to dissect their respective contributions and roles in shaping cortical dynamics and plasticity events (Knöpfel, 2012; Lee et al., 2010; Taniguchi et al., 2011; Zariwala et al., 2011). Beyond subtype identification, optogenetic tools allow us to reversibly and selectively activate and/or silence neuronal classes to probe their causal role in a variety of paradigms (Guo et al., 2014; Kim et al., 2013; Yizhar et al., 2011). To expand the work presented in this thesis one could, with the help of genetic tools, identify various sub-groups such as inhibitory neurons to dissect the circuitry involved in cortical map plasticity, since it has been shown that the transient increase in the excitation versus inhibition ratio correlates with plasticity (Froemke et al., 2012; Yang et al., 2015). Layer 2/3 is particularly interesting, since it is under strong inhibition from GABAergic neurons firing at considerably higher rates than excitatory neurons, and are responsible for the sparse coding (Gentet et al., 2010). Optogenetic manipulations of GABAergic neurons could elucidate their causal role in shaping cortical firing patterns (Guo et al., 2014). Since cholinergic modulation has been implicated as an attentional gateway for plasticity, one could optogenetically silence or activate it to tease out its potential causal role in learning (Ahissar and Hochstein, 1993).

Open questions regarding plasticity and learning

Many questions remain to be addressed regarding neuronal plasticity beginning with the fact that we still do not have a clear understanding of how the cortex processes information. How the brain can learn useful new associations from the stream of incoming and often competing sensory information is still unclear, although computational models of selective attention have tried to elucidate this topic (Dayan et al., 2000). Furthermore,

research is needed regarding the specific roles and modalities of inhibition, how different layers contribute and interact, the sites of plasticity, what are the interactions and respective roles of the three studied levels of plasticity (synaptic, cellular and representational), etc. A vast yet crucial undertaking would be to tease apart the causal link between plasticity and cortical map reorganization since they are classically studied separately. An interesting question that could be easily addressed with our setup is to deepen the understanding of how the behavioral strategy used affects the expression of neuroplasticity (Bieszczad and Weinberger, 2010b). It is important to underline that direct comparison between tasks is difficult due to different levels of motivation, task difficulty, training duration, behavioral responses, task goals, etc.

To deepen our understanding of learning, a critical goal would be to find possible rules that govern it. Classical Hebbian plasticity rules focus on pre-and-post synaptic activity. However currently it is hypothesized that a third neuromodulatory gating factor, coding for novelty and/or reward, should be included (Frémaux and Gerstner, 2016). For example, a reward-modulated Hebbian learning rule suggests that the correlation between presynaptic activity, the difference from the recent mean of the postsynaptic potential, and a neuromodulatory reward signal drives synaptic weight changes (Loewenstein and Seung, 2006). Three-factor learning rules, including dopaminergic activity, have been already studied in corticostriatal synapses (Reynolds and Wickens, 2002), although they have not been rigorously studied experimentally. For reward-modulated learning rules to capture empirical plasticity changes, further research is necessary joining the theoretical modeling of neuronal network activity with experimental validation in behaving animals.

4. References

Adelsberger, H., Garaschuk, O., and Konnerth, A. (2005). Cortical calcium waves in resting newborn mice. Nat. Neurosci. *8*, 988–990.

Adibi, M., and Arabzadeh, E. (2010). A Comparison of Neuronal and Behavioral Detection and Discrimination Performances in Rat Whisker System. J. Neurophysiol. *105*, 356–365.

Adibi, M., Diamond, M.E., and Arabzadeh, E. (2012). Behavioral study of whisker-mediated vibration sensation in rats. Proc. Natl. Acad. Sci. *109*, 971–976.

Ahissar M, Hochstein S. (1997). Task difficulty and the specificity of perceptual learning. Nature 387,401-406.

Ahissar, M., and Hochstein, S. (1993). Attentional control of early perceptual learning. Proc. Natl. Acad. Sci. *90*, 5718–5722.

Ahissar, E., Vaadia, E., Ahissar, M., Bergman, H., Arieli, A., and Abeles, M. (1992). Dependence of cortical plasticity on correlated activity of single neurons and on behavioral context. Science *257*, 1412–1415.

Alexander, W.H., and Brown, J.W. (2011). Medial prefrontal cortex as an action-outcome predictor. Nat. Neurosci. *14*, 1338–1344.

Andermann, M.L. (2010a). Chronic cellular imaging of mouse visual cortex during operant behavior and passive viewing. Front. Cellullar Neurosci.

Andermann, M.L., and Moore, C.I. (2006). A somatotopic map of vibrissa motion direction within a barrel column. Nat. Neurosci. *9*, 543–551.

Anikeeva, P., Andalman, A.S., Witten, I., Warden, M., Goshen, I., Grosenick, L., Gunaydin, L.A., Frank, L.M., and Deisseroth, K. (2011). Optetrode: a multichannel readout for optogenetic control in freely moving mice. Nat. Neurosci. *15*, 163–170.

Arabzadeh, E., Petersen, R.S., and Diamond, M.E. (2003). Encoding of whisker vibration by rat barrel cortex neurons: implications for texture discrimination. J. Neurosci. *23*, 9146–9154.

Aronoff, R., Matyas, F., Mateo, C., Ciron, C., Schneider, B., and Petersen, C.C.H. (2010). Long-range connectivity of mouse primary somatosensory barrel cortex: Long-range connectivity of barrel cortex. Eur. J. Neurosci. *31*, 2221–2233.

Aston-Jones, G., Rajkowski, J., Kubiak, P., and Alexinsky, T. (1994). Locus coeruleus neurons

in monkey are selectively activated by attended cues in a vigilance task. J. Neurosci. *14*, 4467–4480.

Atallah, B.V., Bruns, W., Carandini, M., and Scanziani, M. (2012). Parvalbumin-Expressing Interneurons Linearly Transform Cortical Responses to Visual Stimuli. Neuron *73*, 159–170.

Attwell, D., and Laughlin, S.B. (2001). An energy budget for signaling in the grey matter of the brain. J. Cereb. Blood Flow Metab. *21*, 1133–1145.

Avermann, M., Tomm, C., Mateo, C., Gerstner, W., and Petersen, C.C.H. (2012). Microcircuits of excitatory and inhibitory neurons in layer 2/3 of mouse barrel cortex. J. Neurophysiol. *107*, 3116–3134.

Barinka, F., and Druga, R. (2010). Calretinin expression in the mammalian neocortex: a review. Physiol. Res. *59*, 665.

Bekisz, M., Garkun, Y., Wabno, J., Hess, G., Wrobel, A., and Kossut, M. (2010). Increased excitability of cortical neurons induced by associative learning: an ex vivo study: Learning-induced increase of cortical neuronal excitability. Eur. J. Neurosci. *32*, 1715–1725.

Bender, K.J. (2006). Synaptic Basis for Whisker Deprivation-Induced Synaptic Depression in Rat Somatosensory Cortex. J. Neurosci. *26*, 4155–4165.

Bezdudnaya, T., Cano, M., Bereshpolova, Y., Stoelzel, C.R., Alonso, J.-M., and Swadlow, H.A. (2006). Thalamic Burst Mode and Inattention in the Awake LGNd. Neuron *49*, 421–432.

Bieszczad, K.M., and Weinberger, N.M. (2010a). Representational gain in cortical area underlies increase of memory strength. Proc. Natl. Acad. Sci. U. S. A. *107*, 3793–3798.

Bieszczad, K.M., and Weinberger, N.M. (2010b). Learning strategy trumps motivational level in determining learning-induced auditory cortical plasticity. Neurobiol. Learn. Mem. *93*, 229–239.

Bieszczad, K.M., Miasnikov, A.A., and Weinberger, N.M. (2013). Remodeling sensory cortical maps implants specific behavioral memory. Neuroscience *246*, 40–51.

Blake, D.T., Heiser, M.A., Caywood, M., and Merzenich, M.M. (2006). Experience-Dependent Adult Cortical Plasticity Requires Cognitive Association between Sensation and Reward. Neuron *52*, 371–381.

Brecht, M., Roth, A., and Sakmann, B. (2003). Dynamic Receptive Fields of Reconstructed Pyramidal Cells in Layers 3 and 2 of Rat Somatosensory Barrel Cortex. J. Physiol. *553*, 243–265.

Britten, K.H., Shadlen, M.N., Newsome, W.T., and Movshon, J.A. (1992). The analysis of visual

motion: a comparison of neuronal and psychophysical performance. J. Neurosci. *12*, 4745–4765.

Brown, M. (2004). Perceptual Learning on an Auditory Frequency Discrimination Task by Cats: Association with Changes in Primary Auditory Cortex. Cereb. Cortex *14*, 952–965.

Buonomano, D.V., and Merzenich, M.M. (1998). Cortical plasticity: from synapses to maps. Annu. Rev. Neurosci. *21*, 149–186.

Butt, A.E., Chavez, C.M., Flesher, M.M., Kinney-Hurd, B.L., Araujo, G.C., Miasnikov, A.A., and Weinberger, N.M. (2009). Association learning-dependent increases in acetylcholine release in the rat auditory cortex during auditory classical conditioning. Neurobiol. Learn. Mem. *92*, 400–409.

Buzsáki, G., Bickford, R.G., Ponomareff, G., Thal, L.J., Mandel, R., and Gage, F.H. (1988). Nucleus basalis and thalamic control of neocortical activity in the freely moving rat. J. Neurosci. *8*, 4007–4026.

Cahill, L., McGaugh, J.L., and Weinberger, N.M. (2001). The neurobiology of learning and memory: some reminders to remember. Trends Neurosci. *24*, 578–581.

Carpenter RH. and Williams ML. (1995) Neural computation of log likelihood in control of saccadic eye movements. Nature 377, 59–62.

Carvell, G.E., and Simons, D.J. (1990). Biometric analyses of vibrissal tactile discrimination in the rat. J. Neurosci. *10*, 2638–2648.

Carvell GE., and Simons DJ. (1995). Task- and subject-related differences in sensorimotor behavior during active touch. Somatosens Mot Res 12, 1–9.

Castro-Alamancos, M.A. (2004). Dynamics of sensory thalamocortical synaptic networks during information processing states. Prog. Neurobiol. *74*, 213–247.

Cauller, L.J., Clancy, B., and Connors, B.W. (1998). Backward cortical projections to primary somatosensory cortex in rats extend long horizontal axons in layer I. J. Comp. Neurol. *390*, 297–310.

Chalk, M., Herrero, J.L., Gieselmann, M.A., Delicato, L.S., Gotthardt, S., and Thiele, A. (2010). Attention Reduces Stimulus-Driven Gamma Frequency Oscillations and Spike Field Coherence in V1. Neuron *66*, 114–125.

Chapin, J.K. (1984). Sensorimotor Encoding by Synchronous Neural Ensemble Activity at Multiple Levels of the Somatosensory System. Chemistry *23*, 4519.

Chen, J.L., Andermann, M.L., Keck, T., Xu, N.-L., and Ziv, Y. (2013). Imaging Neuronal

Populations in Behaving Rodents: Paradigms for Studying Neural Circuits Underlying Behavior in the Mammalian Cortex. J. Neurosci. 33, 17631–17640.

Chen, J.L., Carta, S., Soldado-Magraner, J., Schneider, B.L., Helmchen, F., 2013. Behavior-dependent recruitment of long-range projection neurons in somatosensory cortex. Nature 499, 336–340. doi:10.1038/nature12236.

Chen, J.L., Voigt, F.F., Javadzadeh, M., Krueppel, M.R., Helmchen, F. (2016). Long-range population dynamics of anatomically defined neocortical networks. eLife. 5:e14679.

Chen, N., Sugihara, H., and Sur, M. (2015). An acetylcholine-activated microcircuit drives temporal dynamics of cortical activity. Nat. Neurosci. *18*, 892–902.

Chen, T.W., Wardill, T.J., Sun, Y., Pulver, S.R., Renninger, S.L.,Baohan, A., Schreiter, E.R., Kerr, R.A., Orger, M.B., Jayaraman V., Looger, L.L., Svoboda, K., and Kim, D.S. (2013). Ultra-sensitive fluorescent proteins for imaging neuronal activity

Nature. 499(7458): 295–300.

Chia, T.H., and Levene, M.J. (2009). In vivo Imaging of Deep Cortical Layers using a Microprism. J. Vis. Exp.

Chiaia, N.L., Rhoades, R.W., Bennett-Clarke, C.A., Fish, S.E., and Killackey, H.P. (1991). Thalamic processing of vibrissal information in the rat. I. Afferent input to the medial ventral posterior and posterior nuclei. J. Comp. Neurol. *314*, 201–216.

Chung, K., and Deisseroth, K. (2013). CLARITY for mapping the nervous system. Nat. Methods *10*, 508–513.

Clack, N.G., O'Connor, D.H., Huber, D., Petreanu, L., Hires, A., Peron, S., Svoboda, K., and Myers, E.W. (2012). Automated Tracking of Whiskers in Videos of Head Fixed Rodents. PLoS Comput. Biol. *8*, e1002591.

Clayton, E.C. (2004). Phasic Activation of Monkey Locus Ceruleus Neurons by Simple Decisions in a Forced-Choice Task. J. Neurosci. *24*, 9914–9920.

Cohen, M.R., and Maunsell, J.H.R. (2009). Attention improves performance primarily by reducing interneuronal correlations. Nat. Neurosci. *12*, 1594–1600.

Cohen, M.R., and Newsome, W.T. (2009). Estimates of the Contribution of Single Neurons to Perception Depend on Timescale and Noise Correlation. J. Neurosci. *29*, 6635–6648.

Conner, J.M., Culberson, A., Packowski, C., Chiba, A.A., and Tuszynski, M.H. (2003). Lesions of the basal forebrain cholinergic system impair task acquisition and abolish cortical plasticity associated with motor skill learning. Neuron *38*, 819–829.

Conner, J.M., Chiba, A.A., and Tuszynski, M.H. (2005). The Basal Forebrain Cholinergic System Is Essential for Cortical Plasticity and Functional Recovery following Brain Injury. Neuron *46*, 173–179.

Constantinople, C.M., and Bruno, R.M. (2011). Effects and Mechanisms of Wakefulness on Local Cortical Networks. Neuron *69*, 1061–1068.

Crist, R.E., Li, W., and Gilbert, C.D. (2001). Learning to see: experience and attention in primary visual cortex. Nat. Neurosci. *4*, 519–525.

Crochet, S., Poulet, J.F.A., Kremer, Y., and Petersen, C.C.H. (2011). Synaptic Mechanisms Underlying Sparse Coding of Active Touch. Neuron *69*, 1160–1175.

Cybulska-Klosowicz, A., and Kossut, M. (2000). Mice can learn roughness discrimination with vibrissae in a jump stand apparatus. Acta Neurobiol. Exp. (Warsz.) *61*, 73–76.

Danielmeier, C., Allen, E.A., Jocham, G., Onur, O.A., Eichele, T., and Ullsperger, M. (2015). Acetylcholine Mediates Behavioral and Neural Post-Error Control. Curr. Biol. *25*, 1461–1468.

Dayan, P., Kakade, S., and Montague, P.R. (2000). Learning and selective attention. Nat. Neurosci. *3*, 1218–1223.

De Kock, C.P.J., Bruno, R.M., Spors, H., and Sakmann, B. (2007). Layer- and cell-type-specific suprathreshold stimulus representation in rat primary somatosensory cortex: Sensory responses throughout barrel cortex. J. Physiol. *581*, 139–154.

Debowska, W., Liguz-Lecznar, M., and Kossut, M. (2011). Bilateral Plasticity of Vibrissae SII Representation Induced by Classical Conditioning in Mice. J. Neurosci. *31*, 5447–5453.

Dembrow, N.C., Chitwood, R.A., and Johnston, D. (2010). Projection-Specific Neuromodulation of Medial Prefrontal Cortex Neurons. J. Neurosci. *30*, 16922–16937.

Denk, W., Strickler, J.H., and Webb, W.W. (1990). Two-photon laser scanning fluorescence microscopy. Science *248*, 73–76.

Diamond, M.E., and Arabzadeh, E. (2013). Whisker sensory system – From receptor to decision. Prog. Neurobiol. *103*, 28–40.

Diamond, M.E., Huang, W., and Ebner, F.F. (1994). Laminar comparison of somatosensory cortical plasticity. Science *265*, 1885–1888.

Dombeck, D.A., Khabbaz, A.N., Collman, F., Adelman, T.L., and Tank, D.W. (2007). Imaging Large-Scale Neural Activity with Cellular Resolution in Awake, Mobile Mice. Neuron *56*, 43–57.

Dombeck, D.A., Harvey, C.D., Tian, L., Looger, L.L., and Tank, D.W. (2010). Functional imaging

of hippocampal place cells at cellular resolution during virtual navigation. Nat. Neurosci. *13*, 1433–1440.

Douglas, R.J., and Martin, K.A.C. (2004). NEURONAL CIRCUITS OF THE NEOCORTEX. Annu. Rev. Neurosci. *27*, 419–451.

Dringenberg, H.C., Vanderwolf, C.H., and Noseworthy, P.A. (2003). Superior colliculus stimulation enhances neocortical serotonin release and electrocorticographic activation in the urethane-anesthetized rat. Brain Res. *964*, 31–41.

Erlich, J.C., Bialek, M., and Brody, C.D. (2011). A Cortical Substrate for Memory-Guided Orienting in the Rat. Neuron *72*, 330–343.

Fanselow, E.E., and Nicolelis, M.A. (1999). Behavioral modulation of tactile responses in the rat somatosensory system. J. Neurosci. *19*, 7603–7616.

Fanselow, E.E., Sameshima, K., Baccala, L.A., and Nicolelis, M.A. (2001). Thalamic bursting in rats during different awake behavioral states. Proc. Natl. Acad. Sci. *98*, 15330–15335.

Feldmeyer, D., Lübke, J., Silver, R.A., and Sakmann, B. (2002). Synaptic connections between layer 4 spiny neurone-layer 2/3 pyramidal cell pairs in juvenile rat barrel cortex: physiology and anatomy of interlaminar signalling within a cortical column. J. Physiol. *538*, 803–822.

Feldmeyer, D., Brecht, M., Helmchen, F., Petersen, C.C.H., Poulet, J.F.A., Staiger, J.F., Luhmann, H.J., and Schwarz, C. (2013). Barrel cortex function. Prog. Neurobiol. *103*, 3–27.

Frank, M.J., Woroch, B.S., and Curran, T. (2005). Error-Related Negativity Predicts Reinforcement Learning and Conflict Biases. Neuron *47*, 495–501.

Frémaux, N., and Gerstner, W. (2016). Neuromodulated Spike-Timing-Dependent Plasticity, and Theory of Three-Factor Learning Rules. Front. Neural Circuits *9*.

Fritz, J.B. (2005). Differential Dynamic Plasticity of A1 Receptive Fields during Multiple Spectral Tasks. J. Neurosci. *25*, 7623–7635.

Fritz, J.B., Elhilali, M., David, S.V., and Shamma, S.A. (2007). Does attention play a role in dynamic receptive field adaptation to changing acoustic salience in A1? Hear. Res. *229*, 186–203.

Fritz, J., Shamma, S., Elhilali., M., Klein, D. (2003). Rapid task.related plasticity of spectrotermporal receptive fields in primary auditory cortex. Nature Neuroscience *6*.

Froemke, R.C., Carcea, I., Barker, A.J., Yuan, K., Seybold, B.A., Martins, A.R.O., Zaika, N., Bernstein, H., Wachs, M., Levis, P.A., et al. (2012). Long-term modification of cortical synapses improves sensory perception. Nat. Neurosci. *16*, 79–88.

Gallistel, C. (2003). Conditioning from an information processing perspective. Behav. Processes *62*, 89–101.

Galvez, R. (2006). Vibrissa-Signaled Eyeblink Conditioning Induces Somatosensory Cortical Plasticity. J. Neurosci. *26*, 6062–6068.

Gavornik, J.P., Shuler, M.G.H., Loewenstein, Y., Bear, M.F., and Shouval, H.Z. (2009). Learning reward timing in cortex through reward dependent expression of synaptic plasticity. Proc. Natl. Acad. Sci. *106*, 6826–6831.

Gdalyahu, A., Tring, E., Polack, P.O., Gruver, R., Golshani, P., Fanselow, M.S., Silva, A.J., and Trachtenberg, J.T. (2012). Associative Fear Learning Enhances Sparse Network Coding in Primary Sensory Cortex. Neuron *75*, 121–132.

Gentet, L.J., Avermann, M., Matyas, F., Staiger, J.F., and Petersen, C.C.H. (2010). Membrane Potential Dynamics of GABAergic Neurons in the Barrel Cortex of Behaving Mice. Neuron *65*, 422–435.

Gentet, L.J., Kremer, Y., Taniguchi, H., Huang, Z.J., Staiger, J.F., and Petersen, C.C.H. (2012). Unique functional properties of somatostatin-expressing GABAergic neurons in mouse barrel cortex. Nat. Neurosci. *15*, 607–612.

Gerdjikov, T.V., Bergner, C.G., Stüttgen, M.C., Waiblinger, C., and Schwarz, C. (2010). Discrimination of Vibrotactile Stimuli in the Rat Whisker System: Behavior and Neurometrics. Neuron *65*, 530–540.

Gerhard, F., Pipa, G., Lima, B., Neuenschwander, S., and Gerstner, W. (2011). Extraction of Network Topology From Multi-Electrode Recordings: Is there a Small-World Effect? Front. Comput. Neurosci. *5*.

Gilbert, C.D., Sigman, M., and Crist, R.E. (2001). The neural basis of perceptual learning. Neuron *31*, 681–697.

Glazewski, S., Chen, C.M., Silva, A. & Fox, K. (1996). Requirement for alpha-CaMKII in experience-dependent plasticity of the barrel cortex. Science 272, 421–423.

Glazewski, S., and Barth, A.L. (2015). Stimulus intensity determines experience-dependent modifications in neocortical neuron firing rates. Eur. J. Neurosci. *41*, 410–419.

Glazewski, S., and Fox, K. (1996). Time course of experience-dependent synaptic potentiation and depression in barrel cortex of adolescent rats. J. Neurophysiol. *75*, 1714–1729.

Göbel, W., Kampa, B.M., and Helmchen, F. (2007). Imaging cellular network dynamics in

three dimensions using fast 3D laser scanning. Nat. Methods *4*, 73–79.

Goldberg, R.F. (2006). Perceptual Knowledge Retrieval Activates Sensory Brain Regions. J. Neurosci. *26*, 4917–4921.

Goldstone, R.L. (1998). Perceptual learning. Annu. Rev. Psychol. *49*, 585–612.

Greenberg, D.S., Houweling, A.R., and Kerr, J.N.D. (2008). Population imaging of ongoing neuronal activity in the visual cortex of awake rats. Nat. Neurosci. *11*, 749–751.

Grewe, B.F., Langer, D., Kasper, H., Kampa, B.M., and Helmchen, F. (2010). High-speed in vivo calcium imaging reveals neuronal network activity with near-millisecond precision. Nat. Methods *7*, 399–405.

Grewe, B.F., Voigt, F.F., van't Hoff, M., and Helmchen, F. (2011). Fast two-layer two-photon imaging of neuronal cell populations using an electrically tunable lens. Biomed. Opt. Express *2*, 2035–2046.

Grienberger, C., and Konnerth, A. (2012). Imaging Calcium in Neurons. Neuron *73*, 862–885.

Guo, Z.V., Li, N., Huber, D., Ophir, E., Gutnisky, D., Ting, J.T., Feng, G., and Svoboda, K. (2014). Flow of Cortical Activity Underlying a Tactile Decision in Mice. Neuron *81*, 179–194.

Haiss, F., Jolivet, R., Wyss, M.T., Reichold, J., Braham, N.B., Scheffold, F., Krafft, M.P., and Weber, B. (2009). Improved *in vivo* two-photon imaging after blood replacement by perfluorocarbon: *In vivo* two-photon imaging after perfluorocarbon transfusion. J. Physiol. *587*, 3153–3158.

Harris, J.A., and Diamond, M.E. (2000). Ipsilateral and contralateral transfer of tactile learning. Neuroreport *11*, 263–266.

Harris, K.D., and Thiele, A. (2011). Cortical state and attention. Nat. Rev. Neurosci. *12*, 509–523.

Harris, J.A., Petersen, R.S., and Diamond, M.E. (1999). Distribution of tactile learning and its neural basis. Proc. Natl. Acad. Sci. *96*, 7587–7591.

Harris, J.A., Harris, I.M., and Diamond, M.E. (2001). The topography of tactile working memory. J. Neurosci. *21*, 8262–8269.

von Heimendahl, M., Itskov, P.M., Arabzadeh, E., and Diamond, M.E. (2007). Neuronal Activity in Rat Barrel Cortex Underlying Texture Discrimination. PLoS Biol. *5*, e305.

Helmchen, F., and Denk, W. (2005). Deep tissue two-photon microscopy. Nat. Methods *2*, 932–940.

Helmchen, F., Imoto, K., and Sakmann, B. (1996). Ca2+ buffering and action potential-evoked

Ca2+ signaling in dendrites of pyramidal neurons. Biophys. J. *70*, 1069.

Hentschke, H. (2005). Central Signals Rapidly Switch Tactile Processing in Rat Barrel Cortex during Whisker Movements. Cereb. Cortex *16*, 1142–1156.

Hernandez, A., Salinas, E., García, R., and Romo, R. (1997). Discrimination in the sense of flutter: new psychophysical measurements in monkeys. J. Neurosci. *17*, 6391–6400.

Hirata, A. (2006). Noradrenergic Activation Amplifies Bottom-Up and Top-Down Signal-to-Noise Ratios in Sensory Thalamus. J. Neurosci. *26*, 4426–4436.

Hofer, S.B., Mrsic-Flogel, T.D., Bonhoeffer, T., and Hübener, M. (2009). Experience leaves a lasting structural trace in cortical circuits. Nature *457*, 313–317.

Hollerman, J.R., and Schultz, W. (1998). Dopamine neurons report an error in the temporal prediction of reward during learning. Nat. Neurosci. *1*, 304–309.

Holmgren, C., Harkany, T., Svennenfors, B., and Zilberter, Y. (2003). Pyramidal cell communication within local networks in layer 2/3 of rat neocortex. J. Physiol. *551*, 139–153.

Holtmaat, A., and Svoboda, K. (2009). Experience-dependent structural synaptic plasticity in the mammalian brain. Nat. Rev. Neurosci. *10*, 647–658.

Horton, J.C., and Adams, D.L. (2005). The cortical column: a structure without a function. Philos. Trans. R. Soc. B Biol. Sci. *360*, 837–862.

Hromádka, T., DeWeese, M.R., and Zador, A.M. (2008). Sparse representation of sounds in the unanesthetized auditory cortex. PLoS Biol *6*, e16.

Huber, D., Petreanu, L., Ghitani, N., Ranade, S., Hromádka, T., Mainen, Z., and Svoboda, K. (2008). Sparse optical microstimulation in barrel cortex drives learned behavior in freely moving mice. Nature *451*, 61–64.

Huber, D., Gutnisky, D.A., Peron, S., O'Connor, D.H., Wiegert, J.S., Tian, L., Oertner, T.G., Looger, L.L., and Svoboda, K. (2012). Multiple dynamic representations in the motor cortex during sensorimotor learning. Nature *484*, 473–478.

Hui, G.K., Wong, K.L., Chavez, C.M., Leon, M.I., Robin, K.M., and Weinberger, N.M. (2009). Conditioned tone control of brain reward behavior produces highly specific representational gain in the primary auditory cortex. Neurobiol. Learn. Mem. *92*, 27–34.

Hurley, L., Devilbiss, D., and Waterhouse, B. (2004). A matter of focus: monoaminergic modulation of stimulus coding in mammalian sensory networks. Curr. Opin. Neurobiol. *14*, 488–495.

Jaramillo, S., and Zador, A.M. (2011). The auditory cortex mediates the perceptual effects of

acoustic temporal expectation. Nat. Neurosci. *14*, 246–251.

Jenkinson, E.W., and Glickstein, M. (2000). Whiskers, barrels, and cortical efferent pathways in gap crossing by rats. J. Neurophysiol. *84*, 1781–1789.

Ji, W., Gao, E., and Suga, N. (2001). Effects of acetylcholine and atropine on plasticity of central auditory neurons caused by conditioning in bats. J. Neurophysiol. *86*, 211–225.

Jones, E.G. (1999). Making brain connections: neuroanatomy and the work of TPS Powell, 1923-1996. Annu. Rev. Neurosci. *22*, 49–103.

Kampa, B.M., Gobel, W., and Helmchen, F. (2011). Measuring Neuronal Population Activity Using 3D Laser Scanning. Cold Spring Harb. Protoc. *2011*, pdb.prot066597-prot066597.

Karni, A., and Sagi, D. (1991). Where practice makes perfect in texture discrimination: evidence for primary visual cortex plasticity. Proc. Natl. Acad. Sci. *88*, 4966–4970.

Kato, H.K., Gillet, S.N., and Isaacson, J.S. (2015). Flexible Sensory Representations in Auditory Cortex Driven by Behavioral Relevance. Neuron *88*, 1027–1039.

Kawaguchi, Y., and Shindou, T. (1998). Noradrenergic excitation and inhibition of GABAergic cell types in rat frontal cortex. J. Neurosci. *18*, 6963–6976.

Kayser, C., Petkov, C.I., Augath, M., and Logothetis, N.K. (2005). Integration of Touch and Sound in Auditory Cortex. Neuron *48*, 373–384.

Kerr, J.N.D., Greenberg, D., and Helmchen, F. (2005). Imaging input and output of neocortical networks in vivo. Proc. Natl. Acad. Sci. U. S. A. *102*, 14063–14068.

Kerr, J.N.D., de Kock, C.P.J., Greenberg, D.S., Bruno, R.M., Sakmann, B., and Helmchen, F. (2007). Spatial Organization of Neuronal Population Responses in Layer 2/3 of Rat Barrel Cortex. J. Neurosci. *27*, 13316–13328.

Kilgard, M.P., Pandya, P.K., Vazquez, J., Gehi, A., Schreiner, C.E., and Merzenich, M.M. (2001). Sensory input directs spatial and temporal plasticity in primary auditory cortex. J. Neurophysiol. *86*, 326–338.

Kilgard, M.P., Pandya, P.K., Engineer, N.D., and Moucha, R. (2002). Cortical network reorganization guided by sensory input features. Biol. Cybern. *87*, 333–343.

Kim, S.-Y., Adhikari, A., Lee, S.Y., Marshel, J.H., Kim, C.K., Mallory, C.S., Lo, M., Pak, S., Mattis, J., Lim, B.K., et al. (2013). Diverging neural pathways assemble a behavioral state from separable features in anxiety. Nature *496*, 219–223.

Kim, U., and Ebner, F.F. (1999). Barrels and Septa: Separate Circuits in Rat Barrel Field Cortex. J Comp Neurol 408, 489-505.

Kinnischtzke, A.K., Simons, D.J., and Fanselow, E.E. (2013). Motor Cortex Broadly Engages Excitatory and Inhibitory Neurons in Somatosensory Barrel Cortex. Cereb. Cortex.

Knöpfel, T. (2012). Genetically encoded optical indicators for the analysis of neuronal circuits. Nat. Rev. Neurosci.

Knott, G.W., Quairiaux, C., Genoud, C., and Welker, E. (2002). Formation of dendritic spines with GABAergic synapses induced by whisker stimulation in adult mice. Neuron *34*, 265–273.

Knutsen, P.M. (2006). Haptic Object Localization in the Vibrissal System: Behavior and Performance. J. Neurosci. *26*, 8451–8464.

de Kock, C.P., and Sakmann, B. (2009). Spiking in primary somatosensory cortex during natural whisking in awake head-restrained rats is cell-type specific. Proc. Natl. Acad. Sci. *106*, 16446–16450.

Komiyama, T., Sato, T.R., O'Connor, D.H., Zhang, Y.-X., Huber, D., Hooks, B.M., Gabitto, M., and Svoboda, K. (2010). Learning-related fine-scale specificity imaged in motor cortex circuits of behaving mice. Nature *464*, 1182–1186.

Krupa, D.J., Matell, M.S., Brisben, A.J., Oliveira, L.M., and Nicolelis, M.A. (2001). Behavioral properties of the trigeminal somatosensory system in rats performing whisker-dependent tactile discriminations. J. Neurosci. *21*, 5752–5763.

Krupa, D.J., Wiest, M.C., Shuler, M.G., Laubach, M., and Nicolelis, M.A. (2004). Layer-specific somatosensory cortical activation during active tactile discrimination. Science *304*, 1989–1992.

Kuhlman, S.J., O'Connor, D.H., Fox, K., and Svoboda, K. (2014). Structural Plasticity within the Barrel Cortex during Initial Phases of Whisker-Dependent Learning. J. Neurosci. *34*, 6078–6083.

Kwan, A.C., and Dan, Y. (2012). Dissection of Cortical Microcircuits by Single-Neuron Stimulation In Vivo. Curr. Biol. *22*, 1459–1467.

Kwon, S.E., Yang, H., Minamisawa, G., and O'Connor, D.H. (2016). Sensory and decision-related activity propagate in a cortical feedback loop during touch perception. Nat. Neurosci.

Lak, A., Arabzadeh, E., and Diamond, M.E. (2007). Enhanced Response of Neurons in Rat Somatosensory Cortex to Stimuli Containing Temporal Noise. Cereb. Cortex *18*, 1085–1093.

Lak, A., Arabzadeh, E., Harris, J.A., and Diamond, M.E. (2010). Correlated physiological and perceptual effects of noise in a tactile stimulus. Proc. Natl. Acad. Sci. *107*, 7981–7986.

LaMotte, R.H., and Mountcastle, V.B. (1975). Capacities of humans and monkeys to

discriminate vibratory stimuli of different frequency and amplitude: a correlation between neural events and psychological measurements. J. Neurophysiol. *38*, 539–559.

Langer, D., and Helmchen, F. (2012). Post hoc immunostaining of GABAergic neuronal subtypes following in vivo two-photon calcium imaging in mouse neocortex. Pflüg. Arch. - Eur. J. Physiol. *463*, 339–354.

Lawrence, J.J. (2008). Cholinergic control of GABA release: emerging parallels between neocortex and hippocampus. Trends Neurosci. *31*, 317–327.

Lee, A.K., Manns, I.D., Sakmann, B., and Brecht, M. (2006). Whole-Cell Recordings in Freely Moving Rats. Neuron *51*, 399–407.

Lee, S., Hjerling-Leffler, J., Zagha, E., Fishell, G., and Rudy, B. (2010). The Largest Group of Superficial Neocortical GABAergic Interneurons Expresses Ionotropic Serotonin Receptors. J. Neurosci. *30*, 16796–16808.

Lee, S., Kruglikov, I., Huang, Z.J., Fishell, G., and Rudy, B. (2013). A disinhibitory circuit mediates motor integration in the somatosensory cortex. Nat. Neurosci. *16*, 1662–1670.

Lefort, S., Tomm, C., Floyd Sarria, J.-C., and Petersen, C.C.H. (2009). The Excitatory Neuronal Network of the C2 Barrel Column in Mouse Primary Somatosensory Cortex. Neuron *61*, 301–316.

Lennie, P. (2003). The cost of cortical computation. Curr. Biol. *13*, 493–497.

Letzkus, J.J., Wolff, S.B.E., Meyer, E.M.M., Tovote, P., Courtin, J., Herry, C., and Lüthi, A. (2011). A disinhibitory microcircuit for associative fear learning in the auditory cortex. Nature *480*, 331–335.

Li, L. (2005). Chronic Suppression of Activity in Barrel Field Cortex Downregulates Sensory Responses in Contralateral Barrel Field Cortex. J. Neurophysiol. *94*, 3342–3356.

Lin, S.-C., and Nicolelis, M.A.L. (2008). Neuronal Ensemble Bursting in the Basal Forebrain Encodes Salience Irrespective of Valence. Neuron *59*, 138–149.

Loewenstein, Y., and Seung, H.S. (2006). Operant matching is a generic outcome of synaptic plasticity based on the covariance between reward and neural activity. Proc. Natl. Acad. Sci. *103*, 15224–15229.

London, M., Roth, A., Beeren, L., Häusser, M., and Latham, P.E. (2010). Sensitivity to perturbations in vivo implies high noise and suggests rate coding in cortex. Nature *466*, 123–127.

Long, J.D., and Carmena, J.M. (2013). Dynamic changes of rodent somatosensory barrel

cortex are correlated with learning a novel conditioned stimulus. J. Neurophysiol. *109*, 2585–2595.

Luna, R., Hernández, A., Brody, C.D., and Romo, R. (2005). Neural codes for perceptual discrimination in primary somatosensory cortex. Nat. Neurosci. *8*, 1210–1219.

Luo, L., Callaway, E.M., and Svoboda, K. (2008). Genetic Dissection of Neural Circuits. Neuron *57*, 634–660.

Lütcke, H. (2010). Optical recording of neuronal activity with a genetically-encoded calcium indicator in anesthetized and freely moving mice. Front. Neural Circuits.

Lütcke, H., Gerhard, F., Zenke, F., Gerstner, W., and Helmchen, F. (2013a). Inference of neuronal network spike dynamics and topology from calcium imaging data. Front. Neural Circuits *7*.

Lütcke, H., Margolis, D.J., and Helmchen, F. (2013b). Steady or changing? Long-term monitoring of neuronal population activity. Trends Neurosci. *36*, 375–384.

Madisen, L., Mao, T., Koch, H., Zhuo, J., Berenyi, A., Fujisawa, S., Hsu, Y.-W.A., Garcia, A.J., Gu, X., Zanella, S., et al. (2012). A toolbox of Cre-dependent optogenetic transgenic mice for light-induced activation and silencing. Nat. Neurosci. *15*, 793–802.

Maier, D.L., Grieb, G.M., Stelzner, D.J., and McCasland, J.S. (2003). Large-scale plasticity in barrel cortex following repeated whisker trimming in young adult hamsters. Exp. Neurol. *184*, 737–745.

Margolis, D.J., Lütcke, H., Schulz, K., Haiss, F., Weber, B., Kügler, S., Hasan, M.T., and Helmchen, F. (2012). Reorganization of cortical population activity imaged throughout long-term sensory deprivation. Nat. Neurosci. *15*, 1539–1546.

Margrie, T., Brecht, M., and Sakmann, B. (2002). In vivo, low-resistance, whole-cell recordings from neurons in the anaesthetized and awake mammalian brain. Pflägers Arch. Eur. J. Physiol. *444*, 491–498.

Martins, A.R.O., and Froemke, R.C. (2015). Coordinated forms of noradrenergic plasticity in the locus coeruleus and primary auditory cortex. Nat. Neurosci. *18*, 1483–1492.

Mastakov, M.Y., Baer, K., Xu, R., Fitzsimons, H., and During, M.J. (2001). Combined injection of rAAV with mannitol enhances gene expression in the rat brain. Mol. Ther. *3*, 225–232.

Mateo, C., Avermann, M., Gentet, L.J., Zhang, F., Deisseroth, K., and Petersen, C.C.H. (2011). In Vivo Optogenetic Stimulation of Neocortical Excitatory Neurons Drives Brain-State-Dependent Inhibition. Curr. Biol. *21*, 1593–1602.

Matsumora, T., Koida, K., and Komatsu, H. (2008). Relationship Between Color Discrimination and Neural Responses in the Inferior Temporal Cortex of the Monkey. J. Neurophysiol. *100*, 3361–3374.

Matsumoto, M., Matsumoto, K., Abe, H., and Tanaka, K. (2007). Medial prefrontal cell activity signaling prediction errors of action values. Nat. Neurosci. *10*, 647–656.

Mayrhofer, J.M., Skreb, V., von der Behrens, W., Musall, S., Weber, B., and Haiss, F. (2013). Novel two-alternative forced choice paradigm for bilateral vibrotactile whisker frequency discrimination in head-fixed mice and rats. J. Neurophysiol. *109*, 273–284.

Mayrhofer, J.M., Haiss, F., Helmchen, F., and Weber, B. (2015a). Sparse, reliable, and long-term stable representation of periodic whisker deflections in the mouse barrel cortex. NeuroImage *115*, 52–63.

Mayrhofer, J.M., Haiss, F., Haenni, D., Weber, S., Zuend, M., Barrett, M.J.P., Ferrari, K.D., Maechler, P., Saab, A.S., Stobart, J.L., et al. (2015b). Design and performance of an ultra-flexible two-photon microscope for in vivo research. Biomed. Opt. Express *6*, 4228.

Mehta, S.B., Whitmer, D., Figueroa, R., Williams, B.A., and Kleinfeld, D. (2007). Active spatial perception in the vibrissa scanning sensorimotor system. PLoS Biol. *5*, e15.

Mena-Segovia, J., Sims, H.M., Magill, P.J., and Bolam, J.P. (2008). Cholinergic brainstem neurons modulate cortical gamma activity during slow oscillations: Cholinergic neurons during slow wave activity. J. Physiol. *586*, 2947–2960.

Metherate, R., Cox, C.L., and Ashe, J.H. (1992). Cellular bases of neocortical activation: modulation of neural oscillations by the nucleus basalis and endogenous acetylcholine. J. Neurosci. *12*, 4701–4711.

Miasnikov, A.A., McLin III, D., Weinberger, N.M., and others (2001). Muscarinic dependence of nucleus basalis induced conditioned receptive field plasticity. Neuroreport *12*, 1537–1542.

Mitchell, J.F., Sundberg, K.A., and Reynolds, J.H. (2009). Spatial Attention Decorrelates Intrinsic Activity Fluctuations in Macaque Area V4. Neuron *63*, 879–888.

Mitchinson, B., Martin, C.J., Grant, R.A., and Prescott, T.J. (2007). Feedback control in active sensing: rat exploratory whisking is modulated by environmental contact. Proc. R. Soc. B Biol. Sci. *274*, 1035–1041.

Mittmann, W., Wallace, D.J., Czubayko, U., Herb, J.T., Schaefer, A.T., Looger, L.L., Denk, W., and Kerr, J.N.D. (2011). Two-photon calcium imaging of evoked activity from L5 somatosensory neurons in vivo. Nat. Neurosci. 14, 1089–1093.

Miyawaki, A., Llopis, J., Heim, R., McCaffery, J.M., Adams, J.A., Ikurak, M., Tsien, R.Y. (1997). Fluorescent indicators for Ca2+based on green fluorescent proteins and calmodulin. Nature 388.

Molina-Luna, K., Hertler, B., Buitrago, M.M., and Luft, A.R. (2008). Motor learning transiently changes cortical somatotopy. NeuroImage 40, 1748–1754.

Morita, T., Kang, H., Wolfe, J., Jadhav, S.P., and Feldman, D.E. (2011). Psychometric Curve and Behavioral Strategies for Whisker-Based Texture Discrimination in Rats. PLoS ONE *6*, e20437.

Moucha, R., Pandya, P.K., Engineer, N.D., Rathbun, D.L., and Kilgard, M.P. (2005). Background sounds contribute to spectrotemporal plasticity in primary auditory cortex. Exp. Brain Res. *162*, 417–427.

Mountcastle, V.B., and others (1957). Modality and topographic properties of single neurons of cat's somatic sensory cortex. J Neurophysiol *20*, 408–434.

Mountcastle, V.B., Steinmetz, M.A., and Romo, R. (1990). Frequency discrimination in the sense of flutter: psychophysical measurements correlated with postcentral events in behaving monkeys. J. Neurosci. *10*, 3032–3044.

Murayama, M., and Larkum, M.E. (2009). In vivo dendritic calcium imaging with a fiberoptic periscope system. Nat. Protoc. *4*, 1551–1559.

Nagai, T., Yamada, S., Tominaga, T., Ichikawa, M., and Miyawaki, A. (2004). Expanded dynamic range of fluorescent indicators for Ca2+ by circularly permuted yellow fluorescent proteins. Proc. Natl. Acad. Sci. U. S. A. *101*, 10554–10559.

Nicolelis, M.A., and Fanselow, E.E. (2002). Dynamic shifting in thalamocortical processing during different behavioral states. Philos. Trans. R. Soc. Lond. B Biol. Sci. *357*, 1753–1758.

Niell, C.M., and Stryker, M.P. (2010). Modulation of Visual Responses by Behavioral State in Mouse Visual Cortex. Neuron *65*, 472–479.

O'Connor, D.H., Huber, D., and Svoboda, K. (2009). Reverse engineering the mouse brain. Nature *461*, 923–929.

O'Connor, D.H., Peron, S.P., Huber, D., and Svoboda, K. (2010). Neural Activity in Barrel Cortex Underlying Vibrissa-Based Object Localization in Mice. Neuron *67*, 1048–1061.

O'Connor, D.H., Hires, S.A., Guo, Z.V., Li, N., Yu, J., Sun, Q.-Q., Huber, D., and Svoboda, K. (2013). Neural coding during active somatosensation revealed using illusory touch. Nat. Neurosci. *16*, 958–965.

Ohki, K., and Reid, R.C. (2014). In Vivo Two-Photon Calcium Imaging in the Visual System. Cold Spring Harb. Protoc. *2014*, pdb.prot081455-prot081455.

Ohl, F.W., and Scheich, H. (2005). Learning-induced plasticity in animal and human auditory cortex. Curr. Opin. Neurobiol. *15*, 470–477.

Okun, M., and Lampl, I. (2008). Instantaneous correlation of excitation and inhibition during ongoing and sensory-evoked activities. Nat. Neurosci. *11*, 535–537.

Ollerenshaw, D.R., Bari, B.A., Millard, D.C., Orr, L.E., Wang, Q., and Stanley, G.B. (2012). Detection of tactile inputs in the rat vibrissa pathway. J. Neurophysiol. *108*, 479–490.

Olshausen, B., and Field, D. (2004). Sparse coding of sensory inputs. Curr. Opin. Neurobiol. *14*, 481–487.

Otazu, G.H., Tai, L.-H., Yang, Y., and Zador, A.M. (2009). Engaging in an auditory task suppresses responses in auditory cortex. Nat. Neurosci. *12*, 646–654.

Packer, A.M., and Yuste, R. (2011). Dense, Unspecific Connectivity of Neocortical Parvalbumin-Positive Interneurons: A Canonical Microcircuit for Inhibition? J. Neurosci. *31*, 13260–13271.

Packer, A.M., Russell, L.E., Dalgleish, H.W.P., and Häusser, M. (2014). Simultaneous all-optical manipulation and recording of neural circuit activity with cellular resolution in vivo. Nat. Methods *12*, 140–146.

Palm, G. (2013). Neural associative memories and sparse coding. Neural Netw. *37*, 165–171.

Palmer, L.M., Schulz, J.M., Murphy, S.C., Ledergerber, D., Murayama, M., and Larkum, M.E. (2012). The Cellular Basis of GABAB-Mediated Interhemispheric Inhibition. Science *335*, 989–993.

Panteví, C., SobelH, D., and Bloom, F.E. (1993). Modulation of early sensory processing in human auditory cortex during auditory selective attention. Proc Natl Acad Sci USA *90*, 8722–8726.

Pantoja, J., Ribeiro, S., Wiest, M., Soares, E., Gervasoni, D., Lemos, N.A.M., and Nicolelis, M.A.L. (2007). Neuronal Activity in the Primary Somatosensory Thalamocortical Loop Is Modulated by Reward Contingency during Tactile Discrimination. J. Neurosci. *27*, 10608–10620.

Parker, A.J., and Newsome, W.T. (1998). Sense and the single neuron: probing the physiology of perception. Annu. Rev. Neurosci. *21*, 227–277.

Peron, S.P., Freeman, J., Iyer, V., Guo, C., and Svoboda, K. (2015). A Cellular Resolution Map

of Barrel Cortex Activity during Tactile Behavior. Neuron *86*, 783–799.

Petersen, C.C.H. (2007). The Functional Organization of the Barrel Cortex. Neuron *56*, 339–355.

Petersen, C.C.H., and Crochet, S. (2013). Synaptic Computation and Sensory Processing in Neocortical Layer 2/3. Neuron *78*, 28–48.

Pfeffer, C.K., Xue, M., He, M., Huang, Z.J., and Scanziani, M. (2013). Inhibition of inhibition in visual cortex: the logic of connections between molecularly distinct interneurons. Nat. Neurosci. *16*, 1068–1076.

Pi, H.-J., Hangya, B., Kvitsiani, D., Sanders, J.I., Huang, Z.J., and Kepecs, A. (2013). Cortical interneurons that specialize in disinhibitory control. Nature *503*, 521–524.

Pinto, L., Goard, M.J., Estandian, D., Xu, M., Kwan, A.C., Lee, S.-H., Harrison, T.C., Feng, G., and Dan, Y. (2013). Fast modulation of visual perception by basal forebrain cholinergic neurons. Nat. Neurosci. *16*, 1857–1863.

Pleger, B., Blankenburg, F., Ruff, C.C., Driver, J., and Dolan, R.J. (2008). Reward Facilitates Tactile Judgments and Modulates Hemodynamic Responses in Human Primary Somatosensory Cortex. J. Neurosci. *28*, 8161–8168.

Polack, P.-O., Friedman, J., and Golshani, P. (2013). Cellular mechanisms of brain state-dependent gain modulation in visual cortex. Nat. Neurosci. *16*, 1331–1339.

Polley, D.B. (2006). Perceptual Learning Directs Auditory Cortical Map Reorganization through Top-Down Influences. J. Neurosci. *26*, 4970–4982.

Polley, D.B., Chen-Bee, C.H., and Frostig, R.D. (1999). Two directions of plasticity in the sensory-deprived adult cortex. Neuron *24*, 623–637.

Pologruto, T.A. (2004). Monitoring Neural Activity and [Ca2+] with Genetically Encoded Ca2+ Indicators. J. Neurosci. *24*, 9572–9579.

Pologruto, T.A., Sabatini, B.L., and Svoboda, K. (2003). ScanImage: flexible software for operating laser scanning microscopes. Biomed Eng Online *2*, 13.

Pooresmaeili, A., Poort, J., and Roelfsema, P.R. (2014). Simultaneous selection by object-based attention in visual and frontal cortex. Proc. Natl. Acad. Sci. *111*, 6467–6472.

Posluszny, A., Liguz-Lecznar, M., Turzynska, D., Zakrzewska, R., Bielecki, M., and Kossut, M. (2015). Learning-Dependent Plasticity of the Barrel Cortex Is Impaired by Restricting GABA-Ergic Transmission. PloS One *10*, e0144415.

Poulet, J.F.A., and Petersen, C.C.H. (2008). Internal brain state regulates membrane potential

synchrony in barrel cortex of behaving mice. Nature *454*, 881–885.

Prigg, T., Goldreich, D., Carvell, G.E., and Simons, D.J. (2002). Texture discrimination and unit recordings in the rat whisker/barrel system. Physiol. Behav. *77*, 671–675.

Purushothaman, G., and Bradley, D.C. (2005). Neural population code for fine perceptual decisions in area MT. Nat. Neurosci. *8*, 99–106.

Ramanathan, D., Tuszynski, M.H., and Conner, J.M. (2009). The Basal Forebrain Cholinergic System Is Required Specifically for Behaviorally Mediated Cortical Map Plasticity. J. Neurosci. *29*, 5992–6000.

Ramos, R.L., Tam, D.M., and Brumberg, J.C. (2008). Physiology and morphology of callosal projection neurons in mouse. Neuroscience *153*, 654–663.

Ranade, S.P., and Mainen, Z.F. (2009). Transient Firing of Dorsal Raphe Neurons Encodes Diverse and Specific Sensory, Motor, and Reward Events. J. Neurophysiol. *102*, 3026–3037.

Recanzone, Gh. al, Schreiner, C.E., and Merzenich, M.M. (1993). Plasticity in the frequency representation of primary auditory cortex following discrimination training in adult owl monkeys. J. Neurosci. *13*, 87–103.

Reed, A., Riley, J., Carraway, R., Carrasco, A., Perez, C., Jakkamsetti, V., and Kilgard, M.P. (2011). Cortical Map Plasticity Improves Learning but Is Not Necessary for Improved Performance. Neuron *70*, 121–131.

Reyes-Puerta, V., Sun, J.-J., Kim, S., Kilb, W., and Luhmann, H.J. (2014). Laminar and Columnar Structure of Sensory-Evoked Multineuronal Spike Sequences in Adult Rat Barrel Cortex In Vivo. Cereb. Cortex.

Reynolds, J.H., and Chelazzi, L. (2004). ATTENTIONAL MODULATION OF VISUAL PROCESSING. Annu. Rev. Neurosci. *27*, 611–647.

Reynolds, J.N., and Wickens, J.R. (2002). Dopamine-dependent plasticity of corticostriatal synapses. Neural Netw. *15*, 507–521.

Richardson, R.T., and DeLong, M.R. (1990). Context-dependent responses of primate nucleus basalis neurons in a go/no-go task. J. Neurosci. *10*, 2528–2540.

Ringach, D.L. (2009). Spontaneous and driven cortical activity: implications for computation. Curr. Opin. Neurobiol. *19*, 439–444.

Rodgers, C.C., and DeWeese, M.R. (2014). Neural Correlates of Task Switching in Prefrontal Cortex and Primary Auditory Cortex in a Novel Stimulus Selection Task for Rodents. Neuron *82*, 1157–1170.

Roelfsema, P.R., van Ooyen, A., and Watanabe, T. (2010). Perceptual learning rules based on reinforcers and attention. Trends Cogn. Sci. *14*, 64–71.

Rosselet, C., Fieschi, M., Hugues, S., and Bureau, I. (2011). Associative Learning Changes the Organization of Functional Excitatory Circuits Targeting the Supragranular Layers of Mouse Barrel Cortex. Front. Neural Circuits *4*.

Rushworth, M.F.S., and Behrens, T.E.J. (2008). Choice, uncertainty and value in prefrontal and cingulate cortex. Nat. Neurosci. *11*, 389–397.

Rutkowski, R.G., and Weinberger, N.M. (2005). Encoding of learned importance of sound by magnitude of representational area in primary auditory cortex. Proc. Natl. Acad. Sci. U. S. A. *102*, 13664–13669.

Sachidhanandam, S., Sreenivasan, V., Kyriakatos, A., Kremer, Y., and Petersen, C.C.H. (2013). Membrane potential correlates of sensory perception in mouse barrel cortex. Nat. Neurosci. *16*, 1671–1677.

Sato, T.R., Gray, N.W., Mainen, Z.F., and Svoboda, K. (2007). The Functional Microarchitecture of the Mouse Barrel Cortex. PLoS Biol. *5*, e189.

Schultz, W., and Dickinson, A. (2000). Neuronal coding of prediction errors. Annu. Rev. Neurosci. *23*, 473–500.

Schultz, W., Dayan, P., and Montague, P.R. (1997). A neural substrate of prediction and reward. Science *275*, 1593–1599.

Schwarz, C., Hentschke, H., Butovas, S., Haiss, F., Stüttgen, M.C., Gerdjikov, T.V., Bergner, C.G., and Waiblinger, C. (2010). The head-fixed behaving rat—Procedures and pitfalls. Somatosens. Mot. Res. *27*, 131–148.

Shackleton-Jones, N., Gross, R., McIlveen, R. (1999). Psychology. A new Introduction. Houder and Stoughton.

Shaner, N.C., Steinbach, P.A., and Tsien, R.Y. (2005). A guide to choosing fluorescent proteins. Nat. Methods *2*, 905–909.

Shuler MG., Bear MF. (2006). Reward timing in the primary visual cortex. Science 311, 1606-1609.

Shuler, M.G., Krupa, D.J., and Nicolelis, M.A. (2001). Bilateral integration of whisker information in the primary somatosensory cortex of rats. J. Neurosci. *21*, 5251–5261.

Shuler, MG., Krupa DJ., Nicolelis, M.A. (2002). Integration of Bilateral Whisker Stimuli in Rats: Role of the Whisker Barrel Cortices. Cerebral cortex 12, 86-97.

Shulz, D.E., Ego-Stengel, V., and Ahissar, E. (2003). Acetylcholine-dependent potentiation of temporal frequency representation in the barrel cortex does not depend on response magnitude during conditioning. J. Physiol.-Paris *97*, 431–439.

Simons, D.J. (1978). Response properties of vibrissa units in rat SI somatosensory neocortex. J. Neurophysiol. *41*, 798–820.

Siucinska, E., and Kossut, M. (1996). Short-lasting classical conditioning induces reversible changes of representational maps of vibrissae in mouse SI cortex—a 2DG study. Cereb. Cortex *6*, 506–513.

Sofroniew, N.J., Flickinger, D., King, J., and Svoboda, K. (2016). A large field of view two-photon mesoscope with subcellular resolution for in vivo imaging. eLife. 5: e14472.

Steinmetz, N.A., and Moore, T. (2014). Eye Movement Preparation Modulates Neuronal Responses in Area V4 When Dissociated from Attentional Demands. Neuron *83*, 496–506.

Stern, E.A., Maravall, M., and Svoboda, K. (2001). Rapid development and plasticity of layer 2/3 maps in rat barrel cortex in vivo. Neuron *31*, 305–315.

Stirman, J.N., Smith, I.T., Kudenov, M.W., and Smith, S.L. (2016). Wide field-of-view, multi-region, two-photon imaging of neuronal activity in the mammalian brain. Nat. Biotechnol. *34*, 857–862.

Stuttgen, M.C. (2010). Toward Behavioral Benchmarks for Whisker-Related Sensory Processing. J. Neurosci. *30*, 4827–4829.

Stüttgen, M.C. (2011). Mapping spikes to sensations. Front. Neurosci. *5*.

Stüttgen, M.C., and Schwarz, C. (2008). Psychophysical and neurometric detection performance under stimulus uncertainty. Nat. Neurosci. *11*, 1091–1099.

Stuttgen, M.C., and Schwarz, C. (2010). Integration of Vibrotactile Signals for Whisker-Related Perception in Rats Is Governed by Short Time Constants: Comparison of Neurometric and Psychometric Detection Performance. J. Neurosci. *30*, 2060–2069.

Sur, M. (2005). Patterning and Plasticity of the Cerebral Cortex. Science *310*, 805–810.

Svoboda, K., and Yasuda, R. (2006). Principles of Two-Photon Excitation Microscopy and Its Applications to Neuroscience. Neuron *50*, 823–839.

Takahashi, H., Yokota, R., Funamizu, A., Kose, H., and Kanzaki, R. (2011). Learning-stage-dependent, field-specific, map plasticity in the rat auditory cortex during appetitive operant conditioning. Neuroscience *199*, 243–258.

Taniguchi, H., He, M., Wu, P., Kim, S., Paik, R., Sugino, K., Kvitsani, D., Fu, Y., Lu, J., Lin, Y., et

al. (2011). A Resource of Cre Driver Lines for Genetic Targeting of GABAergic Neurons in Cerebral Cortex. Neuron *71*, 995–1013.

Taube, J.S., Muller, R.U., and Ranck, J.B. (1990). Head-direction cells recorded from the postsubiculum in freely moving rats. II. Effects of environmental manipulations. J. Neurosci. *10*, 436–447.

Trachtenberg, J.T., Chen, B.E., Knott, G.W., Feng, G., Sanes, J.R., Welker, E., and Svoboda, K. (2002). Long-term in vivo imaging of experience-dependent synaptic plasticity in adult cortex. Nature *420*, 788–794.

Turrigiano, G.G. (2008). The Self-Tuning Neuron: Synaptic Scaling of Excitatory Synapses. Cell *135*, 422–435.

Turrigiano, G.G., and Nelson, S.B. (2000). Hebb and homeostasis in neuronal plasticity. Curr. Opin. Neurobiol. *10*, 358–364.

Ulanovsky, N. (2004). Multiple Time Scales of Adaptation in Auditory Cortex Neurons. J. Neurosci. *24*, 10440–10453.

Vazdarjanova, A., and McGaugh, J.L. (1998). Basolateral amygdala is not critical for cognitive memory of contextual fear conditioning. Proc. Natl. Acad. Sci. *95*, 15003–15007.

Weinberger, N.M. (2004). Specific long-term memory traces in primary auditory cortex. Nat. Rev. Neurosci. *5*, 279–290.

Weinberger, N.M. (2007). Associative representational plasticity in the auditory cortex: A synthesis of two disciplines. Learn. Mem. *14*, 1–16.

Weinberger, N.M., Javid, R., and Lepan, B. (1993). Long-term retention of learning-induced receptive-field plasticity in the auditory cortex. Proc. Natl. Acad. Sci. *90*, 2394–2398.

Welker, E., Rao, S.B., Dorfl, J., Melzer, P., and Van der Loos, H. (1992). Plasticity in the barrel cortex of the adult mouse: effects of chronic stimulation upon deoxyglucose uptake in the behaving animal. J Neurosci *12*, 153–70.

Wichmann FA, and Hill NJ. (2001). The psychometric function. I. Fitting, sampling, and goodness of fit. Percept Psychophys 63, 1293.

Wiest, M.C. (2005). Heterogeneous Integration of Bilateral Whisker Signals by Neurons in Primary Somatosensory Cortex of Awake Rats. J. Neurophysiol. *93*, 2966–2973.

Wiest, M.C., Thomson, E., Pantoja, J., and Nicolelis, M.A.L. (2010). Changes in S1 Neural Responses During Tactile Discrimination Learning. J. Neurophysiol. *104*, 300–312.

Wurtz, RH. (1968). Visual cortex neurons: response to stimuli during rapid eye movements. Science 162, 1148–1150.

Yan, J., and Zhang, Y. (2005). Sound-guided shaping of the receptive field in the mouse auditory cortex by basal forebrain activation. Eur. J. Neurosci. *21*, 563–576.

Yang, H., Kwon, S.E., Severson, K.S., and O'Connor, D.H. (2015). Origins of choice-related activity in mouse somatosensory cortex. Nat. Neurosci. *19*, 127–134.

Yassin, L., Benedetti, B.L., Jouhanneau, J.-S., Wen, J.A., Poulet, J.F.A., and Barth, A.L. (2010). An Embedded Subnetwork of Highly Active Neurons in the Neocortex. Neuron *68*, 1043–1050.

Yizhar, O., Fenno, L.E., Prigge, M., Schneider, F., Davidson, T.J., O'Shea, D.J., Sohal, V.S., Goshen, I., Finkelstein, J., and Paz, J.T. (2011). Neocortical excitation/inhibition balance in information processing and social dysfunction. Nature *477*, 171–178.

Yotsumoto, Y., Watanabe, T., and Sasaki, Y. (2008). Different dynamics of performance and brain activation in the time course of perceptual learning. Neuron *57*, 827–833.

Yuan, Y., Mao, H., and Si, J. (2015). Cortical neural responses to previous trial outcome during learning of a directional choice task. J. Neurophysiol. 1963–1976.

Zariwala, H.A., Madisen, L., Ahrens, K.F., Bernard, A., Lein, E.S., Jones, A.R., and Zeng, H. (2011). Visual Tuning Properties of Genetically Identified Layer 2/3 Neuronal Types in the Primary Visual Cortex of Cre-Transgenic Mice. Front. Syst. Neurosci. *4*.

Zhou, J., Wen, Y., She, L., Sui, Y. -n., Liu, L., Richards, L.J., and Poo, M. -m. (2013). Axon position within the corpus callosum determines contralateral cortical projection. Proc. Natl. Acad. Sci. *110*, E2714–E2723.

Zhou, M., Liang, F., Xiong, X.R., Li, L., Li, H., Xiao, Z., Tao, H.W., and Zhang, L.I. (2014). Scaling down of balanced excitation and inhibition by active behavioral states in auditory cortex. Nat. Neurosci. *17*, 841–850.

Zhu, J.J., and Connors, B.W. (1999). Intrinsic firing patterns and whisker-evoked synaptic responses of neurons in the rat barrel cortex. J. Neurophysiol. *81*, 1171–1183.

5. Supplementary data

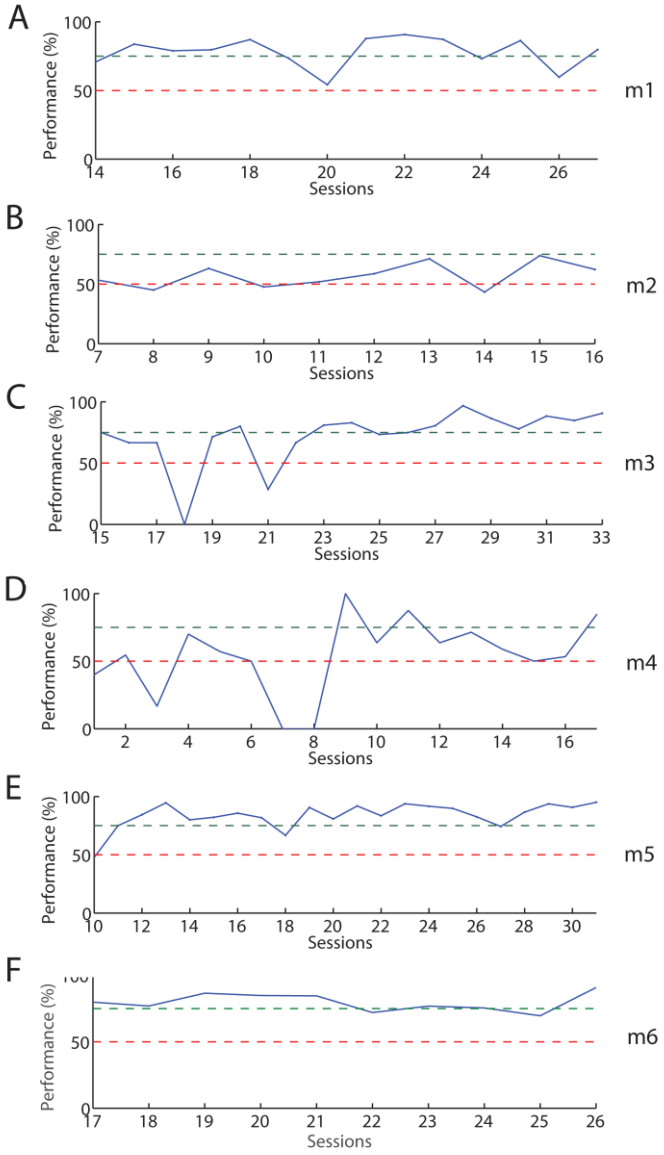

Supplementary figure 1. Behavioral performance across individual sessions on the 2-AFC detection task.

A. m1. **B**. m2. **C**. m3. **D**. m4. **E**. m5. **F**. m6.

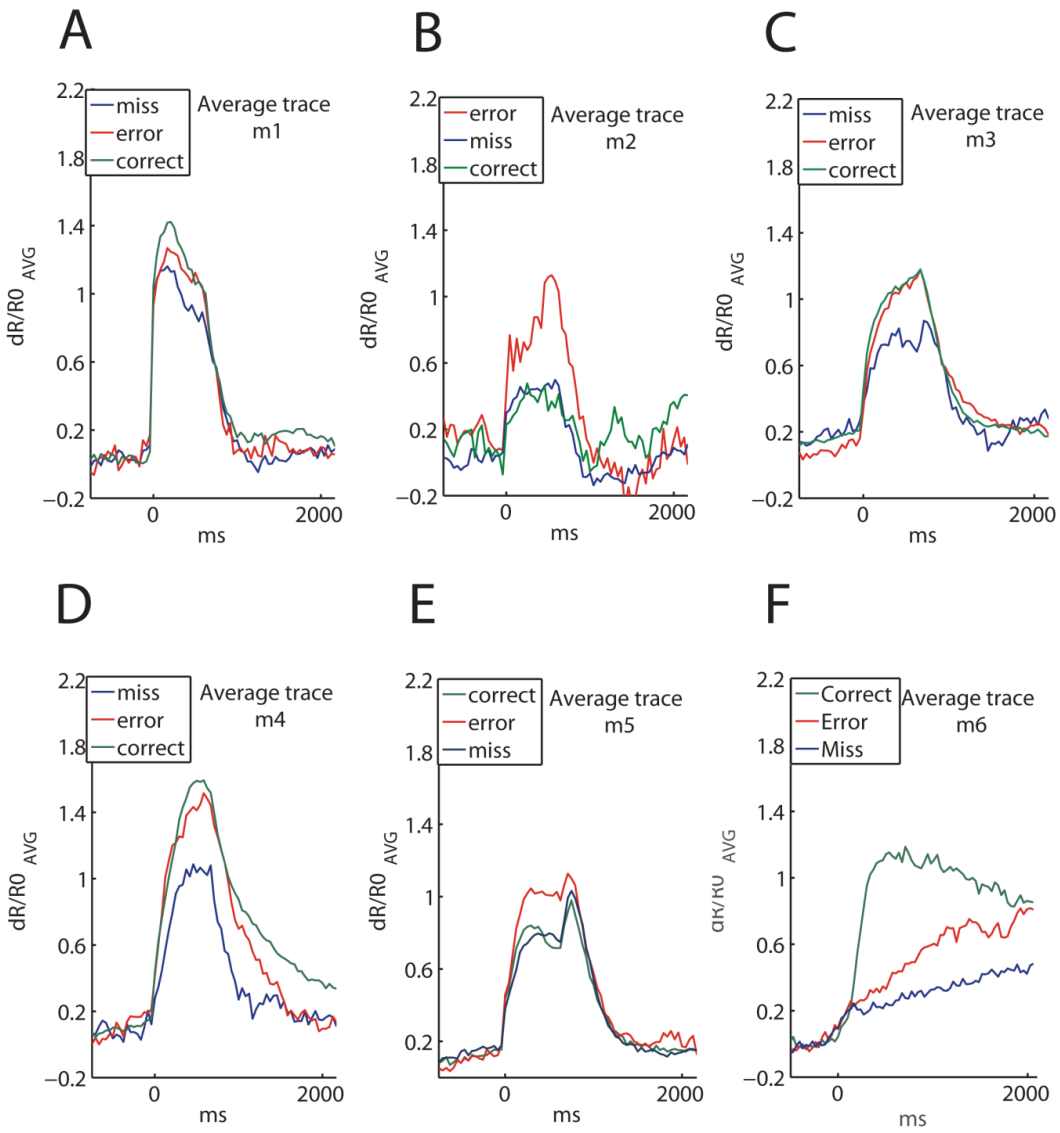

Supplementary figure 2. Average calcium traces for correct, erroneous and missed responses.

A. m1. **B**. m2. **C**. m3. **D**. m4. **E**. m5. **F**. m6.

Animal m1	**Before and after learning**		**Engagement**	
Target side	Contralateral	Ipsilateral	Contralateral	Ipsilateral
Grid search:				
c_opt	1E+02	1E+04	1E-02	1E+05
sigma_opt	1E+01	1E+01	1E+05	1E+01
Performance on whole data set:				
TPR-cl1 (%)	72.4	65.0	46,2	46,0
TPR-cl2 (%)	74.0	59.2	78,7	55,5
TPR-cl3 (%)	-	-	--	--
Bacc (%)	**73.2****	**62.1****	**62,5****	50,7
Chance level estimation:				
1% chance level (%)	57.3	57.4	60,9	61,5

Animal m2	**Before and after learning**		**Engagement**	
Target side	Contralateral	Ipsilateral	Contralateral	Ipsilateral
Grid search:				
c_opt	1E+00	1E-03	1E-04	1E-01
sigma_opt	1E+01	1E+01	1E+04	1E+02
Performance on whole data set:				
TPR-cl1 (%)	71.0	42.4	48,0	52,2
TPR-cl2 (%)	88.4	72.9	58,3	60,2
TPR-cl3 (%)	-	-	-	-
Bacc (%)	**79.7****	57.6	53,1	56,2
Chance level estimation:				
1% chance level (%)	58.3	59.8	57,2	56,5

Animal m3	**Before and after learning**		**Engagement**	
Target side	Contralateral	Ipsilateral	Contralateral	Ipsilateral
Grid search:				
c_opt	1E+00	1E+04	1E+03	1E+00
sigma_opt	1E+01	1E+01	1E+04	1E+01
Performance on whole data set:				
TPR-cl1 (%)	64.3	45.7	63,6	58,8
TPR-cl2 (%)	79.6	77.0	59,9	60,5
TPR-cl3 (%)	-	-	--	--
Bacc (%)	**71.9****	**61.3****	**61,8****	**59,6****
Chance level estimation:				
1% chance level (%)	55.6	54.3	55,2	54,3

Animal m4	**Before and after learning**		**Engagement**	
Target side	Contralateral	Ipsilateral	Contralateral	Ipsilateral
Grid search:				
c_opt	1E+00	1E+01	1E+01	1E-01
sigma_opt	1E+01	1E+01	1E+02	1E+01
Performance on whole data set:				
TPR-cl1 (%)	71.0	88.9	80,2	69,3
TPR-cl2 (%)	64.1	84.6	61,2	63,8
TPR-cl3 (%)	-	-	--	--
Bacc (%)	**86.7****	**67.5****	**66,6****	**70,7****
Chance level estimation:				
1% chance level (%)	54.5	54.4	55,0	54,0

Animal m5	**Before and after learning**		**Engagement**	
Target side	Contralateral	Ipsilateral	Contralateral	Ipsilateral
Grid search:				
c_opt	1E+01	1E+01	1E+00	1E-03
sigma_opt	1E+01	1E+01	1E+01	1E+01
Performance on whole data set:				
TPR-cl1 (%)	85,8	71,9	56,8	56,5
TPR-cl2 (%)	89,1	79,0	68,0	64,8
TPR-cl3 (%)	--	--	--	--
Bacc (%)	**87,4****	**75,5****	**62,4****	**60,7****
Chance level estimation:				
1% chance level (%)	56,3	56,5	58,1	59,7

Supplementary table 1. Best single-trial classification results and optimal non-linear SVM hyper-parameters (copt, σ RBF, opt) found by grid search.

Bold balanced accuracy values (Bacc) indicate results above the 1% chance level. The analyzed time window was 1000ms, and only unilateral 90 Hz stimuli were taken into consideration. “Before and after learning” compares data from before learning (baseline in the awake state) and after learning (after the animals reach a 75% threshold of performance). “Engagement” compared the engaged (correct and error trials) versus the disengaged (missed trials) category. Significance legend: ** = $p<0.01$.

6. Curriculum vitae

Personal Details

Name:	Vida ŠKREB
Place and date of birth:	Zagreb, Croatia, 1st of February, 1984
Citizenships:	Croatian and French

Education

Since January 2010	Ph.D. student in neuroscience at the Faculty of Science, University of Zurich, Switzerland; Supervisor: Dr.Florent Haiss, Steering committee: Prof. Bruno Weber, Prof. Jean-Marc Fritschy, Prof. Fritjof Helmchen
May-September 2009.	Institute of Physiological Chemistry, University of Mainz
March-April 2009.	Biochemistry department, Faculty of science, University of Zagreb
June 2008.	Master thesis in Chemistry at the Faculty of science,"The effect of copper(II) on the absorptions spectra of hydrazones", University of Zagreb (medal for achievements)
2003.-2004.	„Sciences de la vie" Université Paris 7 Denis Diderot, Paris, France
2002.-2003.	Faculty for Food Technology and Biotechnology, University of Zagreb
2002.	Graduation at the Gynasium for mathematics and life science

Publications

Mayrhofer, J. M., Skreb,V., Von der Behrens, W., Musall, S., Weber, B., & Haiss, F. (2013). Novel two-alternative forced choice paradigm for bilateral vibrotactile whisker frequency discrimination in head-fixed mice and rats. Journal of neurophysiology, 109(1), 273–284. doi:10.1152/jn.00488.2012.

Grants

„Forschungskredit“ Grant financed from the „Stiftung für Forschung an der Medizinischen Fakultät allowing one year of funding from the University of Zurich, June 2013

Talks

“Two-photon imaging of neuronal population activity in the rodent somatosensory cortex during perceptual learning” at the Brain-i-Nets plenary meeting 12.-13. November 2012, Graz.

"Cholinergic modulation of sensory responses in the rodent barrel cortex" at the Brain-i-Nets Project Meeting 2011 with EU Review, 8.-10. March 2011, Gif-Sur-Yvette, France.

"Cholinergic modulation of sensory responses in the rodent barrel cortex" at the ZNZ retreat, 12.-14. May 2011.

Posters

“Cholinergic modulation of sensory responses in the rodent barrel cortex”; Skreb,V., Von der Behrens, W., Musall, S., Schaffner, M., Weber, B., & Haiss, F. at The Society for Neuroscience Annual Meeting in Washington D.C., 12.-16. November 2011.

Cholinergic modulation of sensory responses in the rodent barrel cortex”; Skreb,V., Von der Behrens, W., Musall, S., Schaffner, M., Weber, B., & Haiss, F. at the ZNZ day, Zurich, Switzerland, 12.-16. September 2011.

“Cholinergic modulation of sensory responses in the rodent barrel cortex”; Skreb,V., Von der Behrens, W., Schaffner, M., Weber, B., & Haiss, F. at the FENS IBRO Society for Neurosciene School 2011 “Causal Neuroscience: Interacting with neural circuits” Programme in Bertinoro, Italy, 19.-24. June 2011.

7. Acknowledgements

I would like to thank Prof. Bruno Weber and Dr. Florent Haiss for giving me the opportunity to work in such a fascinating field as neuroscience, for offering me their valuable guidance, extensive knowledge, and supportive mentoring until the successful completion of the Ph.D.

I am grateful to Prof. Jean-Marc Fritschy for supporting me during the entire doctorate period and my lab colleagues and fellow students for intellectual exchange, valuable input and helping me maintain my optimism and passion for science.

This thesis would not be possible without the incredible and loving support of my family especially my parents, who were with me at every step of this long and hard path and supporting me financiallyduring the last year and a half. I am also very grateful to for my friends for having faith in me and cheering me along. A special thank you to my love, Nick Shackleton-Jones.